CHALMERS
UNIVERSITY OF TECHNOLOGY

Positioning of Charger Stations for a fully-electrified Swedish Transport System

Consequence on the Power System

Master's thesis in MPEPO

Shenglai Jin

DEPARTMENT OF ELECTRICAL ENGINEERING
SUSTAINABLE ELECTRICAL POWER ENGINEERING AND ELECTROMOBILITY
CHALMERS UNIVERSITY OF TECHNOLOGY
Gothenburg, Sweden 2024
www.chalmers.se

Master's thesis 2024

Positioning of Charger Stations for a Fully Electrified Swedish Transport System

Consequence on the Power System

Shenglai Jin

CHALMERS
UNIVERSITY OF TECHNOLOGY

Department of Electrical Engineering
Sustainable Electrical Power Engineering and Electromobility
Chalmers University of Technology
Göteborg, Sweden 2024

Positioning of Charger Stations for a fully-electrified Swedish Transport System
Consequence on the Power System
Shenglai Jin

Supervisor: Torbjörn Thiringer, Chalmers
Examiner: Torbjörn Thiringer, Chalmers

Master's Thesis 2024
Department of Electrical Engineering
Sustainable Electrical Power Engineering and Electromobility
Chalmers University of Technology
SE-412 96 Göteborg Telephone +46 31 772 1000

Cover: A hypothetical image of a future smart transportation city built with OpenAI.

Typeset in LaTeX
Printed by Chalmers Reproservice
Göteborg, Sweden 2024

Positioning of Charger Stations for a fully-electrified Swedish Transport System
Consequence on the Power System
Shenglai Jin
Department of Electrical Engineering
Chalmers University of Technology

Abstract

In pursuing a fully electrified transportation system, with the promotion of electric vehicles, existing traffic prediction models are showing weakness. The inadequate layout of charging facilities fails to meet demands, and the growing energy consumption has severely impacted the power system.

This study proposes an integrated energy optimization and charging infrastructure framework (EOIET), addressing the challenges during the electrification process. In terms of energy consumption prediction, the study established urban traffic flow energy consumption estimation models UCEM and UTEM based on macro traffic data, and constructed a long-distance traffic flow energy consumption prediction model through the LSTM-GRU model with Rayleigh distribution assumption. For the optimization of charger station layout, the study comprehensively considered the decentralized nature of the urban layout and applied a simulated annealing model and topology optimization techniques to determine the optimal location of long-distance charging stations. The power system impact assessment uses Monte Carlo simulation combined with deep learning algorithms to optimize the power transmission strategy and evaluate the grid stability and load balance.

The study verified the model based on Sweden's historical transportation energy consumption and relevant EU indicators, which confirmed the reliability of the model. It provided a reference for infrastructure development and grid optimization in the context of electrified transportation.

Keywords: Traffic Flow Prediction, EV Charging, Positioning charging infrastructure, Grid Management

Acknowledgements

The years I spent pursuing my master's degree have left me with deep memories. Such a project, in my opinion, is also an important review of the knowledge I have acquired in the last two years or so, and a tangible practice of the body of knowledge I possess.

I am deeply grateful to my supervisor, Professor *Torbjörn Thiringer*, whose wisdom and insight have been instrumental throughout this process. He crafted a research topic that integrated diverse areas of my studies, including electric vehicles, battery technologies, transportation systems, mathematical modeling, machine learning, charging infrastructure planning, and power system analysis. The project's focus on electric vehicle adoption and environmental sustainability not only addresses critical contemporary challenges but also reflects his trust in my abilities to tackle problems. Our regular discussions have been invaluable, helping me refine my models and develop my theoretical framework. His humor, intellect, and encouragement have consistently inspired me to push boundaries.

The patience of the faculty at *Chalmers Tekniska Högskola* enriched my horizon, through well-designed courses, experiments, and seminars to expand my realm of understanding. The exchange semester at *Technische Universität München* during the exchange semester offers a deeper focus on the topic of renewable energies and new insights into the development of sustainable energy systems, particularly from the perspective of the electricity market. I would also like to extend my gratitude to employees at the Swedish Transport Agency (*Trafikverket*), Statistics Agency in Sweden (*SCB*), and the Swedish Energy Agency (*Energimyndigheten*) for their diligent support in data inquiries, which is essential for this study.

The support of friends has been a cornerstone of my learning experience. *Boming Zhao*, a PhD candidate in software engineering, shared invaluable insights into time-series prediction models, guiding my work on machine learning applications. *Changhao Guan*, a software engineer at *Tencent*, offered practical advice on the construction of macro-data models. *Kaichen Niu*, now a lecturer with a background in transportation engineering, provided essential conceptual input for traffic demand modeling. Many others have also supported me, their expertise and generosity have helped me navigate unfamiliar fields, enabling me to expand my skill set and enhance my academic foundation. Their contributions have been nothing short of transformative, and I am deeply appreciative.

The unwavering support of my family has been a source of strength and inspiration. My parents, accomplished professionals in the field of biology, have been my lifelong role models. Their journeys through advanced studies abroad instilled in me the values of perseverance, independence, and self-discipline. They have been instrumental in shaping my ability to approach research with focus and determination,

particularly through their guidance in mastering academic writing and navigating English-language literature. Their encouragement has been a guiding light throughout this process.

Ultimately, I am eternally grateful to everyone who has supported me, be it through direct help, a transfer of wisdom, or being there in spirit. The belief, kindness, and encouragement will always inspire me. Looking beyond, I am ambitious to chase more in the electrical engineering field, seeking my potential and contributing with real value in whatever path lies ahead of me.

Shenglai Jin, Gothenburg, November 2024

List of Acronyms

ÅDT	Annual average 24-hour traffic flow
AIC	Akaike Information Criterion
BIC	Bayesian Information Criterion
EOIET	Integrated optimization and infrastructure framework for fully-electrified transportation
EV	Electric Vehicle
GA	Genetic Algorithm
GRU	Gated Recurrent Unit
LSTM	Long-short term Memory
PSO	Particle Swarm Optimization
RES	Renewable-based Energy Source
SA	Simulated Annealing
TSO	Tabu Search Optimization
UCEM	Urban car energy estimation method
UTEM	Urban transit energy estimation method

Nomenclature

Indices

i,j	Indices for city and province in Sweden
k	Index for type of city
m	Index for type of charger
n	Index for route segment

Parameters

N_i	Population in city i
$N_{car,i}, N_{bus,i}, N_{truck,i}$	Number of vehicles in city i
$e_{car}, e_{bus}, e_{truck}$	Unit energy consumption by vehicles
$N_{H,i}$	Number of houses in city i
$N_{C,i}$	The commuting population in the city i
$X_{Car,i}^{Annual}$	Annual passenger km of cars in the city i
$X_{Car,k}$	Daily average driving distance of the car in type k
$X_{Bus,j}^{Annual}$	Annual offered km of public transport in province j
P_m	Power of charger m
η_m	Charging efficiency of charger m
N_m	Number of charger m
ρ_m	Occupy ratio of charger m
L_n	Length of route n
σ	Scale factor of Rayleigh distribution
λ	Rate parameter in Poisson distribution
$\alpha, \beta, \gamma, \delta$	The tuning parameters used in the model

Contents

1
Introduction

1.1 Background

Reducing greenhouse gas emissions, mitigating global warming, and striving toward carbon neutrality represents proactive responses and shared goals in facing the climate crisis. Under the carbon neutrality framework, the shift to renewable energy is essential in global energy transformation. To this end, the EU has even put forward the strategic goal of fully implementing electric vehicles. Sweden, with its leading electric vehicle industry and abundant renewable energy resources, plays an important role in this process. During the electrification of Swedish transportation, precise forecasting of traffic flow, accurate estimation of vehicle energy consumption, and optimal positioning of charging facilities have become bottlenecks. Meanwhile, as modern society has higher requirements for the stability and balance of the power grid, it is crucial to assess the potential impacts of electrification on the power system is also crucial.

The research aims to utilize extensive Swedish traffic data to build analytical models that support accurate traffic flow predictions, improving the optimal sitting of critical charging infrastructure and assessing its potential impact on the grid as well. Moreover, the research contributes to the development of renewable energy within the framework of carbon neutrality.

1.2 Literature Review

Accurate traffic prediction is essential for the development of electrified transport systems. Previous research predominantly focuses on temporal and spatial feature extraction. Generally, prediction models can be categorized into three types: Naïve, parametric, and non-parametric models[1]. The naïve model adopts historical data as a decision-making standard, and cannot accurately reflect variation tendency of traffic flow. Parametric models, for example, the Autoregressive Moving Average model (ARIMA) are widely used in short-term prediction[2]. Its extended version, combined with the GARCH model, improves the ability to capture conditional means and heteroskedasticity[3][4]. However, the reliance of parametric models on the assumption of data linearity limits their performance in complex nonlinear relationships, especially in long-term forecasts. With the rise of deep learning, non-parametric methods have become mainstream. For example, KNN can effectively

capture historical fluctuation characteristics, but it is limited to periodic change characteristics[5][6]. LSTM offers improved handling of nonlinear scenarios compared to parametric models [7][8][9], yet its performance is insufficient when dealing with short-term fluctuations. To address this, the encoder-decoder structure and light-BGM were coupled with LSTM[10][11][12][13], unexpectedly resulting in increased computational complexity and risk of overfitting. Meanwhile, the combination of GRU and encode-decode sacrifice medium and long-term prediction ability although simplifies the computation[14]. In addition, RNN and GCN-based operations have improved the spatiotemporal feature extraction in prediction[15]-[20]. However, such methods are usually limited to small-scale applications. Reviewing related models, the flexibility and accuracy of non-parametric models make them stand out[21]. It is frustrating that it is highly difficult to consider both multi-dimensional time predictions and the simplicity of the model. The improvements may come from the attendance of external factors [22].

Building on traffic prediction, vehicle energy consumption estimation is also crucial. Studies have shown that most electric vehicle users tend to charge when the battery is low[23], keeping the battery charge between 20% and 80% has been shown to be beneficial to battery health[24]. These factors exacerbate the "mileage anxiety" of electric vehicles, while fast charging facilities proved to contribute to overcoming it[25][26]. As for the vehicle energy consumption calculation, an approach integrating specific driving data provides high accuracy[27], however, lacks the ability to quantify the overall fleet. In comparison, models based on queuing theory are suitable for fleet calculations[19]. With the popularization of EVs, the potential interaction between individual user behavior and energy consumption has gradually attracted attention. Although relevant studies have shown that this relationship still has great uncertainty, urban commuting demand may tend to stabilize due to the multifactorial impacts[28]. Theoretically, the charging station siting models can be categorized into mathematical optimization, multi-criteria decision-making(MCDM), and heuristic algorithms[29]. Notably, mathematical optimization models are constrained to small-scale and fixed-parameter scenarios. MCDM typically considers external factors such as cost[30], making it less relevant in demand-driven cases. In contrast, heuristic algorithms have demonstrated promise in large-scale planning. The genetic algorithms optimize site selection layout by simulating user charging behavior[32][33], while whale optimization algorithms plan based on charging waiting time[34]. European research further provides standardized suggestions for charging station parameters[31], and recommends setting up a light vehicle charging station every 60 kilometers and a heavy vehicle charging station every 100 kilometers in the EU core network[35][36]. The Swedish Transport Agency conducted a review of existing electric vehicle charging facilities[37][38].

Along with the rolling out of charging facilities, the criteria for evaluating whether the power grid can meet daily charging needs and maintain smooth operation has become a research focus. Evidence has shown that EV users usually charge at night which overlaps with the evening peak, increasing the burden on the power grid[25].

Addressing this problem, an analytical framework has been proposed, especially for the power peak and equipment overload problems caused by charging[39]. Long-term models suggested that the increase in EV usage may lead to an increase in the power system's dependence on fossil energy[40]. Meanwhile, smart charging technologies have demonstrated effectiveness in reducing peak loads and enhancing renewable energy utilization[41]. Additionally, probabilistic models of vehicle energy consumption and power generation provide quantitative insights for grid stability analysis[42].

The review of the previous learnings reveals that while substantial progress has been made in traffic flow prediction, vehicle energy consumption estimation, charging station layout, and grid impact assessment, limitations still exist. Most prediction models have obstacles in capturing both short and long-term characteristics, particularly performing worse regarding nonlinear sequences. In addition, current vehicle energy consumption models lack specificity for different traffic scenarios (e.g. cities and highways). Concerning the positioning of chargers, high computational complexity, especially for large-scale cases, and insufficient consideration of multidimensional factors do matter. As for the consequence of the power system, there is a lack of systematic generation and load modeling, and the overlooking of the energy market is missing as well.

1.3 Purpose

Based on the above analysis, the purpose of the study is to establish an LSTM-GRU model to enhance the ability to capture both short-term fluctuation and long-term trends. Furthermore, an additional target is setting energy consumption models specifically tailored for urban commuting and long-distance travel along highways. Moreover, designing an algorithm to determine the placement of the charging stations. In addition, a goal is to assess the stability of the power system by Monte Carlo analysis under multiple decision-making strategies, providing a reference for the operation aligned with power market policy.

2
Theory

This chapter mainly presents some known research theories, which will help the subsequent development of this study.

2.1 Traffic Flow Forecast

For national-level analysis, long-term trend forecasting of traffic flows is crucial for understanding future traffic patterns and demand trends, which play a crucial role in planning and constructing the overall layout of the charging infrastructure. Meanwhile, short-term fluctuation prediction helps to optimize the daily operation of charging stations, particularly in response to fluctuations caused by special events (e.g., holidays, large parties, etc.). This enables more appropriate resource allocation, adjusting and optimizing charging stations' specific location and capacity. Relying solely on either a single long-term or short-term model presents some limitations in the analysis. Therefore, combining the strengths of both long-term and short-term forecasting into a multi-level analytical framework becomes the primary topic of this study.

Based on the discussion on prediction modeling in Section 1.2, this study adopts LSTM combined with GRU. The following is a brief introduction to the structure of LSTM and GRU.

2.1.1 LSTM

The LSTM model is dominated by the learning prediction of long-term dependencies. It completes the prediction through the forgetting gate, input gate, state update, and output gate. The forget gate determines which part of the previous cell state C_{t-1} should be kept. It takes the previous hidden state h_{t-1} and the current input x_t, and applies a Sigmoid activation to produce a value between 0 and 1 for each component of the cell state

$$f_t = \sigma(W_f \cdot |h_{t-1,}x_t| + b_f) \tag{2.1}$$

where W_f is the weight matrix for the forget gate, b_f is biased for the forget-gate, and σ is the sigmoid activation function.

Then the candidate cell state C_t is generated using a hyperbolic tangent function as

an activation function, creating a new set of values that could be added to the cell state, expressed as

$$\tilde{C}_t = \tanh(W_C \cdot |h_{t-1}, x_t| + b_C) \tag{2.2}$$

W_i, W_C are the weight matrices for the input gate and candidate cell state, b_i, b_C are the basis for the input gate and candidate cell state.

The cell state is updated by combining the retained information from the previous cell state and the new information, denote by

$$C_t = f_t C_{t-1} + i_t \tilde{C}_t \tag{2.3}$$

This allows the LSTM model to retain long-term dependencies by deciding what to forget and what to update.

Finally, it is the output gate that determines the next hidden state h_t, also the LSTM cell's output. It decides which part of the cell state should be passed to the next layer or time step. The output gate is expressed as

$$o_t = \sigma(W_o \cdot |h_{t-1}, x_t| + b_o) \tag{2.4}$$

where W_o is the weight matrix for the output gate, b_o is the bias for the output gate. The hidden state is calculated by applying an active function to the updated cell state, and then scaling it by the output gate

$$h_t = o_t \cdot \tanh(C_t) \tag{2.5}$$

2.1.2 GRU

GRU is a recurrent neural network with a simplified structure that only includes update and reset gates to more efficiently handle short-term fluctuation feature extraction prediction. The update gate controls how much of the previous hidden state should be passed on to the current hidden state, determining the amount of pass information to carry forward at each time step, expressed as

$$z_t = \sigma(W_z \cdot |h_{t-1}, x_t| + b_z) \tag{2.6}$$

where W_z is the weight matrix for the update gate, b_z is the bias for the update gate.

The reset gate determines how much of the previous hidden state to forget. It also decides how much of the past information to discard when computing the new hidden state, denoted as

$$r_t = \sigma(W_r \cdot |h_{t-1}, x_t| + b_r) \tag{2.7}$$

The candidate's hidden state h_t is computed using the reset gate. When r_i is close to 0, the influence of the previous hidden state is reduced, allowing GRU to reset and focus on the new input x_t. The above process can be denoted by

$$\tilde{h}_t = \tanh(W \cdot |r_t h_{t-1}, x_t| + b) \tag{2.8}$$

Where W is the weight matrix for the candidate's hidden state. b is biased for the candidate's hidden state. The hidden state h_t is then updated by combining the previous hidden state h_{t-1} (scaled by z_t) and the candidate hidden state h_t (scaled by $1 - z_t$). This interpolation allows the GRU to maintain important information over time while discarding less relevant information.

2.2 Energy Demand Estimation

2.2.1 Energy Consumption per EV

Typically, battery efficiency is around 90%. To accurately assess the average energy consumption (kWh/km) of an electric vehicle while traveling, it is necessary to understand the drive resistance and the key factors that affect it. Below is an energy consumption calculation method based on key factors such as vehicle driving resistance and battery efficiency.

Vehicle driving resistance consists of two main components. The rolling resistance, which is generated by the friction between the tires and the ground, can be calculated as

$$F_{roll} = C_r mg \tag{2.9}$$

where C_r is the rolling resistance coefficient, m is the mass of the vehicle, and g is the acceleration due to gravity (generally valued at $9.8\text{kg} \cdot \text{m/s}^2$). The air resistance can be expressed as

$$F_{frag} = 0.5 C_d A \rho v^2 \tag{2.10}$$

where C_d is the air resistance coefficient, A is the windward area of the vehicle, ρ is the air density, and v represents the traveling speed.

In general, vehicles traveling through various scenarios experience events such as acceleration, deceleration, and kinetic energy recovery from braking, all of which trigger fluctuations in energy consumption. However, individual fluctuations tend to offset each other out in large-scale fleets, allowing for analysis under a constant-speed driving case. In steady-state driving, the vehicle traction is balanced with the driving resistance. Therefore the vehicle energy consumption per kilometer traveled can be calculated as

$$e = \frac{P}{\eta} \frac{1}{v} = \frac{F_{roll} + F_{drag}}{\eta} \tag{2.11}$$

In this study, the relevant parameters of cars, buses, and large trucks are referenced in the following table.

Table 2.1: Parameters of the investigated Electric Vehicles

Parameter	Car	Bus	Truck
m	1300 kg	10000 kg	15000 kg
C_r	0.009	0.007	0.0075
C_d	0.25	0.55	0.65
A	2.4 m^2	7.5 m^2	7 m^2
ρ		1.225 kg/m^3	
η		90%	

Combined with the general speed at which vehicles travel, the study can take the energy consumption of 0.2kWh/km for small cars, 1.2kWh/km for buses, and 1.5kWh/km for large trucks.

2.2.2 Energy Consumption Model

In the analysis of energy consumption of large-scale transportation systems at the national scale, the driving distance and energy consumption of different EVs exhibits randomness and volatility. The probability distribution models can effectively describe this uncertainty and quantify the energy consumption characteristics in different scenarios, thus providing reliable estimates of average daily energy consumption. Acknowledging that the vehicle traveling distance obeys a specific probability distribution, the average daily energy consumption of a certain type of electric vehicle can be expressed as

$$E_{avg} = \int_0^\infty exf(x) \cdot dx \tag{2.12}$$

Here e is the average energy consumption per kilometer of each type of vehicle proposed in 2.2.2, x denotes the daily driving distance, and $f(x)$ denotes the probability density function obeyed by the driving distance of the vehicle.

In this scenario, if the fleet has N electric vehicles, its total energy consumption can be expressed as

$$E_{tot} = NE_{avg} \tag{2.13}$$

In practice, the probability distribution smoothes out the extreme driving distance of individual vehicles into an overall average, making the average daily energy consumption more representative. This model can effectively reflect the average energy consumption level of a large-scale fleet. Proposing appropriate probability distribution models for different scenarios has becomes one of the key issues to be addressed in this study.

2.3 Position of Charger Station

The location of charging stations is a multi-dimensional decision-making process that takes into account factors such as charging station utilization, vehicle accessibility,

etc., and it is a typical discrete optimization problem. Adopting multiple constraints to quantify the corresponding factors and solving the objective function, which can provide a solution for layout of the charging station to meet the actual demand. This decision-making process can be expressed as

$$\min / \max Z = \sum_{j=1}^{n} c_j x_j \tag{2.14}$$

Satisfying

$$\sum_{j=1}^{n} a_j x_j \leq b_j \tag{2.15}$$

where, Z is the objective function, which is the weighted sum of the factors affecting the charging station location decision, x_j and c_j represent the factor and its weight, respectively. a_j and b_j represent the moderators in the constraints.

In practical decision-making, following the European Union's principle of prioritizing demand-driven usage[31], this study focuses on charging station coverage and usage rate as the main decision-making factors. Meanwhile, different constraints and objective functions are established for different scenarios. For example, in the city, the focus is on the distribution of stations consistent with the city's structure, whereas on the highway, ensuring accessibility within a certain distance. Establishing a reasonable influencing factor system and selecting an appropriate heuristic algorithm to solve the multi-objective function has also become one of the focuses of this study.

2.4 Consequence of the Power System

2.4.1 Assessment of Energy Supply and Demand

As the demand for EV charging increases, the balance of supply and demand within the power system becomes increasingly complex. Using probability distribution models to fit the patterns of power generation and consumption enables a precise understanding of the distributional characteristics of supply and demand fluctuations, facilitating a more accurate assessment of supply-demand dynamics across different periods. To accurately characterize the data, measures such as symmetry, skewness, and kurtosis can assist in determining the distributional trend of the data and matching the applicable probability model.

Skewness is mainly used to characterize the direction and degree of asymmetry of the data distribution. A positive skewness indicates that the distribution is right-skewed, negative suggests left-skewed, and a zero skewness illustrating that the distribution is roughly symmetric. The formula followed as

$$Sk = \frac{1}{n} \sum_{i=1}^{n} \left(\frac{x_i - \bar{x}}{\sigma}\right)^2 \tag{2.16}$$

Kurtosis measures the degree of spikiness of the data distribution and is calculated as

$$Ku = \frac{1}{n}\sum_{i=1}^{n}\left(\frac{x_i - \bar{x}}{\sigma}\right)^4 - 3 \tag{2.17}$$

In the above expression, x_i represents the sample data, $\bar{x}$ is the sample mean, σ is the standard deviation, n is the sample size.

In general, the commonly used probability distribution models include normal distribution, Poisson distribution, exponential distribution, Weibull distribution, log-normal distribution and so on. Normal distribution is suitable for describing the case of symmetric distribution, the probability density function is

$$f(x) = \frac{1}{\sqrt{2\pi\sigma^2}} e^{-\frac{(x-\mu)^2}{2\sigma^2}} \tag{2.18}$$

where μ is averageσ is the standard error.

The Poisson distribution is often used to describe short bursts of events with a probability density function of

$$P(x = k) = \frac{\lambda^k e^{-\lambda}}{k!} \tag{2.19}$$

where λ refers to the average frequency of events and k represents the number of events in a period.

And the exponential distribution is expressed as

$$f(x) = \lambda e^{-\lambda x} \tag{2.20}$$

The Weibull distribution applies to random variables with right or left skewness and is expressed as

$$f(x) = \frac{1}{x\sigma\sqrt{2\pi}} e^{-\frac{(\ln x - \mu)^2}{2\sigma^2}} \tag{2.21}$$

where, μ and σ correspond to the mean and standard deviation after logarithmizing the sequence, respectively. After determining the approximate available probability distribution model, maximum likelihood estimation (MLE) is a commonly used parameter estimation method to determine the distribution parameters. For the sample $x_1, x_2, ...x_n$ and parameter θ, the likelihood function expresses the joint probability of the sample data under the parameter

$$L(\theta) = f(x_1|\theta)f(x_2|\theta)...f(x_n|\theta) \tag{2.22}$$

By solving for the optimal parameters $\hat{\theta}$, the corresponding log-likelihood function is maximized, i.e.

$$\frac{d}{d\theta} \ln L(\hat{\theta}) = 0 \tag{2.23}$$

After completing the initial model fitting, it is necessary to conduct a goodness-of-fit test and comparison to determine the final distribution model. Useful criteria include

Akaike Information Criterion (AIC)

$$\mathrm{AIC} = 2k - 2\ln L(\hat{\theta}) \tag{2.24}$$

Bayesian Information Criterion (BIC)

$$\mathrm{BIC} = k\ln(n) - 2\ln L(\hat{\theta}) \tag{2.25}$$

where k represents the number of model parameters and n represents the sample size, these two criteria measure the simplicity of the model.
Kolmogorov-Smirnov Test (K-S Test)

$$D = \sup_x |F_n(x) - F(x)| \tag{2.26}$$

$F_n(x)$ is the empirical cumulative distribution function and $F(x)$ is the theoretical distribution cumulative function. The criterion measures the maximum difference between the fitted distribution and the theoretical distribution.

After confirming the probability distribution model for power generation and consumption, Monte Carlo analysis can be applied to simulate power supply and demand under various scenarios, therby assessing the impact of charging demand on system stability. This approach simulates diverse supply and demand scenarios by generating multiple random samples of input variables (e.g., generation, load demand) to evaluate the performance of the power system under different load conditions. System reliability is represented by the lost load probability (LOLP)

$$LOLP = \frac{Time\_loadloss}{Time\_total} \tag{2.27}$$

A well-performed power system requires an LOLP of less than 0.1%, which provides a useful reference for subsequent studies.

2.4.2 Assessment of Electricity Market Policies

In addition to the supply and demand, energy market policies also reflect the supply and demand and price dynamics of the power system in real-time. The following is a description of the commonly used market impact mechanisms.

The Merit Order Effect is a mechanism that prioritizes the dispatch of generating units based on the cost of generation, with lower-cost units being dispatched prioritized, and higher-cost units starting up only when demand is high. Since the marginal cost of renewable energy is nearly zero, it might lower the average price

of electricity in the overall electricity market. Quota Obligation is a policy implemented in Sweden, requires generating companies to meet a certain percentage of renewable energy in their electricity supply. This obligation can lead to fluctuations in electricity prices, especially in case of clean energy shortage.

By analyzing historical volatility data on electricity prices, these two mechanisms can effectively assess the impact on the electricity market as electric vehicles are promoted and renewable energy sources increase. These policy analyses will provide a key economic principle for charging station placement and charging strategy optimization.

3

Case Set-Up

Based on the theoretical foundation of this study, this chapter will elaborate on the overall technical route of the research and organize multi-dimensional data related to Sweden, such as vehicle data, human geography information, traffic flow, and power systems, to ensure the reliability of the research. The research structure is shown in the figure below.

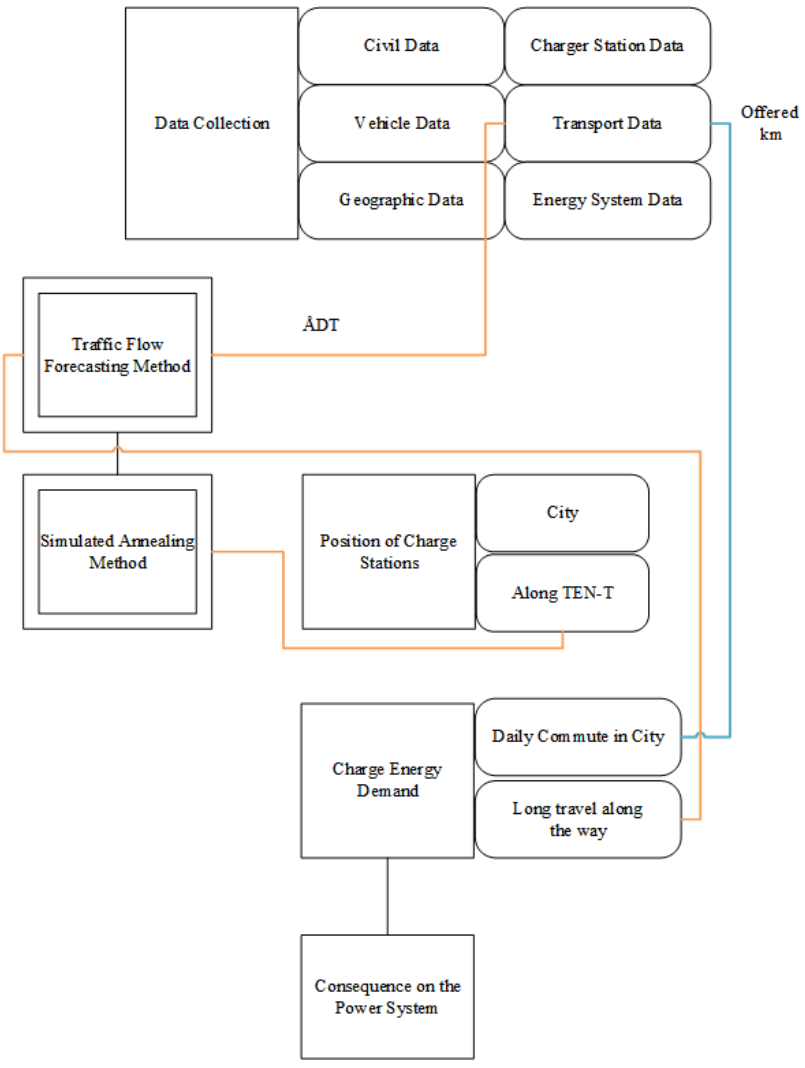

Figure 3.1: Structure of the Research

The study relies on official statistical data from the European Union and Sweden, integrating traffic prediction, energy consumption estimation, charging station optimization algorithm, and power system evaluation model, to propose a research framework for integrated energy optimization and charging infrastructure for electrified transportation (EOIET). Additionally, various historical datasets play a crucial role in verifying the rationality of the model results.

The data for this study comes from multiple official and public channels, covering vehicle parameter information [43][44], population, area, and housing ratio of each city [45], Swedish geographic information [46], registered vehicles, historical commuting information [47], average daily traffic flow on major roads [48], charging station specification parameters [31], power system power generation, electricity price [49], etc. The details are shown in the table.

Table 3.1: Data and its resource

Type of Data	Content	Note	Reference
Vehicle Data	Unit Energy Consumption of Vehicles	$e_{car}, e_{bus}, e_{truck}$	Volvo, Scania
Civil Data	Population	N_i	KVR
	Number of houses	$N_{H,i}$	
	Number of apartments	$N_{Ap,i}$	
	Number of commuters	$N_{C,i}$	
Transport Data	Number of Cars	$N_{Car,i}$	SCB
	Number of Buses	$N_{Bus,i}$	
	Number of Trucks	$N_{Truck,i}$	
	Annual Passenger km of Cars in each city	$X_{\mathrm{Car},i}^{Annual}$	
	Annually offered km of Buses in each län	$X_{Bus,j}^{Annual}$	
	Annual average of daily traffic flow	$\text{Å}DT$	Trafikverket
Geographic Data	Shapefile of Swedish City	-	Open map
	Shapefile of roads in Sweden	-	
Charging Station Data	Power of Charger in Sweden	P_m	EU Masterplan
	Charging Efficiency	η_m	
	Occupy Ratio	ρ_m	
Energy System Data	Annual Generation	G	Energimyndigheten
	Electricity Price	C	

The availability and interpretation of data provided by some official agencies are presented in Appendix A. To ensure the consistency and accuracy of the data, all

types of data must be cleaned and normalized after being introduced. Missing values in localized areas are supplemented using a linear weighted interpolation method. Additionally, ArcGIS software is employed to process traffic flow and charging station layout, offering visualization results as well.

The research employed several simplifications to facilitate the analysis. First, in terms of the research object, the typical energy consumption parameters of electric vehicles were selected to analyze large-scale fleets, ignoring the variations between individual vehicles. In addition, in the context of the research scenario, electric vehicle users were divided into two groups: daily urban commuters and long-distance highway travelers. Distinct models were then constructed based on the characteristics of each group, which, while simplifying the process, overlap demand.

The analysis part of the report is presented in Chapters 4-6. Chapter 4 mainly proposes the estimation of vehicle energy consumption in cities and highways. Chapter 5 builds a model to determine the placement of charging stations in cities and highways; and introduces the initial SoC setting combined with the Monte Carlo process to determine the charger consumption along the highway. Chapter 6 analyzes the impact on the power system under full electrification of the transport system.

4

Analysis I
Traffic and Energy Forecast

This chapter focuses on predicting electric vehicle traffic and energy consumption to support modeling and assessment of urban commuting and highway travel demands. Building on the previous discussions, this study utilizes traffic forecasting models, average vehicle energy consumption metrics, and relevant distribution models as foundational references. The study classifies its subjects into passenger cars, buses, and heavy trucks, and further categorizes scenarios into urban daily commuting demands and long-distance highway travel demands.

In terms of predictive accuracy and demand characteristics, the relatively stable nature of urban daily travel needs and public transit systems allows for traffic and energy consumption forecasts based on historical commuting data and other macro-level statistical indicators. In contrast, given the greater variability in highway travel demand, a non-parametric forecasting model is introduced to quantify and predict fluctuations, thereby obtaining more reliable traffic and energy consumption data.

4.1 Urban Travel and Energy Consumption

To address urban commuting demands, the study introduces models for estimating daily commuting demand and energy consumption for cars and buses, referred to as UCEM and UTEM, detailed in sections 4.1.1 and 4.1.2, respectively. The models aim to quantify the daily usage characteristics of different types of EVs within urban settings. Note that heavy trucks are generally excluded from the urban scenario. However, due to the specific requirements of logistic transport, heavy trucks are considered in Sweden's metropolitan cities, namely, Stor Stockholm, Stor Göteborg, and Stor Malmö. The relevant analysis is presented in section 4.1.3.

4.1.1 Urban Car Estimation Model (UCEM)

Based on the classification of city characteristics, an analysis was conducted on the commuting patterns and energy consumption of vehicles in urban areas. The Swedish Bureau of Statistics provides comprehensive data on essential urban metrics, including population, area, registered vehicles, and historical commuting data[46][47]. The method for classifying cities, as shown in table 4.1, follows the guidelines proposed by the SKR[50]. This classification framework allows for a nuanced approach

to understanding commuting and energy consumption dynamics across different urban contexts.

Table 4.1: Classification of Swedish Municipalities

Code	Description
A1	Large cities: Municipalities with a population of at least 200000 inhabitants, with at least 200000 inhabitants in the largest urban area.
A2	Commuting municipalities near large cities: Municipalities where more than 40% of the working population commute to work in a large city or municipality near a large city.
B3	Medium-sized towns: Municipalities with a population of at least 50000 inhabitants, with at least 40000 inhabitants in the largest urban area.
B4	Commuting municipalities near medium-sized towns: Municipalities where more than 40% of the working population commute to work in a medium-sized town.
B5	Commuting municipalities with a low commuting rate near medium-sized towns: Municipalities where less than 40% of the working population commute to work in a medium-sized town.
C6	Small towns: Municipalities with a population of at least 15000 but less than 40000 inhabitants in the largest urban area.
C7	Commuting municipalities near small towns: Municipalities where more than 30% of the working population commute to work in a small town/urban area or more than 30% of the employed day population lives in another municipality.
C8	Rural municipalities: Municipalities with a population of less than 15000 inhabitants in the largest urban area, very low commuting rate (less than 30%)
C9	Rural municipalities with a visitor industry: Municipalities in rural areas that fulfill at least two criteria for the visitor industry, i.e., number of overnight stays, retail-restaurant-hotel turnover per head of population.

The results of the city classification are shown in Figure 4.1. It reveals that higher-level cities are predominantly concentrated in southern Sweden, while Class C cities are more located in the northern region.

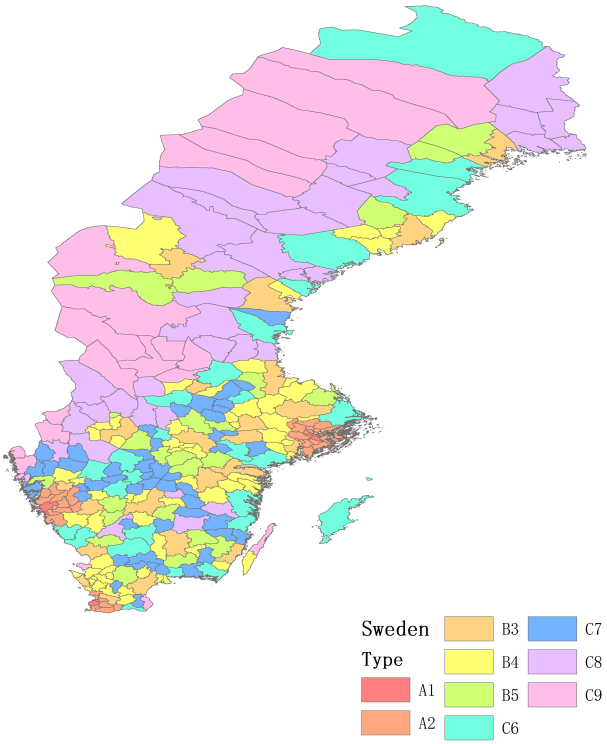

Figure 4.1: City Type in Sweden

After completing the city classification, based on the Annual Passenger Kilometers of Cars published by SCB in Sweden[47], denoted as $X_{Car,i}^{Annual}$, for each city in Sweden, along with the population and the number of cars, the average daily distance traveled per car can be estimated

$$X_{Car,i} = \frac{X_{\mathrm{Car},i}^{Annual}}{N_i} N_{Car,i} \tag{4.1}$$

This dataset provides an accurate depiction of the average daily commuting distance for each city over multiple years. Considering the definitions of city categories, the study assumes that daily average commuting distances within each city type fluctuate within a limited range. By analyzing the historical distribution of these distances, a characteristic value can be derived to represent each city category, as illustrated in Figure 4.2.

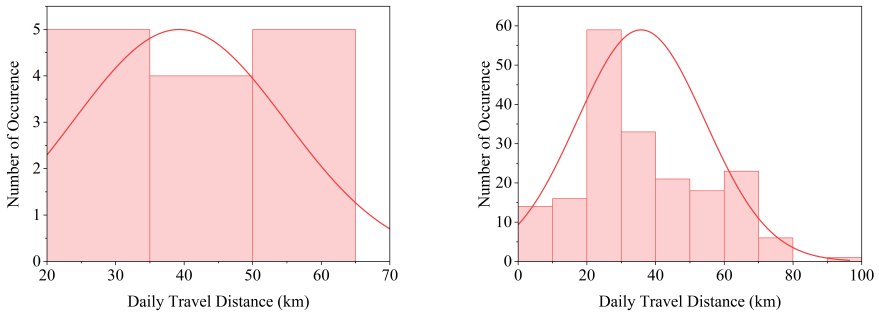

(a) A1 **(b)** A2

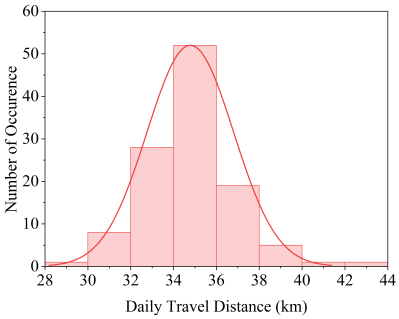

(c) B3

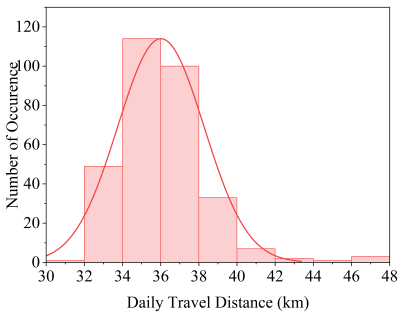

(d) B4

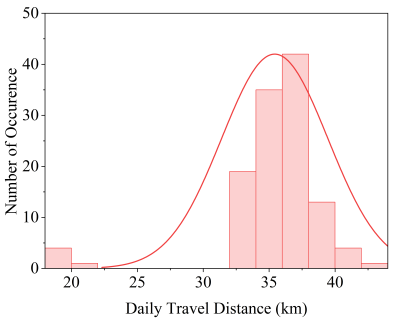

(e) B5

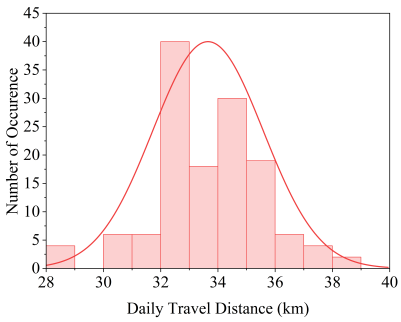

(f) C6

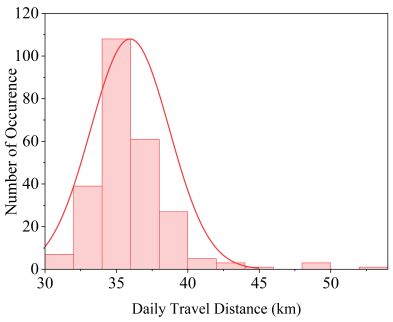

(g) C7

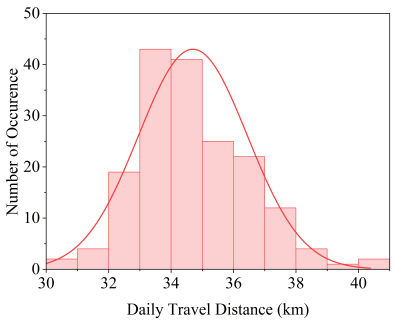

(h) C8

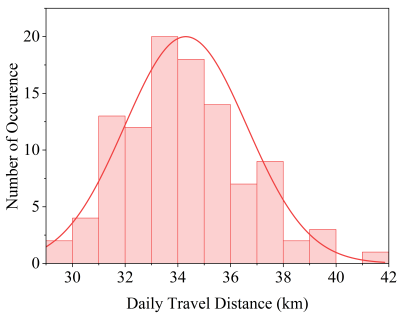

(i) C9

Figure 4.2: Daily travel distance in each type of city, where annual data from SCB[47], the study calculates and sketches the average daily distance from 2019 to 2023 to observe the distribution.

It can be observed that the average daily commuting distance for cities within the same category fluctuates around a specific value. The study identifies the most densely concentrated value within this distribution as the characteristic daily commuting distance for each city category, denoted as . The specific values are presented in Table 4.2.

Table 4.2: Daily Travel Distance in Each Type of Cities, taking the characteristic value according to the historical daily commuting distance distribution of each city

A1	A2	B3	B4	B5	C6	C7	C8	C9
40 km	38 km	35 km	36 km	35 km	34 km	36 km	35 km	34 km

The study also introduces a variable: the commuting rate R_i. Defined as the proportion of a city's commuting population to its total population over a specific time period, the commuting rate reflects the intensity of connections and transportation demand between cities or within metropolitan areas, calculated by

$$R_i = \frac{N_{i,com}}{N_i} \tag{4.2}$$

where $N_i, N_{i,com}$ represents total population and commuting population, respectively. As mentioned in Chapter 3, there is some overlap between urban commuters and long-distance travelers. In order to minimize this effect and avoid double-accumulating energy consumption, the study assumes that only the commuting population follows the average daily travel distance specific to each city category. As for the remaining population, an adjustment factor of 5km per day is applied as a reference. The vehicle energy consumption in a city is then calculated as

$$E_{Car,i} = 0.2kWh/km \cdot X_j R_i N_{Car,i} + 1kWh(1 - R_i)N_{Car,i} \tag{4.3}$$

Calculation results for some Sweden cities are shown in Table 4.3 below. The complete data across Sweden is presented in Appendix A.

Table 4.3: Daily Urban Cars, where number of cars offered by SCB[47], combined with commuting rate derived in research to get the energy demand.

City	Number of Cars	Commuting Rate	Energy Demand (MWh/day)
Stockholm	353523	48.21%	1546.5
Malmö	125388	32.29%	408.8
Göteborg	197528	30.82%	623.7
Upplands-Väsby	19024	52.11%	84.5
Vallentuna	16329	50.44%	70.7
Österåker	22610	39.50%	81.5
Värmdö	19556	42.44%	74.3
Järfälla	31097	53.30%	140.5
Ekerö	12956	41.35%	48.4
Huddinge	38886	66.13%	208.6

The daily energy consumption of cars in various cities in Sweden is visualized,via ArcGIS, as shown in Figure 4.3.

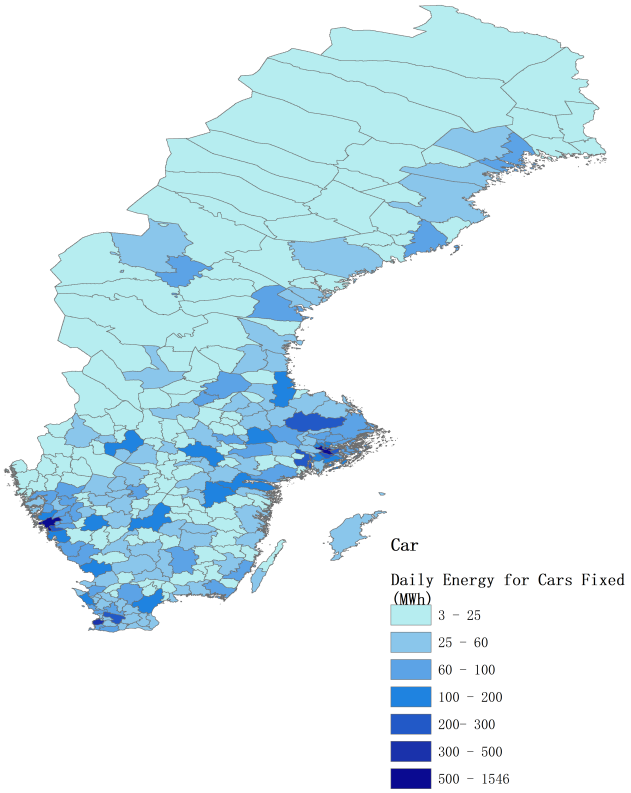

Figure 4.3: Daily Energy Consumption of Cars in City, following UCEM model

4.1.2 Consumptions for Public Transport in City (UUTE)

In analyzing the driving demand and energy consumption of buses within cities, the research proposed the UTEM framework, diverging from the approach used for passenger cars and not relying on historical data. Given that bus operations strictly adhere to transportation planning, estimating urban public transport energy consumption based on official transportation plans provided by Swedish governments proves to be an effective approach. Annual target mileage and the number of buses[47] are then utilized, integrating transportation planning documents from twenty-one Swedish provinces, including Skåne, Västra Götaland, etc.[51-71].

These planning documents offer comprehensive details on the use of public transport for commuting, encompassing route planning, energy consumption design, and other multidimensional factors. Here, a regulatory function is introduced to model the integration of this information.

The average distance traveled per bus in each city can be expressed as

$$X_{Bus,i} = f(X_{Bus,j}^{Annual} \frac{N_{Bus,i}}{N_{Bus,tot,k}} \frac{1}{365}) \tag{4.4}$$

Where,
$X_{Bus,j}^{Annual}$ is the annual mileage of one province.
$N_{Bus,i}$ and $N_{Bus,tot,k}$ are the number of buses in the city and the whole province, respectively.
f is the regulatory function.

Then according to the energy consumption formula, the daily energy consumption of buses in a city can be calculated as

$$E_{Bus,i} = 1.2kWh/km \cdot X_{Bus,i} N_{Bus,i} \tag{4.5}$$

Table 4.4 provides examples illustrating the energy consumption levels associated with urban transit systems. These examples offer insight into the varying energy demands across different public transportation networks within urban areas. The complete data across Sweden is presented in Appendix B.

Table 4.4: Daily Urban Buses Energy Consumption, number of Bus offered by SCB[47], energy demand calculated through model

City	Number of Buses	Energy Demand (MWh/Day)
Stockholm	697	155.8
Malmö	362	65.57
Göteborg	2038	237.26
Linköping	213	34.34
Örebro	38	21.05
Västerås	501	9.37
Helsingborg	246	43.55
Norrköping	159	25.88
Jönköping	79	23.73
Umeå	118	17.84
Vilhelmina	53	8.01
Arvidsjaur	1	1.09
Pajala	11	1.84
Övertorneå	11	1.19

It is worth mentioning that the number of registered buses in Gothenburg far exceeds that in Stockholm, but considering that in actual management the capital lacks sufficient space for parking many public vehicles, it still makes sense to drive to other cities for charging. After calculating the estimated average daily energy consumption for buses across different cities in Sweden, the results are presented in a visual format to provide a clearer comparison and understanding of the data. This visualization, shown in Figure 4.4, highlights regional variations and allows for a more accessible analysis of energy usage trends among urban transit systems in diverse locations.

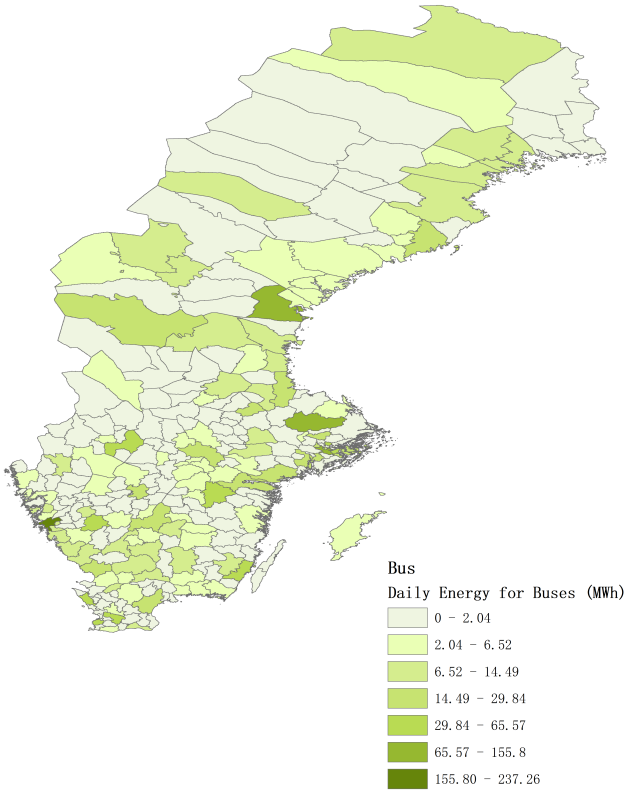

Figure 4.4: Daily Energy Consumption of Buses in City, following UTEM model

4.1.3 Urban Truck Analysis

As explained above, large trucks in cities only operate around Sweden's major urban areas. The study estimates the energy consumption of large urban trucks based on the data from these core urban areas provided by the Statistics Bureau. The relevant data are shown in Table 4.5.

Table 4.5: Travel for Trucks in City

Region	Stor-Stockholm	Stor-Göteborg	Stor Malmö
Number of LGVs	72	33	22
Vehicle Kilometers	1005896	498988	298926
Km per day	83	84	73

Similarly, taking the average energy consumption of a truck as 1.5 kWh/km. Then the result of the daily energy demand for trucks in the city shall be calculated by

$$E_{truck,n} = 1.5kWh/km \cdot N_{Truck,i}x_t \tag{4.6}$$

The figure below shows the corresponding regional truck energy consumption.

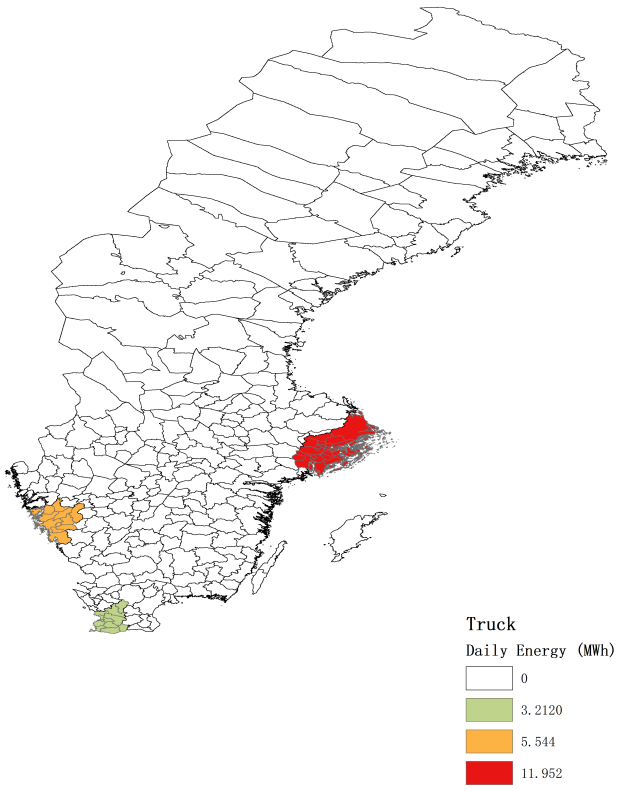

Figure 4.5: Daily Energy Consumption of Trucks in Core Region

4.2 Highway-Long Travel and Energy Consumption

Section 2.2 claimed that employing probabilistic models to quantify the average daily travel distance of vehicles is an effective approach. In urban areas, due to the relative stability of commuting, a classification-based marc-level statistical model is introduced in section 4.1. However, vehicles on highways experience significant variability in travel distances. A more detailed prediction and probabilistic model for accurate depiction is essential for highway analysis. It can be noticed that the Rayleigh distribution is particularly effective in representing a variable positively skewed and constrained to non-negative values. Most occurrences concentrated around a range in the Rayleigh distribution model, aligned with real-highway travel.

The study used the LSTM-GRU model for traffic prediction and simulated the driving distance through the Rayleigh distribution model to complete the energy consumption estimation.

4.2.1 Traffic Flow Prediction

The study identifies the traffic flow in Sweden at first. Sweden Transport Agency provides the average daily traffic flow[38], denoted as ÅDT. Using ArcGIS for visu-

alization, it is evident that traffic volume is significantly higher along the Göteborg-Malmö corridor (E6 highway), and the major roads near Stockholm (E18 and E20 highway). The traffic levels on other Sweden's core highways are also substantially higher than those on standard roads, further validating the rationale for separating urban commuting and highway commuting in the research.

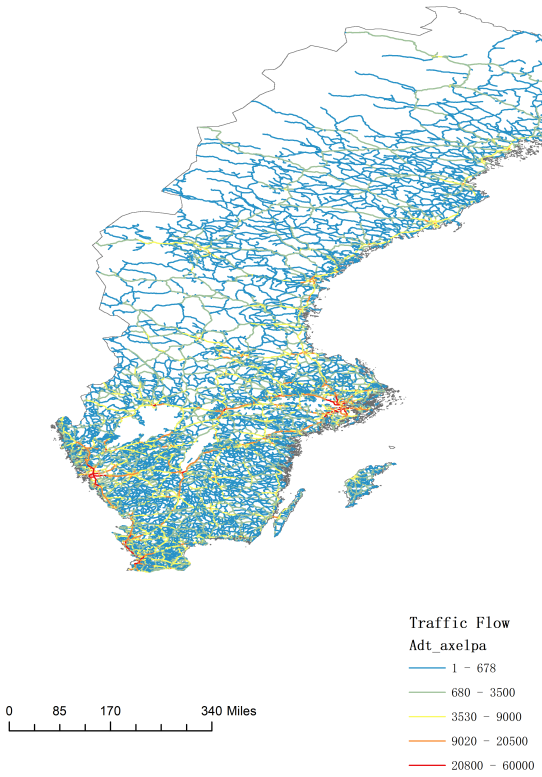

Figure 4.6: Traffic Flow in Sweden, data from Trafikverket[38]

Note that the Swedish Transport Agency does not provide detailed traffic flow data for everyday throughout the year. Instead, measurements are conducted four times annually, with two measurements taken on weekends and two on weekdays. As a result, an average daily traffic flow Å$DT$is derived. Consequently, using the provided average flow data directly for predictive studies presents limitations, as it disregards variations across seasons and months and fails to account for sudden traffic peaks. To address this, the study incorporates a traffic sequence expansion approach, using ÅDT combined with fluctuation provided by the Swedish Transport Agency[38]. Figure 4.7 illustrates traffic fluctuations from 2019 to 2023.

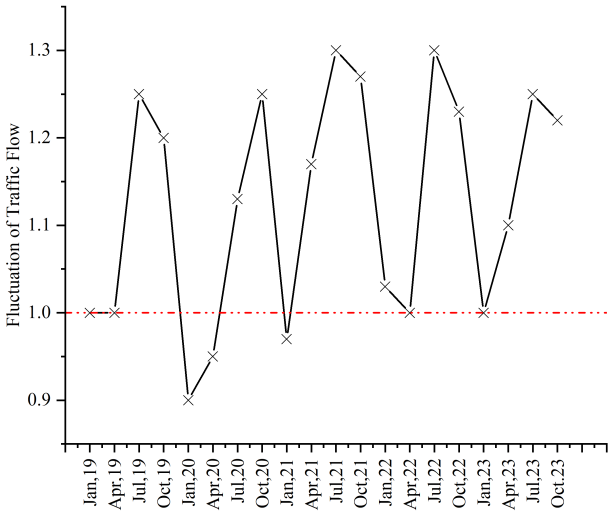

Figure 4.7: Fluctuation of Traffic Flow

This expansion approach mitigates the effects of smoothing out long-term trends, while also capturing short-term fluctuations overlooked by the average flow, thereby enhancing the reliability of the traffic analysis.

Through the expansion, a more detailed traffic series is obtained, allowing for future trend predictions when integrated with a forecasting model. The research addresses both long-term trends in electric vehicle adoption, which are crucial for planning the overall charging network layout, and short-term demand fluctuations, which are essential for guiding demand response on the power grid side. The LSTM-GRU model is particularly well-suited for this dual focus, as it can capture long-term dependencies while remaining sensitive to short-term variations in traffic flow. Additionally, as a non-parametric model, the LSTM-GRU can dynamically adapt to changes in traffic flow, ensuring it is an ideal selection for the predictive need in this research.

A customized LSTM-GRU model is then constructed. The model integrates two LSTM layers, each equipped with gates for memory management, which collectively capture long-term dependencies essential for identifying persistent traffic trends. These dual LSTM layers enable deeper abstraction of long-term characteristics in the data, improving the model's ability to handle complex temporal patterns. The GRU layer is then utilized to focus on short-term variations, adapting to dynamic shifts in traffic flow. Dropout layers are included throughout to prevent overfitting by randomly omitting neurons during training, ensuring robust and generalized learning. Following these layers, a fully connected layer consolidates the extracted features to compute the final output. Finally, a regression layer applies the Mean Squared Error (RMSE) loss function to compare the predicted values with actual values, guiding the model towards greater accuracy. This multi-layered architecture allows the LSTM-GRU model to capture both long-term stability and short-term

fluctuations effectively, making it highly suitable for precise traffic flow forecasting. The structure of the prediction model is shown in Figure 4.8.

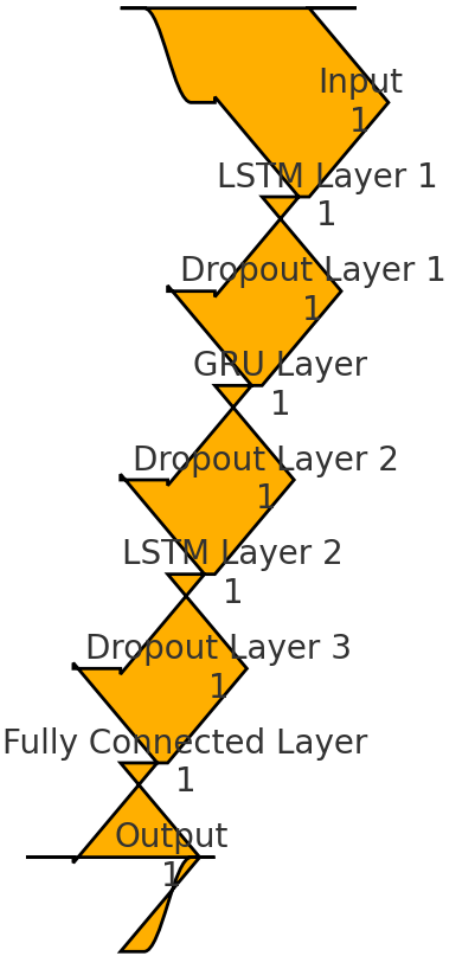

Figure 4.8: Structure of the prediction model

The developed model is subsequently applied to forecast existing traffic flow patterns, enabling an assessment of its predictive accuracy. A comparison between the original observed traffic flow and the model's predicted flow is presented in Figure 4.9.

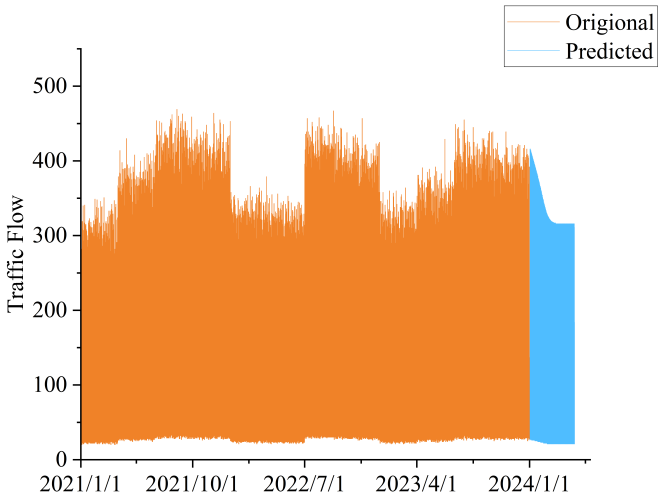

Figure 4.9: Predicted and Original Traffic Flow, a set of historical traffic is randomly selected and presented using the prediction model

Based on the predicted sequence, we can still get a new average flow, denoted as ÅDT'. We select the flow of each core section of Swedish highways and repeat the above prediction process. We compare the new average flow with the original average flow to get Figure 4.10.

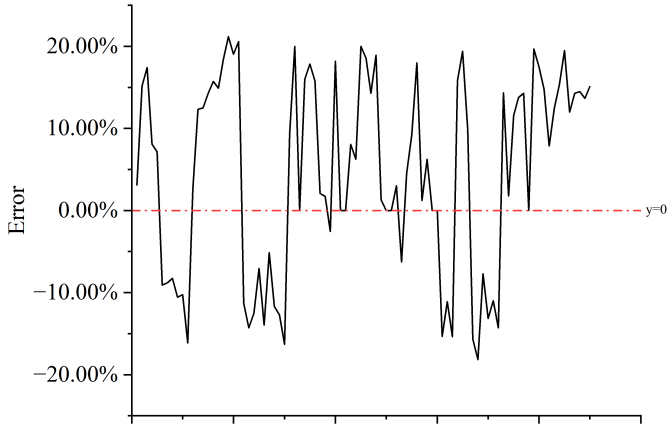

Figure 4.10: Predicted ÅDT compared with historical data

According to the comparison, it can be seen that the historical flow average and the flow average obtained by the research model are basically within an acceptable difference range. It can be inferred that ÅDT can be used as a parameter basis for subsequent energy consumption and site selection.

4.2.2 Energy Consumption for Vehicles along TEN-T

Based on the concentrated distribution characteristics of Rayleigh distribution, the study assumes that the vehicle travel distance on each highway section follows this distribution. The scale factor is one of the most important parameters within

Rayleigh distribution model, and the mathematical expectation of this distribution can be expressed as

$$E(X) = \sigma\sqrt{\frac{\pi}{2}} \tag{4.7}$$

Here, $E(X)$ reflects the average driving distance of the entire fleet. The energy consumption of the entire fleet can be expressed as

$$E = ADT \times E(X) \times e \tag{4.8}$$

where, e is the unit energy consumption. Choosing the proper value of the scale factor σ to realize reliable energy consumption is vital. Stating that different scale factors should be set according to different road sections and periods to ensure the rationality of the expected value of vehicle driving distance. Specifically, the model parameters are calibrated according to the characteristics of highways, as well as the traffic flow patterns at different times of day. The ideas are as follows.

For the quite short road, take the factor $\sigma = 0.8L$.

As for the road bit longer than the short road, taking the scale factor as

$$\sigma = \begin{cases} \alpha_1 L + \Delta, \ daytime \\ \alpha_2 L + \Delta, \ evening \\ \alpha_3 L + \Delta, \ night \end{cases}, L_{short} \leq L \leq L_{medium} \tag{4.9}$$

For the medium-length road, setting the scale factor by

$$\sigma = \begin{cases} \beta_1 L + \Delta, \ daytime \\ \beta_2 L + \Delta, \ evening \\ \beta_3 L + \Delta, \ night \end{cases}, L_{medium} \leq L \leq L_{long} \tag{4.10}$$

For the long-length road, one more smoothing factor is introduced, and the scale factor would be calculated by

$$\sigma = \begin{cases} \gamma_1 L^{\delta_1} + \Delta, \ daytime \\ \gamma_2 L^{\delta_2} + \Delta, \ evening \\ \gamma_3 L^{\delta_3} + \Delta, \ night \end{cases}, L \geq L_{long} \tag{4.11}$$

The above design idea introduces variables such as $\alpha, \beta, \gamma, \delta, \Delta$ to adjust the scale parameters of the Rayleigh distribution model. Moreover, introducing the correction factor Δ prevents the scale parameter from changing suddenly and ensures the prediction results' smoothness. The study follows heuristic rules to set the parameters in scale factor determination for various road types and commuting times, shown in Table 4.6.

Table 4.6: Parameter settled in the Rayleigh distribution model, following the heuristic parameter design concept

Parameter	Car	Truck
L_{short}	10 km	15 km
L_{medium}	50 km	50 km
L_{long}	100 km	100 km
$\alpha = [\alpha_1, \alpha_2, \alpha_3]$	[0.1, 0.15, 0.2]	[0.1, 0.15, 0.2]
$\beta = [\beta_1, \beta_2, \beta_3]$	[0.05, 0.07, 1]	[0.08, 0.12, 0.22]
$\gamma = [\gamma_1, \gamma_2, \gamma_3]$	[0.15, 0.17, 0.2]	[0.4, 0.5, 0.55]
$\delta = [\delta_1, \delta_2, \delta_3]$	[0.7, 0.75, 0.8]	[0.7, 0.72, 0.75]

The variables established based on the above empirical values can be used to determine the Rayleigh distribution scale parameters followed by each road section. The total vehicle energy consumption of the corresponding road section can be calculated according to the formula.The complete energy consumption calculation results for each highway section are presented in Appendix C. Here, taking the Swedish E4 and E45 highways as an example, the energy consumption distribution of each road section is shown in Figure 4.11.

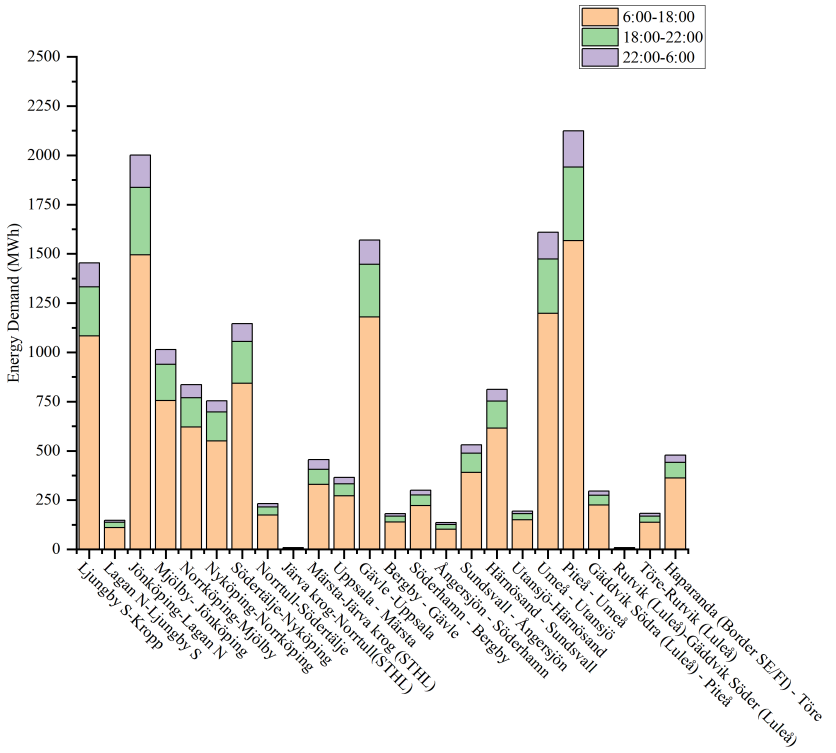

(a) E4

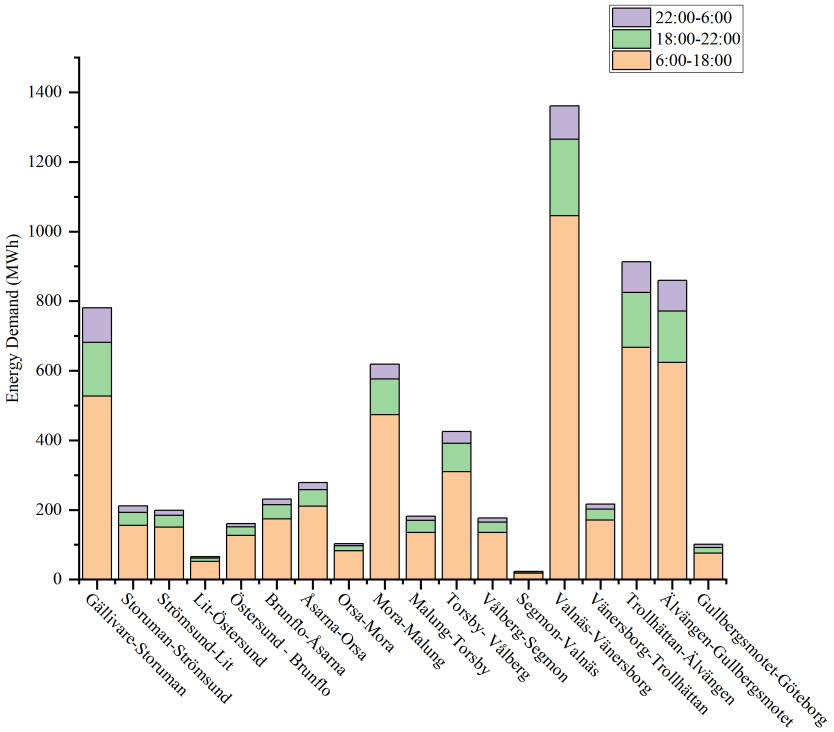

(b) E45

Figure 4.11: Energy Consumption of cars along E4 & E45 highway, calculated through the proposed Rayleigh distributed energy consumption framework

4.3 Verification of the Energy Consumption Result

This study provides preliminary energy consumption estimates for urban commuting and highway traveling in Sweden. Then the verification of these results will be illustrated based on geographical location and traffic data. In the city, the energy consumption per unit area is obtained by dividing the total energy consumption of each city, as shown in Section 4.1, by the area of the city[45]. According to the real society, areas with relatively higher energy consumption per unit area are expected to be concentrated in southern Sweden, especially in the core urban areas. The visualization results of unit area energy consumption are shown in Figure 4.13.

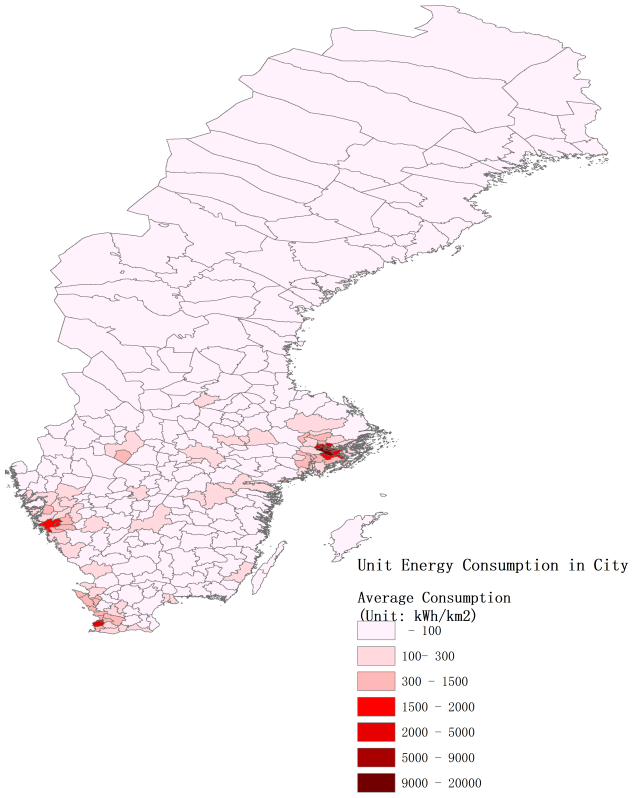

Figure 4.12: Unit Energy Consumption in City (kWh/km^2), in which energy consumption in the city is calculated by the UCEM UTEM model proposed

The figure shows that areas with significantly higher energy consumption per unit area are mainly located in southern Sweden. This pattern is particularly evident in major urban and industrial centers such as Stockholm, Gothenburg, and Malmö, where population density and industrial activity drive up energy demand. The results of the calculations are well aligned with observed real-world facts, confirming the robustness and validity of the model for energy consumption in urban areas. It also shows that the model is well suited to capture the spatial distribution of energy demand in different parts of Sweden.

Parallel validation was also carried out in the case of highway driving using a similar averaging method to ensure the accuracy of the model under different driving conditions. Specifically, the energy consumption per unit length was calculated by dividing the total energy consumption by the length of the individual roadway segments, resulting in a value in kWh/km. This energy consumption per km is then analyzed along with the traffic flow per unit length to identify any consistent trends or correlations. This approach allows for a detailed assessment of energy consumption patterns specific to freeway traffic, validating the model's application to high-speed, long-distance travel scenarios. As an example, the E4 freeway is shown in Figure 4.13.

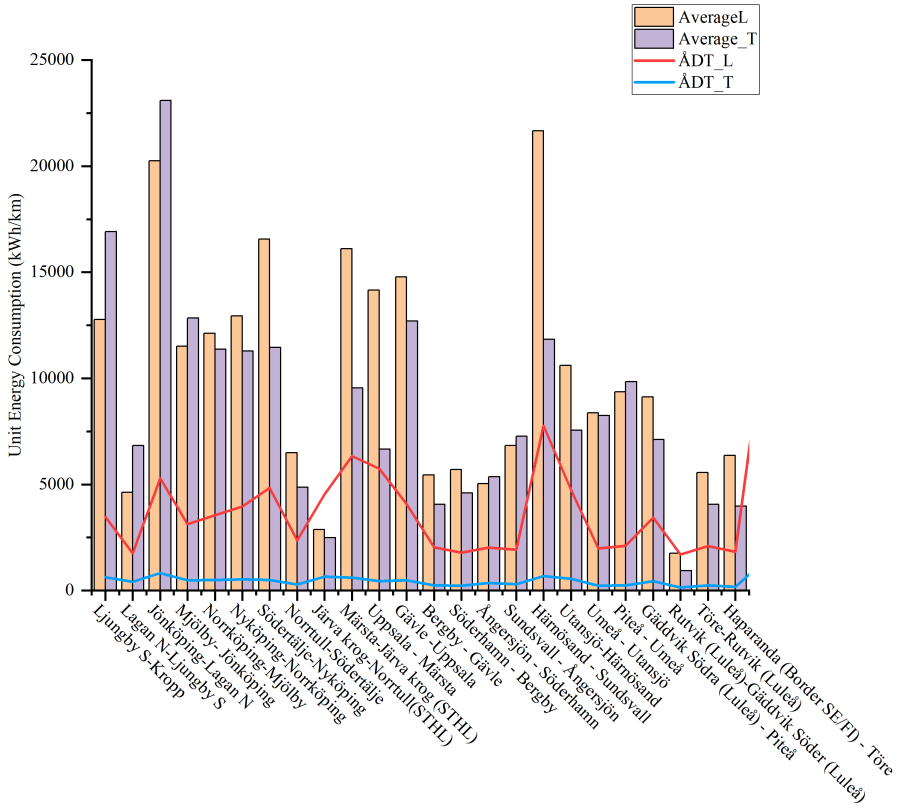

Figure 4.13: Compare Unit Energy Consumption with Traffic Flow along E4, in which the energy consumption data of each road section is calculated by the Rayleigh distribution assumption model proposed

The results indicate a certain correlation between the unit energy consumption of the E4 highway and the trend of unit traffic flow. To further validate the findings, distribution maps of unit energy consumption and unit traffic flow for highway sections throughout Sweden were generated, as shown in Figure 4.14.

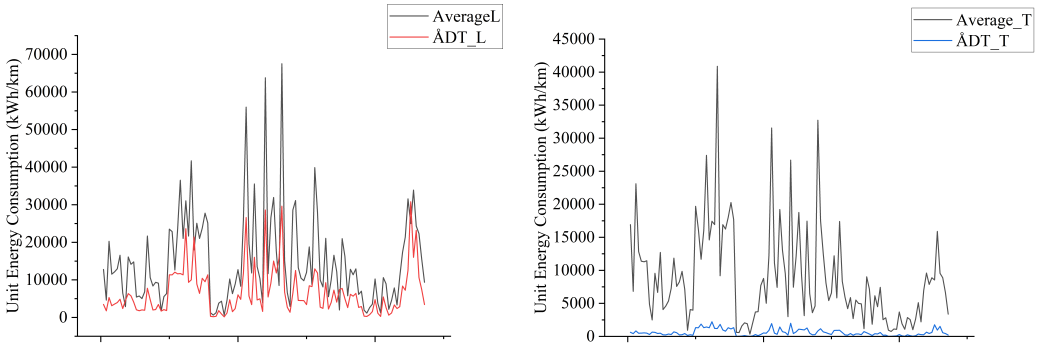

(a) Light Cars **(b)** Trucks

Figure 4.14: Comparison of Unit Energy Consumption and Traffic Flow, presenting all consumption per unit length and traffic flow per unit length within Swedish highways

It shows that the average energy consumption of cars and trucks is highly consistent with the average traffic flow trend, which also proves the rationality of the Rayleigh distribution estimation approach.

To sum up, this chapter classified EV users into urban commuters and highway travelers. A macro-level historical data was used for urban flow prediction, and the UCEM and UTEM models were developed to estimate the daily energy consumption for passenger cars and buses within cities. Additionally, urban truck usage was considered in the core city based on foundational data. As for highways, an LSTM-GRU model and a Rayleigh distribution-based energy consumption estimation model were constructed to achieve accurate flow prediction and energy consumption estimation for highway travel. Validation of the model's accuracy was implemented by normalizing energy consumption results and comparing them with real-world conditions. This chapter provides a robust framework for predicting travel patterns and energy consumption distribution of electric vehicle users, establishing a data and model foundation for the subsequent chapters on charging infrastructure planning and grid impact assessment.

5

Analysis II
Positioning of Charging Facilities

With the average daily energy consumption data of urban and highway settings obtained, this chapter will focus on proposing targeted charging station site selection strategies. First, in Section 5.1, the charging infrastructure standards proposed by the EU will be introduced. Section 5.2 addresses charging stations within cities. Since site selection in urban areas is highly constrained by urban structure, a qualitative analysis is conducted to determine the positioning scope. Section 5.3 covers the construction of charging stations along highways. It establishes an optimization algorithm to conduct a quantitative analysis of the site selection and combines the road topology and user cost to calculate the optimal construction location. Section 5.4 introduces assumptions of the initial SoC, determining the ratio of EVs that need to charge via the Monte Carlo process, and specifying the charging facilities along the highway.

5.1 Identify the Charging Facilities

According to the Masterplan on the construction of electric vehicle charging facilities released by the European Commission[31], electric vehicle charging facilities can be divided into nine categories, as shown in Table 5.1.

Table 5.1: Type of Charging Points, defined by EU

Power	Charging Efficiency	Description
AC 3.7kW-7.4kW	80-85%	Home Charge
AC 11kW	85-90%	Community
AC 22kW	92%	
DC 25kW	92%	Fast Charge, especially in commercial areas and along highways
DC 50kW	93%	
DC 100kW	94%	
DC 150kW	95%	
DC 350kW	96%	
DC 500kW	97%	

Meanwhile, the EU has put forward suggestions on the number ratio of charging

ports for each model in the Masterplan[31], as shown in Figure 5.1.

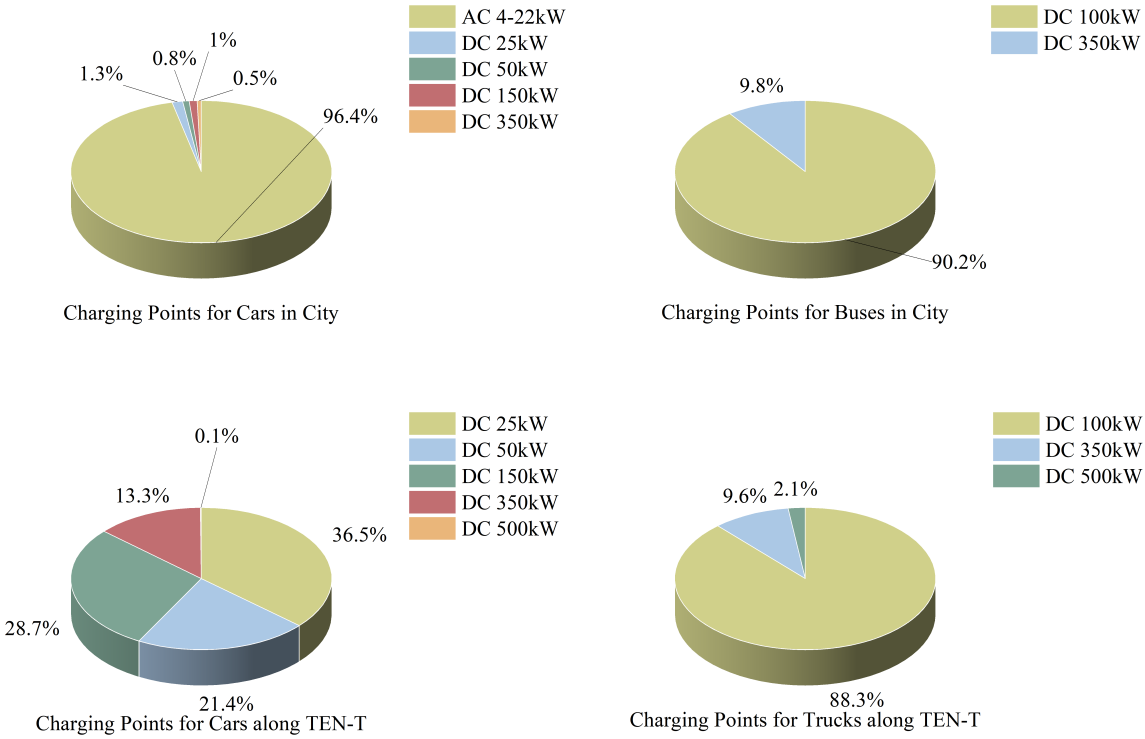

Figure 5.1: Ratio of different Charging Points, according to the abstracted descriptions from EU documents

This recommended ratio details the location of charging points for cars and buses in the city, as well as cars and trucks along highways. Subsequent research will refer to this ratio and optimize the solution in combination with energy consumption requirements.

5.2 Charging Points in City

In the city, the charging behavior of EV users can be characterized by high-frequency, low-power slow charging, and patterns influenced by working behavior. Generally, charging scenarios are mainly concentrated in residential, communities, transportation hubs, and commercial zones. Home charging, also denoted as residential charging, usually uses low-power AC slow charging of 3.7-7.4kW. The number of such charging stations should be consistent with the number of single-family or townhouses in Sweden, constrained by a reasonable layout regulation. The main usage period for home charging is concentrated after getting off work until the next day.

Community charging primarily serves apartment residents and relies on AC slow charging as well, with its usage times aligning with home charging. Charging in commercial zones, catering to consumers, utilize DC fast charging equipment during business hours. Moreover, charging facilities at public transportation hubs serve

buses, which require a full charge after a range of driving. Their daily occupancy time coincides with the operation time of buses.

The study summarizes the use time of relevant scenarios in Table 5.2 below.

Table 5.2: Charging scenarios and corresponding operating period

Charging Scenarios	Operating Periods
Home	15h/day
Community	15h/day
Commercial zones	8h/day
Transportation Hubs	20h/day

The study assessed charging station usage across various scenarios to understand demand patterns and infrastructure needs. By integrating these findings with the average daily energy consumption results for each city, as established in Section 4.1, determining the required number of charging facilities becomes a straightforward allocation task.

The allocation can be calculated using the following approach, ensuring that infrastructure aligns with projected energy needs and usage rates in each scenario, expressed as

$$\begin{cases} E = \sum_{m}^{All} P_m N_m T_m \eta_m \\ N_m = \rho_m \times \sum N_m \end{cases} \tag{5.1}$$

Where:
N_m is the number of charging points of a given type,
T_m is the daily operating time,η_m is the charging efficiency,
ρ_m is the ratio of charger type m.

The calculation of the number of charging points for each type across different cities was conducted to understand the distribution and availability of charging infrastructure. The results of these calculations are detailed in Table 5.3, providing a comprehensive view in charging point types and quantities across urban areas.

Table 5.3: Charging Points in City, energy demand derived in Chapter 4, number of facilities calculated through formula 5.1

	AC			DC			
City	3.7-7.4kW	11kW	22kW	25kW	50kW	150kW	350kW
Bleking	1399	448	391	541	270	142	263
Dalarna	4615	726	825	1493	746	150	614
Gävleborg	2838	655	599	882	440	466	410
Gotland	247	98	77	93	47	57	50
Halland	1571	1587	923	451	220	416	490
Jämtland	2687	270	317	584	296	118	239
Jönköping	3373	1047	903	1234	615	771	608
Kalmar	3643	487	617	1202	602	135	473
Kronoberg	2258	503	498	800	398	356	353
Norrbotten	4287	463	497	854	433	386	368
Örebro	3361	971	799	1017	509	437	524
Östergötland	3509	1506	1041	956	477	175	622
Skåne	8075	7645	4673	2879	1412	432	2528
Södermanland	1970	930	676	695	346	169	418
Stockholm	4144	19358	9914	1170	507	273	4453
Uppsala	1946	1432	928	708	349	153	526
Värmland	4903	691	786	1418	711	166	585
Västerbotten	4851	438	438	709	363	245	321
Västernorrland	2042	532	469	653	326	246	317
Västmanland	2441	982	728	777	387	34	453
Västra Götaland	13380	8411	5516	4367	2160	833	3144

The locations of charging points were plotted on the map, as illustrated in the accompanying figure. In this representation, each marked point corresponds to a cluster of 100 charging points, providing a clear visual overview of the spatial distribution and density of charging infrastructure across the area. This approach allows for an efficient assessment of coverage and highlights regions with higher or lower concentrations of charging facilities. The specific data for each city are presented in Appendix D.

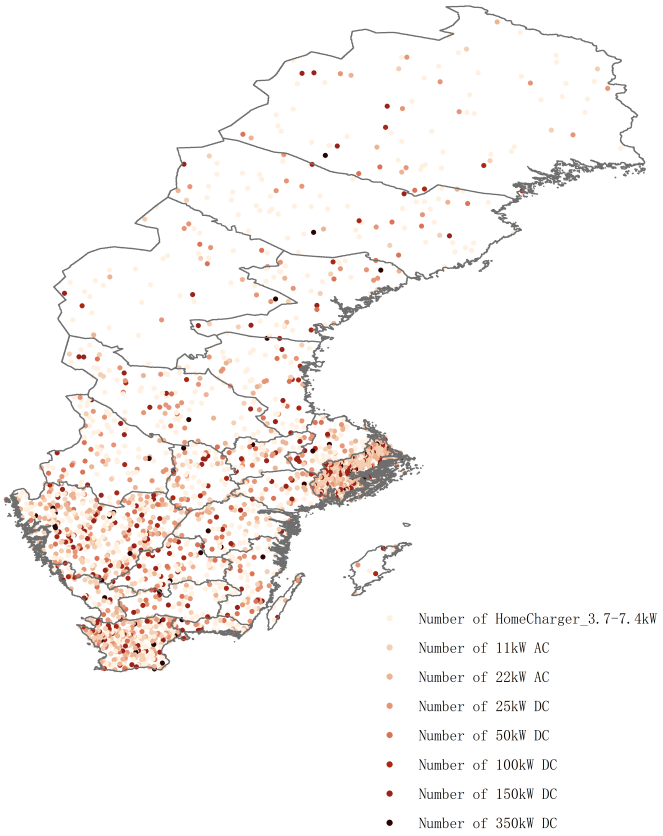

Figure 5.2: Charging Points in City in Sweden, derived by model proposed

It indicates that densely populated cities in southern Sweden require a tremendous number of charging facilities to support daily commuting needs. High-power charging stations are widely utilized in areas around Gothenburg, Jönköping, and Stockholm. In contrast, only a limited number of high-power charging stations are installed in Norrbotten County.

5.3 Charging Stations along Highway

In contradict to urban charging stations, which are typically built within residential buildings, public parking lots, and other infrastructure, highway charging stations are generally constructed along the route. Selecting optimal locations along the highway requires a comprehensive evaluation of factors such as traffic flow at different times, location, and utilization rates. This section will employ multi-objective planning and topological analysis to determine the most suitable locations for charging stations along highways.

5.3.1 Selection of Charging station based on SA

The research first needs to establish a method to quantify the key metrics in the positioning process, and then establish a model to solve multiple objectives problem. The simulated annealing algorithm is particularly advantageous for solving multiple

objective cases due to its ability to effectively explore a vast solution space and escape local optima, thereby enhancing the likelihood of finding a global optimum. It is also crucial in complex scenarios with multiple competing objectives, as it allows for a balanced solution that meets diverse requirements. Following this, the study will introduce the objective function and the specific settings for the simulated annealing algorithm to guide the highway charging station placement.

5.3.1.1 Objective function

Multiple parameters are introduced to quantify the impact of charging station location selection, where $\alpha, \beta, \gamma, \lambda, \varepsilon, \sigma$ are weight coefficients and are dynamically adjusted according to actual needs. L_n represents the length of a specific road, and $ADT_t(n)$ refers to the traffic flow within a road during period t.

Firstly, the study establishes a traffic flow balance parameter, denoted as f_{fl}, aiming at prioritizing the placement of charging stations in high-traffic zones with greater charging demand. It can be expressed as

$$f_{fl} = \text{Flow}_{\text{Capture}} = \alpha \times \sum_t \left(\frac{ADT_t(n)}{1 + |x - 0.5L_n|^{\lambda}}\right) \tag{5.2}$$

Then the section length balance factor f_{le} is introduced. Given that the endpoints of a road represent cities, long-distance drivers are more likely to charge along routes after driving a bit long distance. It encourages charging stations to be positioned close to the midpoint of the section, in other words, as far as possible from the city. Relevant factor can be determined by

$$f_{le} = \text{Length}_{\text{weight}} = \beta \times \left(1 - \frac{x}{L_n}\right) \tag{5.3}$$

Similarly, a time balance factor, denoted as f_t, is introduced to balance peak and non-peak flow, ensuring efficient utilization of charging stations. Time balance factor is calculated as

$$f_t = \text{Time}_{\text{balance}} = \gamma \times \sum_t \left(w_t \times \frac{ADT_t(n)}{1 + |x - 0.5L_n|^{\lambda}}\right) \tag{5.4}$$

Finally, a boundary penalty parameter f_p is settled to discourage stations locating at extreme positions. For example, the endpoints are often less effective since most vehicles are either entering or leaving the city, so lower charging requirements here. Expressed as

$$f_p = \text{Penalty}{=}\delta \times \left\{\frac{1}{1 + e^{-\varepsilon(x - 0.1L_n)}} + \frac{1}{1 + e^{-\varepsilon(1 - 0.1 - \frac{x}{L_n})}}\right\} \tag{5.5}$$

Notably, when designing these parameters, the study applies a monotonicity principle common in mathematical modeling. It implies that larger parameter values reduce the likelihood that the proposed station location will meet optimal requirements for usage rate and traffic flow, guiding the algorithm towards locations with

higher alignment to demand patterns. Combining the above parameters, the multi-objective planning function is expressed as

$$\min(f_{fl} + f_{le} + f_t + f_p) \tag{5.6}$$

The above variables involve some weight coefficients. Similarly, this study sets the initial values based on heuristic theory. The specific parameters are shown in Table 5.4.

Table 5.4: Weighted coefficients in the objective function

Weight coefficient	Cars	Truck
α	0.5	0.5
β	0.3	0.4
γ	0.2	0.1
δ	10	2.1

5.3.1.2 Constraints in the Simulated Annealing Algorithm

After constructing the objective function, certain constraints must also be incorporated into the simulated annealing algorithm, to ensure that the generated charging station locations meet practical requirements. These include legality, which ensures that the locations of charging stations fall within the effective range of the road segment. Additionally, appropriate spacing between charging stations is essential. EU guidelines stipulate that charging stations for cars should be no more than 60 km apart, while those for heavy trucks should be spaced no more than 100 km apart[35]. Finally, a minimum distance constraint is set between charging stations and the boundaries of the section, assumed here to be 5 km. So, the constraints can be expressed as

$$\begin{cases} 0 \leq x \leq L \\ \min_{dis} \leq |x_{i+1} - x_i| \leq \max_{dis} \\ \min_{bd} \leq x \leq L - \min_{bd} \end{cases} \tag{5.7}$$

5.3.1.3 Settlement of SA Algorithm

After constructing the objective function and constraints, further configuration of the simulated annealing algorithm is required. In each iteration, the algorithm slightly perturbs the charging station location, generating new candidates randomly near the current solution. The algorithm then calculates the 'score' of the new solution based on the objective function, incorporating factors such as traffic flow capture, section length balance, time balance, and boundary penalties. If the new solution outperforms the current one, it is accepted directly; if slightly inferior, it is accepted with a certain probability of maintaining diversity and exploration capacity. As the temperature gradually decreases, the acceptance probability of suboptimal solutions also decreases, allowing the algorithm to converge to a global optimum and thus determine the optimal charging station locations.

The study sets specific parameters for the algorithm. Setting the initial temperature to 1000 to explore a broad solution space at the outset, and the final temperature settled to 1 to allow stable convergence of the solution. The cooling rate is then defined as 0.95 to ensure a gradual temperature decrease, enhancing convergence in the later stages. The maximum number of iterations per temperature is 500, ensuring sufficient exploration at each temperature level. Using Sweden's E4 highway as an example, the model calculates the optimal locations of charging stations along each section, as shown in Figure 5.3.

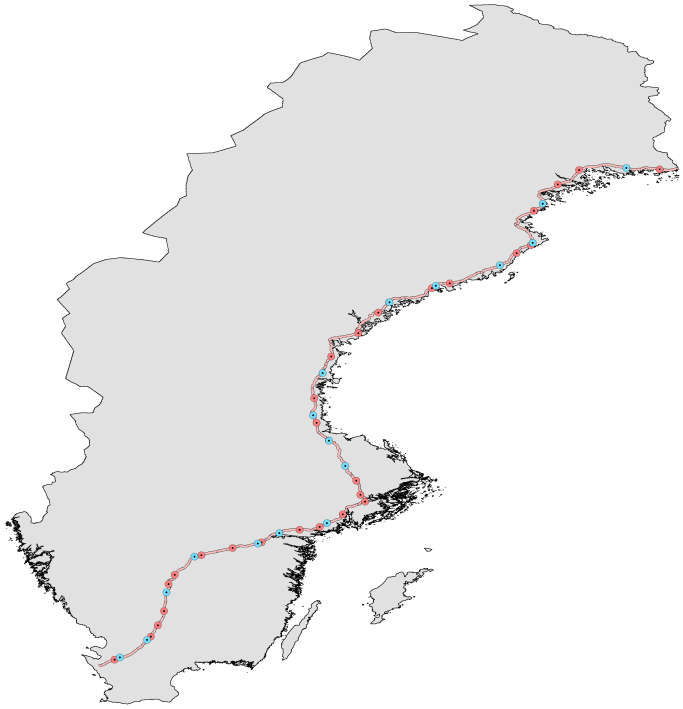

Figure 5.3: Charging Station along E4, red point refers to charging stations for cars, blue points represent charging stations for trucks

5.3.2 Global Optimization of the Charging Station

The model behaved well in single highway analysis, as it treats charging station placement as a one-dimensional, isolated system strategical problem. However, when expanding to Sweden's entire highway network, addressing highway intersection points becomes essential and inevitable. Additionally, as Sweden's highway system is not a closed network, terminal points, such as border locations with neighboring countries, must be reconsidered.

This section aims to propose a comprehensive optimization plan that, based on bilateral user cost and policy considerations, integrates a road topology model to optimize key nodes, thereby enabling a more adaptable charging station deployment across the network.

5.3.2.1 National Border

Pricing poses a significant consideration, as electric vehicle users naturally tend to favor charging stations that offer lower costs. Recognizing this trend, the company Mer has provided an approximate overview of charging costs for users across Scandinavian countries, offering insights into regional pricing variations. This information, with specific data outlined in Table 5.5, helps to highlight cost differences that may influence charging behavior and station preference among users.

Table 5.5: Charging Price in Nordic Countries, according to Mer[37]

	Slow Charger	**Rapid Charger**	**High Power Charger**
Sweden	4.79 SEK/kWh	5.99 SEK/kWh	5.99 SEK/kWh
Norway	4.79 NOK/kWh	5.99 NOK/kWh	5.99 NOK/kWh
Finland	0.29 EUR/kWh	0.39 EUR/kWh	0.39 EUR/kWh
Denmark	3.5 DKK/kWh	3.5 DKK/kWh	3.69 DKK/kWh

The table clearly shows that charging costs in Denmark are slightly higher than in Sweden. Therefore, it is a promising option to load a charging station on the E65 highway at the Swedish-Danish border.

Note that cargo clearance procedures are faced by large trucks. For Norway, as a non-EU country, the transportation of goods from Sweden is subject to customs clearance. These trucks are required to make a customs declaration and undergo possible inspections when crossing the border. Waiting times for clearance at the border vary depending on the situation, but in general, during peak hours (e.g. weekday mornings and evenings) there may be a wait of one to two hours. Meanwhile, Denmark and Finland, same as Sweden, are also part of the EU Single Market and Customs Union, which means that there is no need for customs clearance procedures when goods are transported between these countries. Based on this argument, it is also a credible option to add charging stations specifically for large trucks at the Norway-Sweden border to facilitate waiting in queues.

5.3.2.2 The intersection of Highway

From a transportation network perspective, interchanges play a critical role, functioning as key nodes within the broader network structure. By applying network analysis methods, the significance or centrality of these nodes can be quantified, allowing for an assessment of their strategic importance. This analysis serves to validate that intersections are indeed optimal locations for establishing charging stations, supporting efficient connectivity and accessibility within the network.

To create a comprehensive road network topology model, the research define the intersections along highways as nodes, represented as

$$V = \{v_1, v_2, ..., v_n\} \tag{5.8}$$

Then, define the roads of the highway as edges, represented as

$$E = \{e_1, e_2, ..., e_m\} \tag{5.9}$$

The structure of Sweden's high-speed transportation network can be visualized by defining edges and nodes that represent the connections and intersections across the system. This topology, which captures the spatial and structural relationships within the network, is illustrated in Figure 5.4.

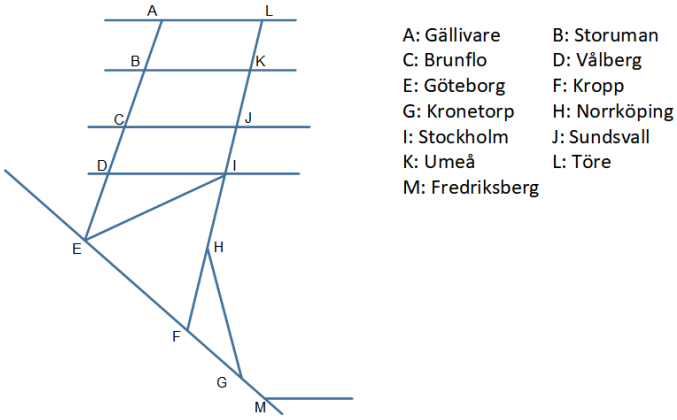

Figure 5.4: Topology Graph of TEN-T

After completing the establishment of the topological structure, the adjacency matrix needs to be defined. Here, the study summarizes the significant data of each road section, including traffic flow, section length, etc., as shown in Table 5.5.

Table 5.6: Parameters of road topology

From	To	Distance (km)	Traffic Flow (Car)	Traffic Flow (Truck)
A	B	404.03	46956	2413
B	C	293.67	20308	4563
C	D	565.42	202109	14401
D	E	215.37	378180	25549
E	F	205.57	697845	82858
F	G	58.38	226125	27411
G	H	462.67	677412	47645
H	I	163.2	216699	25189
I	J	354.06	380306	44988
J	K	247.76	252970	26620
K	L	264.65	199615	23982
L	A	171.81	17280	2707
K	B	254.84	81185	3940
J	C	174.65	90140	6472
I	D	366.09	1021361	87338
I	E	433.69	872863	104030
H	F	401.43	628184	80716
M	G	10.1	39131	4447

Correspondingly, considering the car and truck flow and the length of each road segment, the weight coefficient is set to

$$w_{ij}(t) = \frac{\alpha_L T_{ij}^L(t) + \alpha_H T_{ij}^H(t)}{d_{ij}} \tag{5.10}$$

The weighted adjacency matrix for the graph would be

$$A_{ij}(t) = \begin{cases} w_{ij}(t), edge \\ 0, no\_edge \end{cases} \tag{5.11}$$

After completing the construction of the adjacency matrix, the key nodes can be studied using matrix-specific research methods. Eigenvector centrality measures the influence of a node within the network, which can be calculated as

$$C(v_i) = \frac{1}{\lambda} \sum_{v_j \in V} a_{ij} C(v_j) \tag{5.12}$$

The centrality index of all nodes can be calculated, as shown in Figure 5.5.

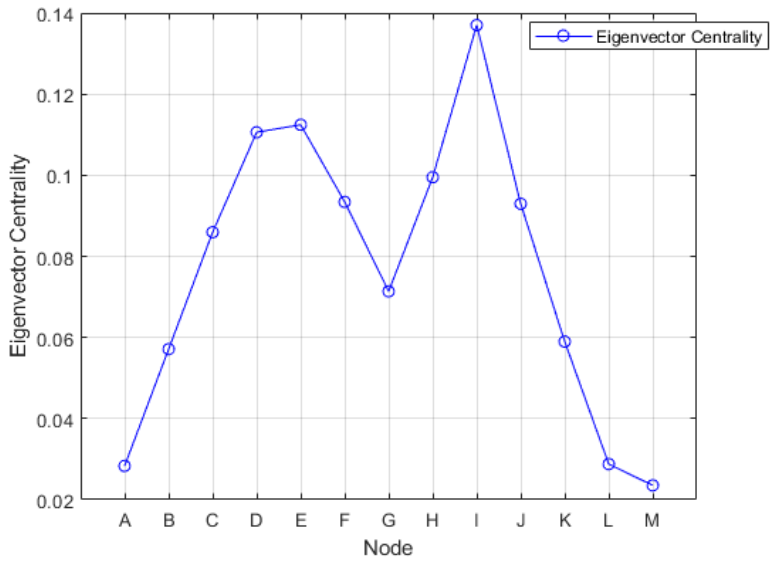

Figure 5.5: Importance of nodes quantified by Eigenvector Centrality

Eigenvector centrality, as an effective method for measuring node importance, assigns higher scores to nodes connected to other important nodes, aiding in identifying core or bridging nodes within complex networks. According to Figure 5.5, there are relatively few nodes with centrality values above 0.1, and these nodes exhibit significantly higher centrality than others. Therefore, nodes D, E, H, and I are considered particularly important in the topology of this study.

Relying solely on matrix-vector centrality to determine node importance can easily overlook nodes that play a critical role in maintaining the overall connectivity of the

network. Therefore, a connectivity-based approach to assess system robustness is introduced. By simulating node failures and observing changes in network connectivity, the impact of each node on the overall network structure can be evaluated, helping identify nodes that are essential for sustaining network robustness. Let the graph after removing node v_i expressed by

$$G' = G - v_i \tag{5.13}$$

Compute the size of the largest connected component before and after removal, which is the relative connectivity

$$\mathrm{RC}(\mathrm{v}_i) = \frac{\left|C_{\max}(G')\right|}{|C_{\max}(G)|} \tag{5.14}$$

The robustness test results of each node are presented in Figure 5.6.

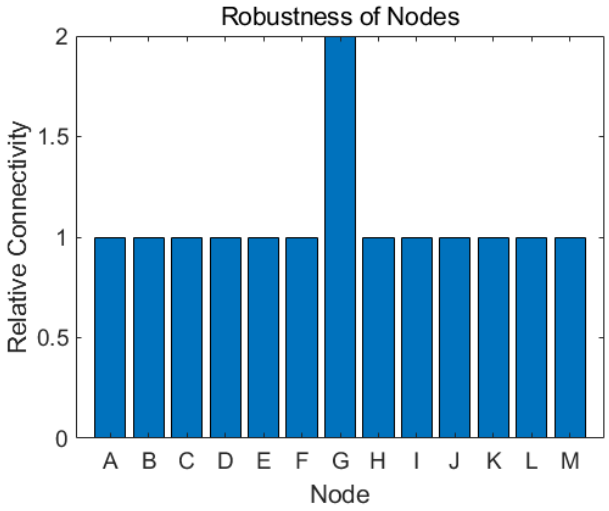

Figure 5.6: Robustness of all nodes, proving node G as a key point

Building on the charging station placement calculations from the simulated annealing algorithm, this study incorporates factors such as eigenvector centrality within the network topology, node impact on system robustness, and constraints related to user costs and freight policies at national borders. Together, these considerations optimize and present the distribution of charging stations across Sweden's highways, as shown in Figure 5.7.

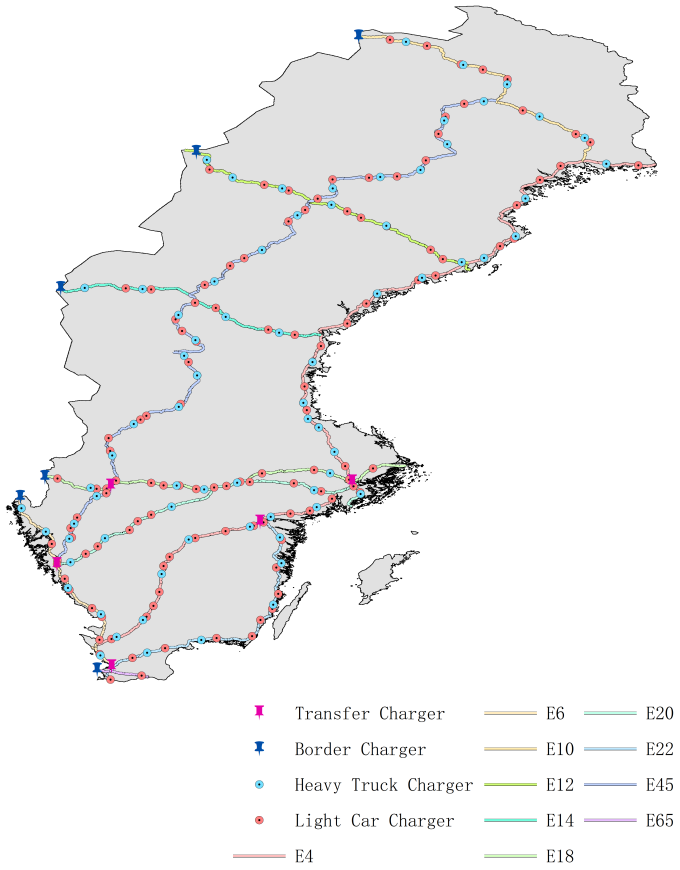

Figure 5.7: Charging Stations along Highway, proposed by Simulated annealing model and Global Optimization illustrated in Section 5.3.2

The figure above provides a comprehensive illustration of the strategic approach developed in this study for optimal siting of charging stations along various highways in Sweden. In this layout, red dots indicate designated car charging stations that are strategically located to support EV traffic on major traffic routes. Blue dots mark the locations of charging stations designed specifically for trucks to meet the unique energy needs and longer travel distances of heavy-duty vehicles. In addition, blue pins mark supplementary charging stations located at national borders to ensure that cross-border trucks have easy access to charging facilities before entering or leaving Sweden. Meanwhile, pink pins indicate additional charging stations located at key highway intersections where traffic density and route convergence place higher demand on charging infrastructure.

5.4 Energy of Charger along Highway

Different from the qualitative analysis of charging in the city, this section will introduce the SoC hypothesis of vehicles traveling along the highway. Combined with the Rayleigh model proposed in Section 4.2.2, Monte Carlo analysis is performed on the vehicles on each road section to determine the remaining SoC at the end of the trip and analyze the charging behavior.

Specifically, assuming that the initial SoC is 20%-100%, and the random variable is given by Beta distribution, expressed as

$$\mathrm{SOC}_{ini} = 20 + x(100 - 20) \tag{5.15}$$

where $x \sim \beta(2, 8)$, random value by beta model. Section 4.2.2 sets the travel distance $X(\sigma)$. Then the SoC when stop driving can be expressed as

$$\mathrm{SOC}_{end} = \mathrm{SOC}_{ini} - \frac{X}{\dot{X}} \tag{5.16}$$

where $\dot{X}$ is the full driving distance of a general electric vehicle, and the ratio to the driving distance can represent the SoC consumed. According to the charging habits of users, it is considered that charging on the highway will only be done when SoC is less than 20% when stopping driving, which is recorded as a charging event. Then the Monte Carlo process can be applied, which is repeating the initial SoC-driving distance-final SoC test for all vehicles on a road section. The proportion of vehicles that need to be charged can be determined as

$$r = \frac{\mathrm{Ch\,arg\,e\_Event}}{\mathrm{Total}} \tag{5.17}$$

Combined with the vehicle energy consumption of the road section determined in Section 4.2.2, as shown by Formula 4.8, the charging energy consumption on a road can be determined by

$$E_{char} = E \cdot r \tag{5.18}$$

In a similar approach, by integrating the proportion of charging points required for each vehicle model with the specific energy demands of each highway segment, a comprehensive scheme for installing charging points along Sweden's highways was developed, as shown in Table 5.6.

Table 5.7: Charging Points along Highway, the number of charging stations determined by the simulated annealing model and topographical optimization. Charging energy is determined by Monte Carlo process, according to formula 5.15-5.18. Using formula 5.1 to get the number of chargers

	Charging Station		Number of Charger					
Highway	Light	Heavy	25kW	50kW	100kW	150kW	350kW	500kW
E4	36	17	282	165	522	233	173	40
E6	9	6	227	133	432	183	135	19
E10	8	6	9	6	18	10	9	6
E12	9	7	29	17	34	24	17	4
E14	6	5	35	20	42	28	20	4
E18	10	6	73	43	83	60	42	12
E20	11	6	207	122	473	165	131	20
E22	13	5	69	41	45	50	38	14
E45	37	19	104	64	115	89	64	22
E65	2	1	8	4	3	6	5	3

In terms of quantity, the density of charging equipment required along highway charging stations seems to be relatively high, but considering the future scenario of full electrification of transportation, high-density coverage of charging facilities is somehow reasonable.

This chapter refined the layout of urban charging facilities to align with city infrastructure. As for highways, a simulated annealing model was established using multi-parameter quantification to assess various influencing factors, coupled with key node analysis based on highway topology. This approach ultimately defined a comprehensive highway charging station placement plan. The setting of charging stations proposed in this chapter provides a solid foundation for power system evaluation.

6

Analysis III
Consequence on the Power System

In previous chapters, the study focused on estimating traffic flow and energy consumption and selecting charging station locations for urban and highway scenarios. This chapter further integrates the division of Sweden's power regions to evaluate the energy supply and demand balance across these areas. By applying Monte Carlo analysis and incorporating power market information, this section aims to assess the impacts of transportation electrification on power system management and operational stability.

Primarily, section 6.1 provides a summary and analysis of the energy supply and demand conditions in each power region, offering a preliminary examination of the effects brought about by transportation electrification. Section 6.2 introduces a probabilistic modeling approach to regional power generation and consumption. For regions facing energy shortages, Section 6.3 utilizes multiple optimization algorithms combined with Monte Carlo analysis to propose strategic recommendations for grid management. Finally, Section 6.4 builds on Swedish energy policies and power market theories to further explore the implications of electrified transportation.

6.1 Identify Supply and Demand

The diagram below illustrates the four distinct regions of Sweden's power system, labeled SE1 through SE4. This regional division supports a partitioned approach in this study, enabling a more detailed analysis of each area's unique energy demands and resource characteristics. By examining each region separately, this framework allows for a more targeted assessment of energy distribution and infrastructure needs, contributing to a comprehensive understanding of the power system's functionality across different geographic areas.

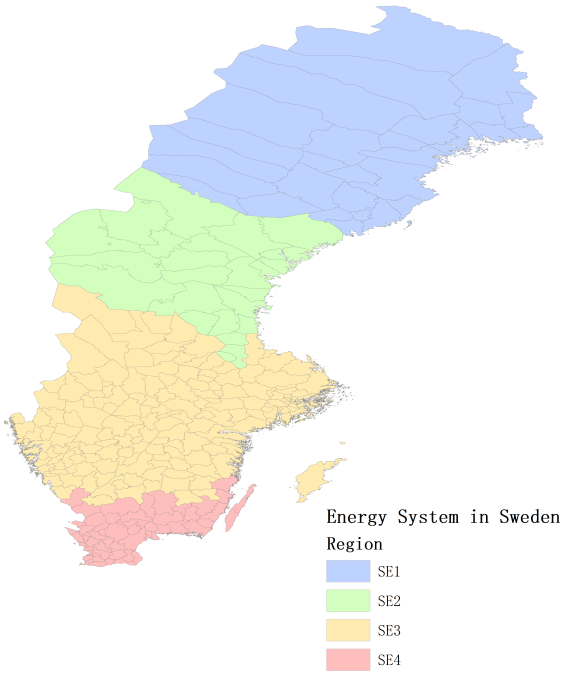

Figure 6.1: Energy System Division in Sweden

The Swedish Energy Agency provided power generation data for each power region in 2024[49]. The study first drew the power generation curve, as shown in Figure 6.2.

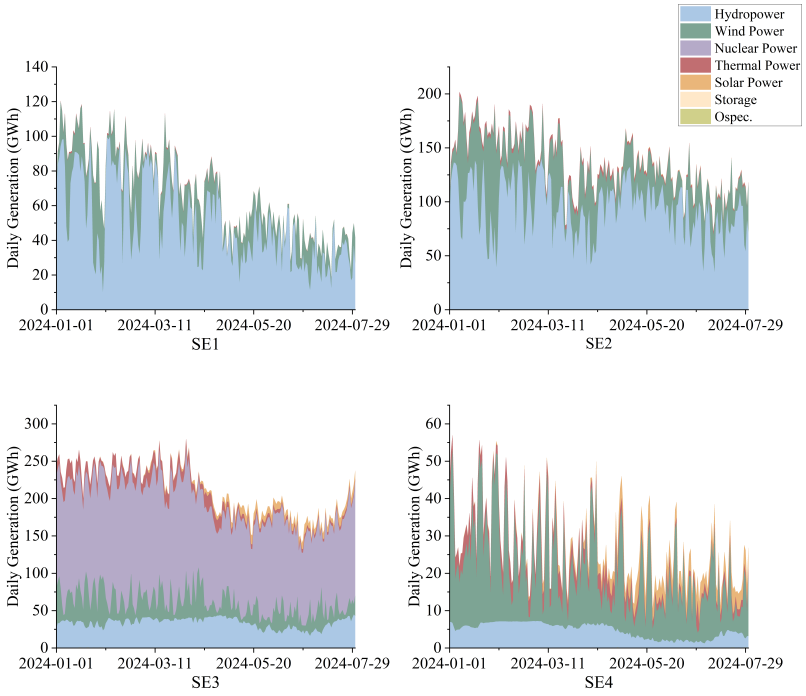

Figure 6.2: Daily Generation in each region, unit: GWh/day, generation data from energimyndigheten[49]

Significant differences can be seen in each region's generation mix, with the north generally relying more on hydropower and the south relying more on nuclear, wind and solar. Regions SE1 and SE2 exhibit seasonal fluctuations in power generation, which correspond to the hydropower regulation mechanisms during wet and dry periods. SE3, where nuclear power is the main source, demonstrates a stable generation pattern. SE4, predominantly reliant on wind power, shows significant intraday variations. Similarly, the energy consumption of vehicles in each region is summarized. The relevant data are shown in Table 6.1.

Table 6.1: Daily Transportation Consumption in each region, according to the traffic flow-consumption model proposed

Region	**SE1**	**SE2**	**SE3**	**SE4**
Consumption (GWh)	14.09	8.74	99.39	22.08

The study compares the average daily traffic energy consumption and power generation curves of each region, as shown in Figure 6.3.

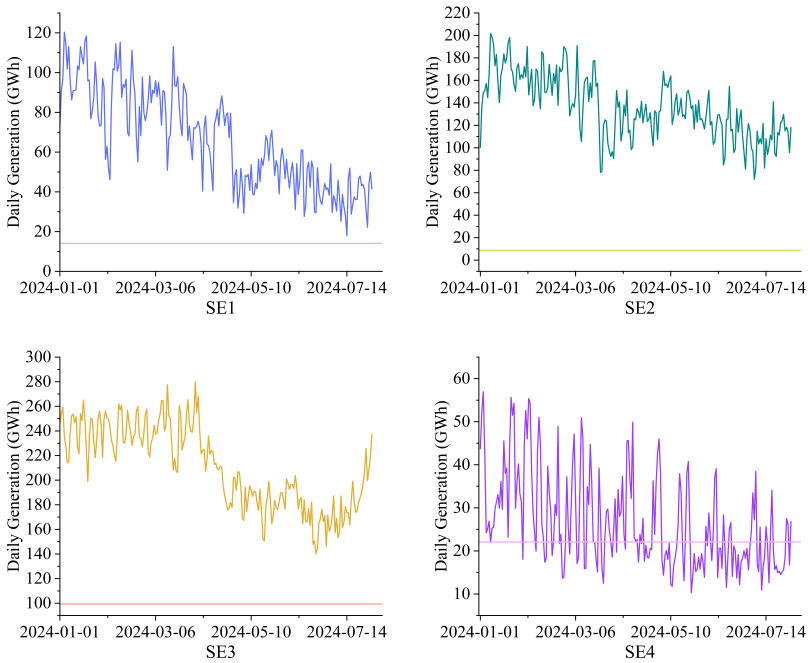

Figure 6.3: Comparison of supply and demand in each region

Preliminary findings show that the power generation of SE1-SE3 can meet the needs of the transportation sector, and SE4 may have some load deficiency. Furthermore, the study explored the ratio of transportation energy consumption to power generation in each region, as shown in Figure 6.4.

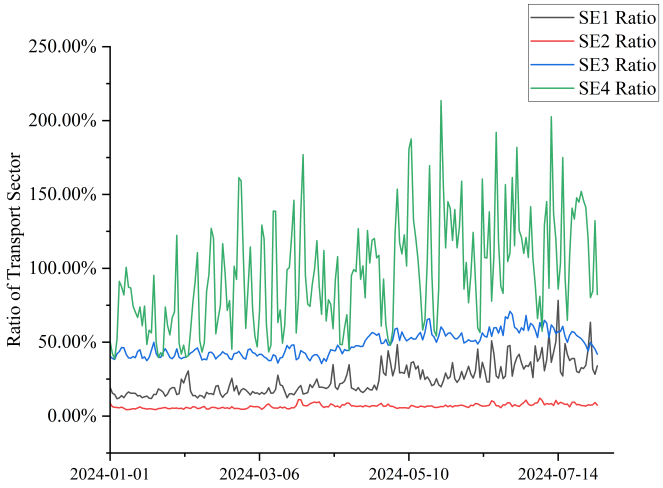

Figure 6.4: Ratio of occupation by transportation

SE1 and SE2 have the lowest populations, resulting in low transportation energy consumption. The abundant hydropower resources in these regions mean that they both have sufficient surplus power generation. SE3 is a densely populated region in Sweden, and transportation energy consumption also accounts for a large proportion, but it still has a certain amount of surplus power generation. SE4, as the most densely populated region, shows a large deficiency of production.

Based on the analysis of the power supply and demand relationship in each region, SE4 will be used as the research target to explore the scenario of energy transmission between different regions.

6.2 Probablistic Model Fitting

6.2.1 Load Curve of SE4

Utilizing probability distribution to evaluate power system stability is an effective approach. In this section, it is proposed to model the fluctuation of energy consumption in the SE4 region using a normal distribution and to introduce a Poisson process to model the instantaneous peak demand during holidays. The combination of seasonal fluctuations and the mean shift process makes the energy consumption curve more realistic, calculated as

$$e(t) = \sum_{i=0}^{n} w_i \{E \cdot f_{season}(t-i) \cdot [1 + P(\lambda)] \cdot N(1, \sigma)\} \tag{6.1}$$

where, f_{season} takes 0.95, 1, 1.1 for winter, summer, and other seasons, respectively. λ is the factor for Poisson distribution, settled by 0.2 here. σ is the scale factor of normal distribution, equal to 0.1. The SE4 energy consumption time curve is shown in Figure 6.5.

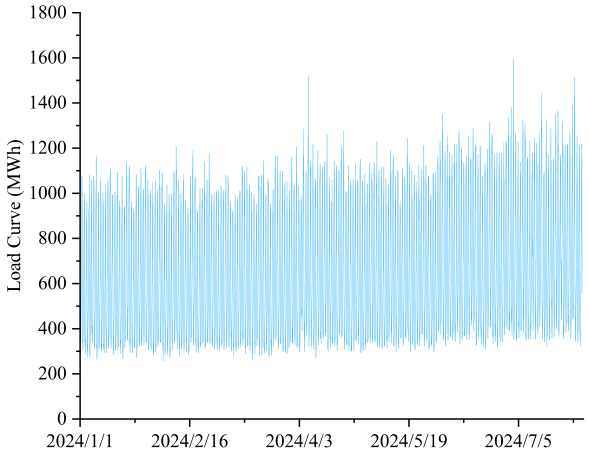

Figure 6.5: Load Curve of SE4

6.2.2 Generation Model for SE1-SE4

The study first performed a characteristic examination for the SE1 to SE4, creating histograms to visualize the distributions and fitting the probability distribution models accordingly, as illustrated in Figure 6.6.

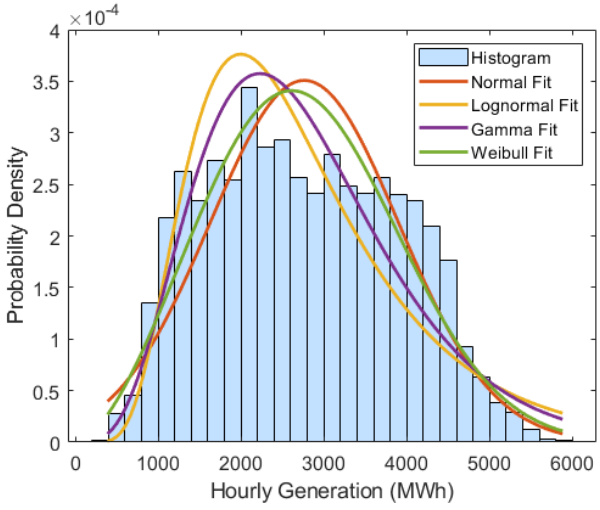

(a) SE1

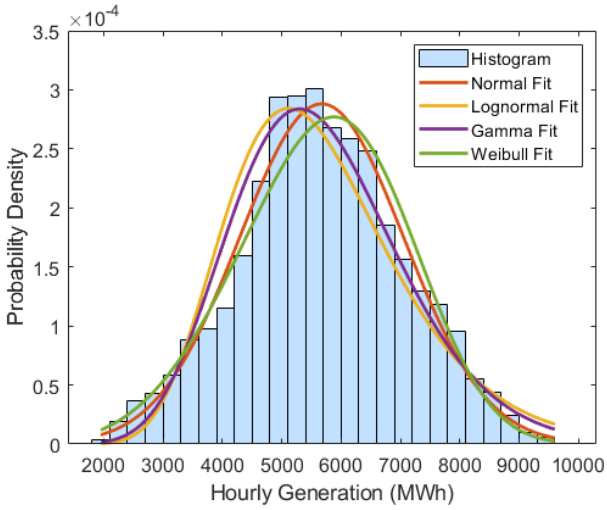

(b) SE2

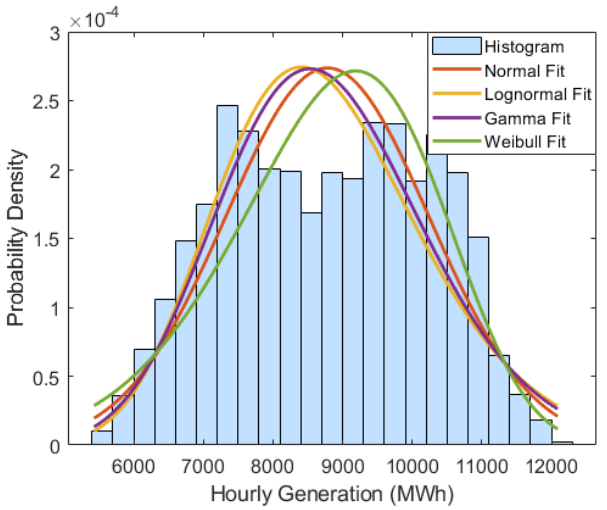

(c) SE3

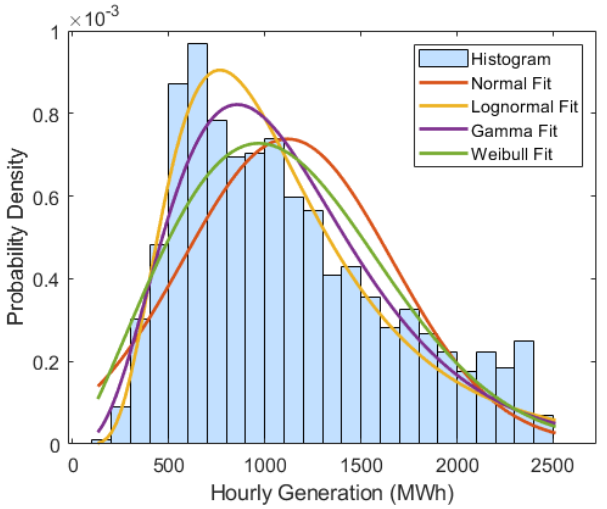

(d) SE4

Figure 6.6: Probabilistic Distribution Fitting of Generation Data

Meanwhile, the SE1-SE4 generation fitting process was carried out by combining AIC, BIC, and K-S tests, and the results are shown in Table 6.2

Table 6.2: Criteria for generation fitting process, in which calculate methods mentioned in Chapter 2

(a) SE1

	Normal	**Lognormal**	**Gamma**	**Weibull**
AIC	86448	86884	86462	86210
BIC	86461	86897	86475	86223
K-S Test	8.77E-12	1.19E-12	6.19E-16	1.99E-08

(b) SE2

	Normal	**Lognormal**	**Gamma**	**Weibull**
AIC	88462	88955	88673	88489
BIC	88475	88968	88687	88502
K-S Test	0.16041	3.33E-13	5.13E-07	0.0002

(c) SE3

	Normal	**Lognormal**	**Gamma**	**Weibull**
AIC	88984	89107	89033	89004
BIC	88997	89121	89046	89017
K-S Test	8.63E-15	2.95E-24	1.62E-20	1.05E-21

(d) SE4

	Normal	**Lognormal**	**Gamma**	**Weibull**
AIC	78843	78070	78009	78206
BIC	78856	78083	78022	78219
K-S Test	4.25E-29	4.70E-06	3.40E-08	3.50E-11

Based on the comparison of fitting images and related parameters, this study gives priority to the goodness of fit, i.e., the K-S Test results. Whereas, AIC and BIC, as the simplicity of the model, are only used as reference when the conclusion cannot be drawn through the K-S Test results. The study obtained the probability distribution model of comprehensive energy generation in each region of SE-SE4.

SE 1 obeys the Weibull distribution

$$f(x) = \frac{2.6623}{3116.8}\left(\frac{x}{3116.8}\right)^{2.6623-1} \exp\left(-\left(\frac{x}{3116.8}\right)^{2.6623}\right), x \geq 0 \tag{6.2}$$

SE2 and SE3 obeys the Normal distribution

$$f(x) = \frac{1}{1384.5\sqrt{2\pi}} \exp(-\frac{(x-5672.8)^2}{2 \cdot (1384.5)^2}), x \geq 0 \tag{6.3}$$

$$f(x) = \frac{1}{1457.2\sqrt{2\pi}} \exp(-\frac{(x-8781)^2}{2 \cdot (1457.2)^2}), x \geq 0 \tag{6.4}$$

SE4 obeys the gamma distribution

$$f(x) = \frac{261.8654^{4.2628} x^{4.2628-1} e^{-261.8654x}}{\Gamma(4.2628)}, x \geq 0 \tag{6.5}$$

6.3 Monte Carlo Analysis

After obtaining the distribution model of power generation in each region and the SE4 load curve model, Monte Carlo analysis is performed for the SE4 region, and LOLP is used as the basis for evaluating the determination of system stability and reliability. Note that this section focuses on the relationship between the surplus transmission of each region and the energy demand of SE4, without considering the actual grid transmission path (refer to the “virtual power plant” theory).

6.3.1 Transmission Ability of SE1-SE3

The study first evaluates the situation of surplus power generation from SE1-SE3 supplying SE4. Note that this analysis treats the surplus power generation of each region as a "pool" to observe the differences in system stability. The study sets a surplus energy transmission ratio of 5%-65% for SE1-SE3, and conducts a Monte Carlo simulation on SE4. The loss of load probability (LOLP) is shown in Figure 6.7.

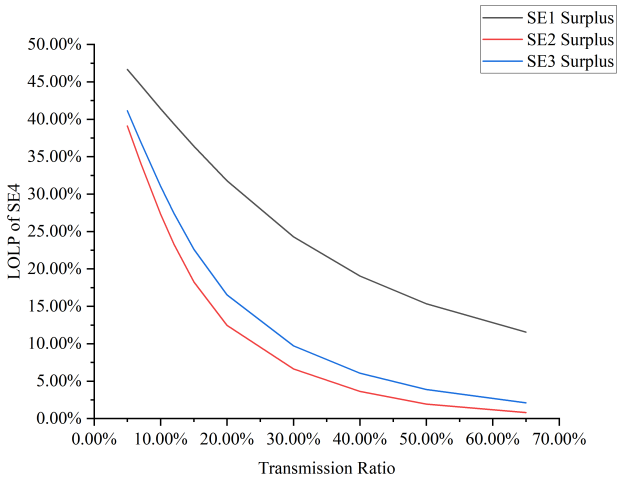

Figure 6.7: LOLP of SE4 with different transmission levels

Though the LOLP of SE4 is effectively mitigated with the increase in the proportion of surplus transmission from SE1, the effect is inferior to that of SE2 under the same transmission ratio. To sum up, to meet the demand for load in SE4, the SE2 power transmission scheme should be prioritized in practical applications, supplemented by the surplus power of SE1 and SE3 to improve the overall power system's reliability and stability.

6.3.2 Comprehensive transmission scenario

This section examines the changes in the loss-of-load probability (LOLP) in the SE4 region under integrated dispatch scenarios across regions, as well as the impacts on grid decision-making response mechanisms. Due to the sensitivity of data involved in actual grid decision-making strategies, this study simulates real-world dispatch scenarios by applying various optimization algorithms. For simplification, cross-border transmission is excluded from the integrated grid dispatch analysis, focusing instead on surplus energy from regions SE1 to SE3 being proportionally transmitted to SE4. This process can be expressed as

$$\begin{cases} PowerSE4 = G_4 + Sur_1 \cdot x_1 + Sur_2 \cdot x_2 + Sur_3 \cdot x_3 \\ LOLP < 0.1 \\ x_1, x_2 < x_3 \\ \min(x_1 + x_2 + x_3), 0 < x < 1 \end{cases} \tag{6.6}$$

In this model, x_1, x_2, x_3 represents the proportion of surplus energy transferred from SE1, SE2, and SE3 to SE4, respectively. while Sur denotes the surplus energy in each region. Different optimization algorithms were applied to simulate decision-making pathways under these conditions, with the results illustrated in Figure 6.8.

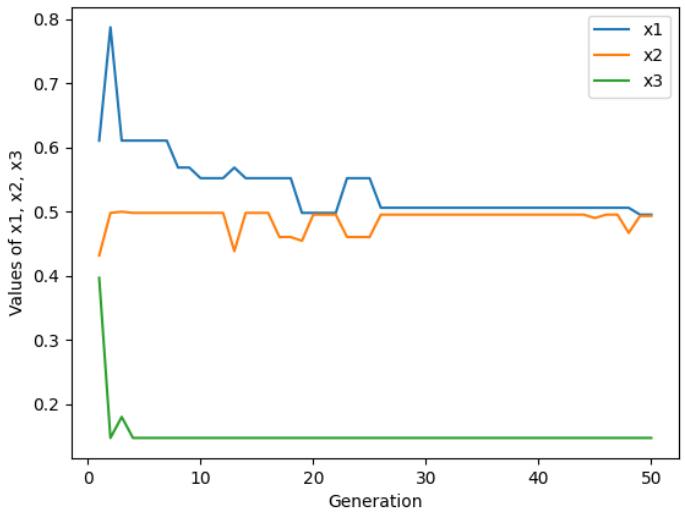

(a) GA Model

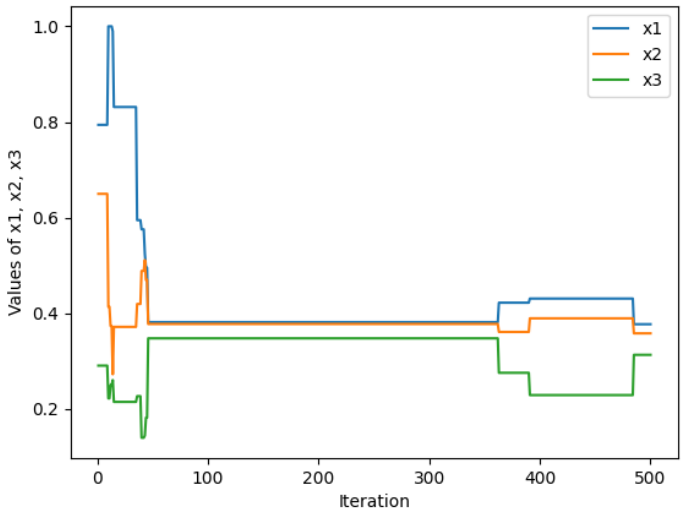

(b) SA Model

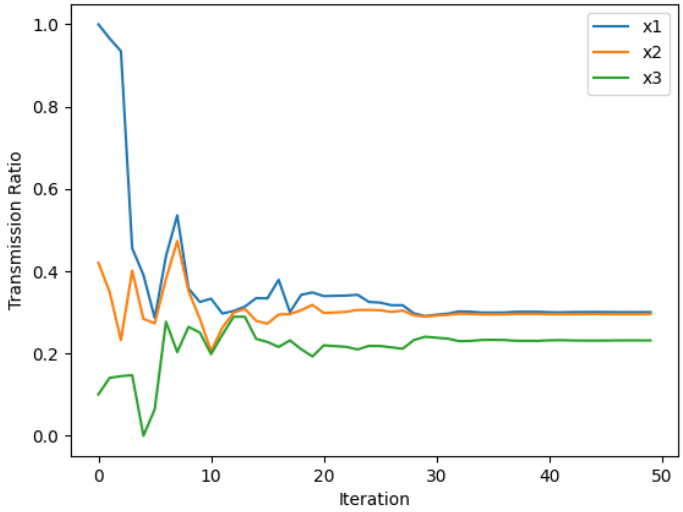

(c) PSO Model

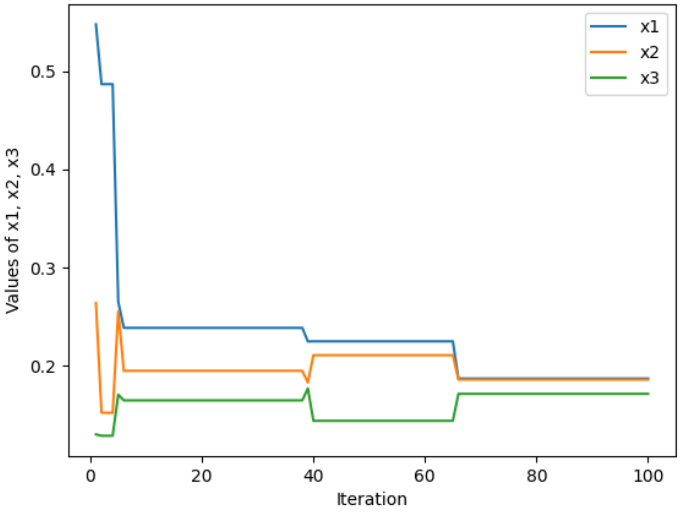

(d) TSO Model

Figure 6.8: Result of different Strategies

The research explores inter-regional power transmission strategies, and although factors like economic benefits were not considered, different decision algorithms exhibited distinct tendencies in dispatching. For instance, GA and SA tended to rely more on regions with stronger transmission capabilities to satisfy the LOLP (Loss of Load Probability). In contrast, PSO and TSO leaned toward balancing power transmission distribution across regions.

Moreover, the study explored the LOLP distribution of SE4 under the integrated transmission scenario, as shown in Figure 6.9.

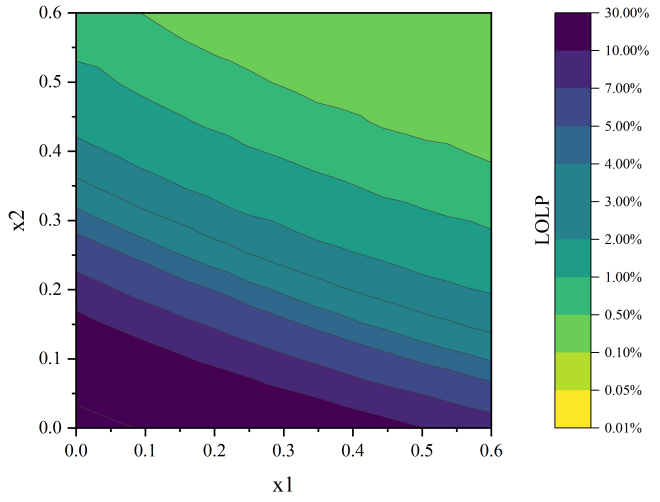

(a) Fix x3=3%, LOLP

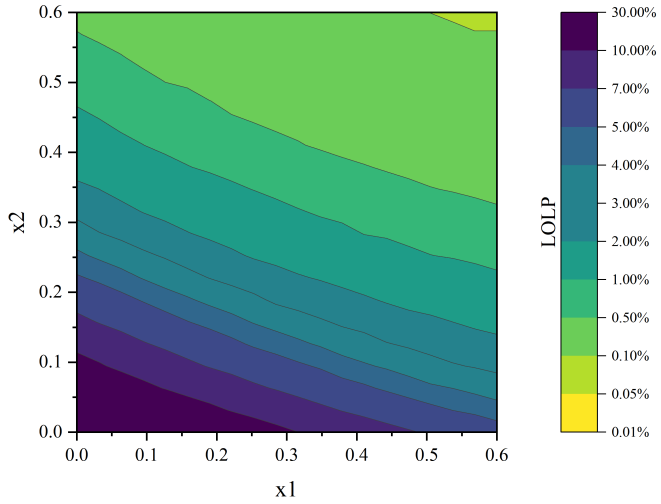

(b) Fix x3=6%, LOLP

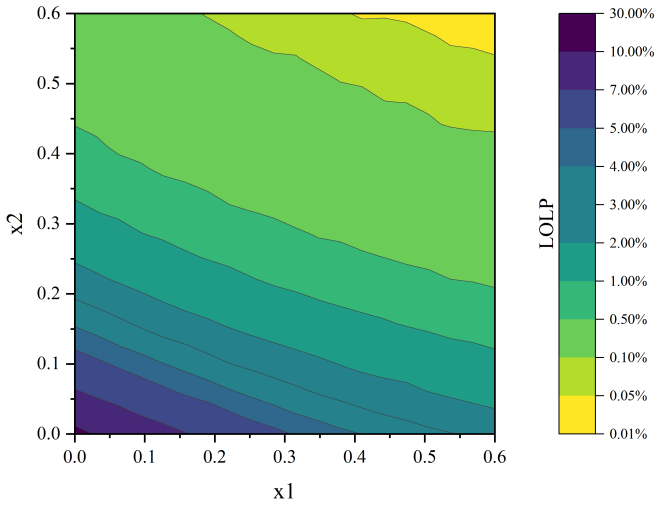

(c) Fix x3=12%, LOLP

Figure 6.9: Monte Carlo result for different transmission levels per each region, LOLP<0.1% is required in modern energy system

The above images show that when the SE3 transmission ratio is controlled at 12%, there is a combination of SE1 and SE2 transmission ratios that meets the requirements so that the system stability meets the requirements. However, the ratios required to achieve this goal appear to be too large. Each region must prioritize the maintenance of sufficient standby capacity to meet frequency regulation, voltage control, and other stability requirements, especially in response to sudden or unforeseen events. .

The study uses a simplified model that focuses only on a single energy supply and demand scenario and excludes the influence of other dynamic factors. However, even under these simplified assumptions, significant differences emerged between the various decision-making strategies. And in the realities of grid operations, numerous social and economic factors add complexity and make grid management even more challenging. The volatility of power markets directly affects generation adjustments, and the vulnerability of actual grid loads to unplanned interruptions necessitates that regions maintain higher levels of spare capacity. In addition, cross-border power trading introduces another dimension of complexity that affects supply stability and resource allocation on the interconnected grid.

Given these circumstances, highlighting the challenge of strategy-making in system management, flexibility in grid operations and balanced resource allocation are becoming increasingly important. A more comprehensive and adaptive mechanism is needed to manage the increasing complexity of scheduling strategies to maintain stability and resilience in the changing energy landscape.

6.4 Analysis of Energy Market

This section highlights some of the key challenges that the Swedish electricity market would face with the electrification of the Swedish transportation system.

Based on the discussion of SE4 energy supply and demand dynamics in the previous chapter and the analysis of transmission strategies and system stability, it is becoming increasingly clear that SE4 will need to incorporate a greater percentage of renewable energy in the future. For SE4, it is of vital significance to enhance transmission and storage solutions to maintain a balanced and stable grid. It aims to ensure that the region's power needs can be met as the electrification of the transportation system progresses, ensuring adequate backup power during peak loads or unplanned outages, and improving the overall stability and resilience of the grid.

To illustrate the role of SE4 in Sweden's interconnected power system, the Swedish Energy Agency has developed a schematic diagram that shows the grid connections within Sweden and in neighboring countries. The diagram is shown in Figure 6.10.

Figure 6.10: Energy System Structure around Sweden, provided by Swedish Energy Agency[49]

In terms of grid structure, the main source of energy in SE4 and its surrounding area is wind power. Considering the economics of power dispatch and transmission, SE4's choice to directly import wind power is a relatively convenient and low-cost option. Meanwhile, SE4 itself needs to continuously enhance the development of locally advantageous resources, such as wind and photovoltaic power generation, according to demand, to supplement its power supply capacity and enhance its energy independence and stability.

However, the large-scale introduction of renewable energy sources such as wind power also brings new challenges. According to the "Merit-Order Effect", as illustrated in Chapter 2, since the marginal cost of renewable energy is close to zero, a large number of new energy sources will depress the market price of electricity. While this is beneficial to consumers, when electricity prices remain low, power producers may find it difficult to recover operating costs, resulting in reduced profits or even losses. This "loss problem" is particularly pronounced in electricity markets with a high share of wind power, as shown in Figure 6.11.

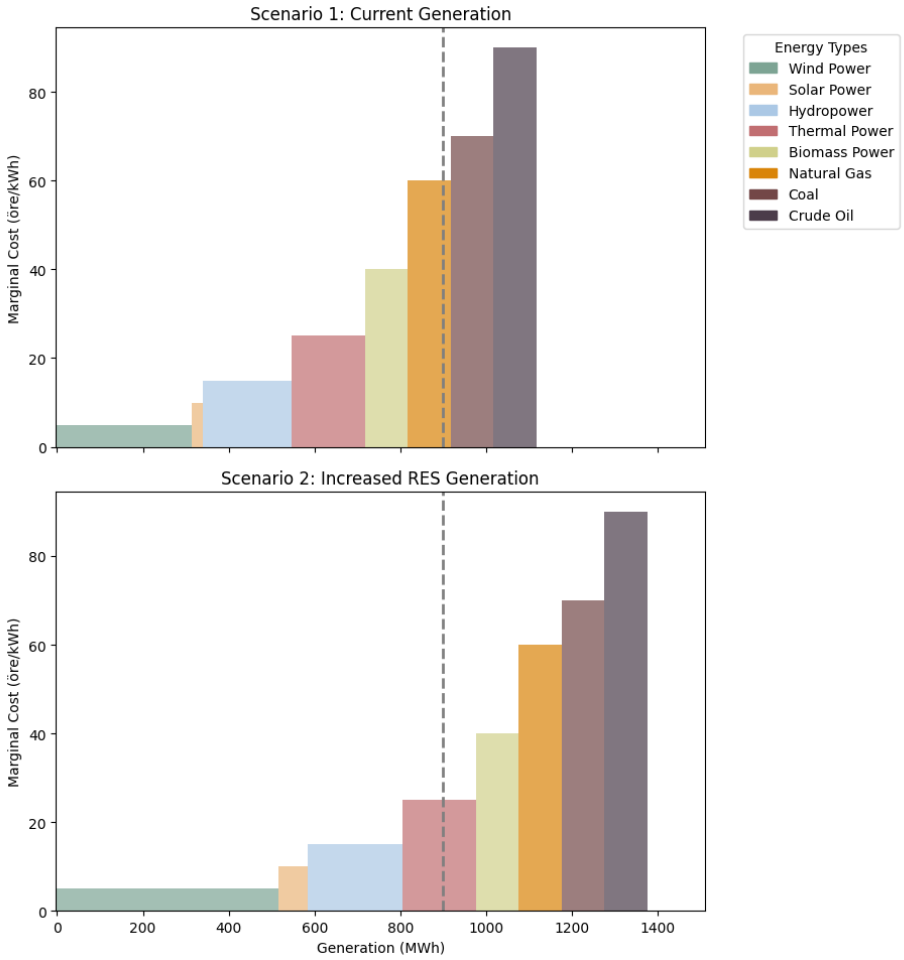

Figure 6.11: Merit Order Effect in Energy Market, taking one moment in Sweden as an example

It is obvious that under the same energy demand scenario, under the assumption that the proportion of other power generation remains unchanged, the increase in wind power generation will eventually lead to a decrease in the market equilibrium price. To address this problem, electricity markets may need to apply new mechanisms to balance the economic benefits of renewable energy with the long-term profitability of firms. Moreover, although the electricity certificate policy adopted by Sweden provides energy companies with an additional source of income, this income may not be enough to fully offset the losses caused by falling market prices when electricity prices fluctuate. Enterprises may increase electricity prices to maintain profitability and pass the costs on to consumers, thus increasing the financial burden on users. Especially under the long-term downturn in market prices, the impact of this increased cost on low-income users is more significant.

It is worth acknowledging that the contradiction between corporate profits and consumer burden is a potential obstacle to promoting renewable energy. The continued rise in electricity prices may cause dissatisfaction among users, especially when these cost increases contrast with the renewable energy environment with sufficient electricity supply. From the perspective of social impact, this contradiction may lead to a decline in public support for renewable energy policies, which in turn affects the effectiveness of policy implementation and the continued promotion of renewable energy. Therefore, policymakers need to strike a balance between supporting corporate profits and protecting the economic interests of users to ensure the long-term development of renewable energy.

To conclude, this chapter provides a comprehensive analysis of the impact of transportation electrification on Sweden's power system, highlighting significant challenges. From the perspective of energy supply and demand, a severe energy deficit is anticipated in the key SE4 region. As a densely populated area, SE4 will struggle to meet the increased demand without additional energy resources. Power dispatch simulations indicate that the increasing electricity demand will complicate future grid management, calling for improvements in existing dispatch mechanisms. From a power market perspective, increased electricity demand combined with a rise in renewable energy integration could not only place added pressure on grid stability but also raise economic burdens for businesses and consumers.

The research recommends enhancing support for clean energy reserves and flexible dispatch mechanisms at the policy and planning levels to ensure a sustainable power supply. Additionally, optimizing inter-regional power dispatch and reinforcing grid interconnections will be crucial in meeting the growing demand driven by electrification. These findings and recommendations offer valuable insights for Sweden and other nations advancing electrification, providing a foundation to address future power system management challenges effectively.

7

Results

Based on the analysis framework EOIET proposed, the study has initially derived the energy demand, charging infrastructure location plan, and impacts on the power system under a fully electrified transportation scenario in Sweden. This chapter will summarize these findings and further assess their validity through a multi-faceted analysis. Section 7.1 discusses the results related to EV energy consumption, Section 7.2 reviews the charging infrastructure location plan, and Section 7.3 evaluates the potential impacts on the power system.

7.1 EV Flow and Energy Consumption

The study categorizes Swedish EV users into urban daily commuters and highway long-distance travelers, with specific consideration given to the driving characteristics and daily energy consumption of passenger cars, buses, and trucks in different scenarios. Detailed energy consumption calculations are presented in Appendix B. Daily energy consumption data have been converted to annual averages for ease of evaluation and analysis, as shown in Table 7.1.

Table 7.1: Energy Consumption by EVs in different scenarios, city's energy demand calculated in Section 4.1, highway's energy demand derived in section 4.2. Here provide the sum-up results of the study.

Scenario	Annual Energy Consumption (TWh/year)
Car in City	5.56
Bus in City	0.74
Truck in City	0.0076
Car along Highway	26.62
Truck along Highway	19.76
Total	**52.9876**

Meanwhile, the Swedish Energy Agency provided data on energy consumption in the transport sector over the years[49], as shown in Table 7.2.

Table 7.2: Energy consumption of the Swedish transport sector over the years (Unit: TWh/year)

Year	Petrol	Diesel	Others	Total
2008	40.9	36.8	10.3	88.1
2009	40.1	35.9	10.1	86.1
2010	37.5	39.6	10.6	87.8
2011	34.7	40.9	11.8	87.4
2012	31.6	40.0	12.5	84.1
2013	29.9	39.6	13.9	83.4
2014	28.6	39.0	16.1	83.8
2015	27.8	40.7	17.4	85.9
2016	26.6	38.5	20.5	85.6
2017	25.4	38.8	22.3	86.4
2018	23.7	36.7	24.1	84.5
2019	23.1	37.2	23.0	83.4
2020	21.1	35.7	22.0	78.9

Based on the above data, a clear decreasing trend can be observed in the use of Petrol, the conventional energy source for passenger cars, while Diesel, commonly used for heavy-duty vehicles, shows a more gradual change. Other energy sources, including electricity and biofuels, represent emerging clean energy alternatives and demonstrate a significant upward trend in recent years. Historical changes in energy consumption are visualized in Figure 7.1.

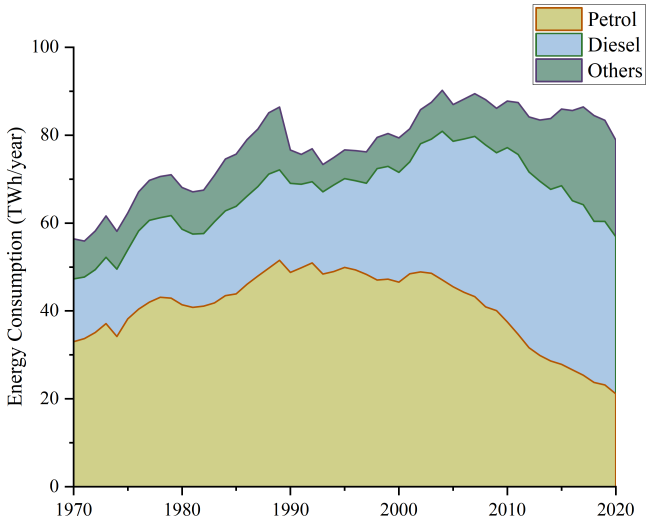

Figure 7.1: Different Energy usage in Sweden, 1970-2020. Data from Energy Agency in Sweden[49]. Note that other energy here represents biofuels and electricity and other rare amount of energy

It can be observed that the share of renewable energy in the transportation sector

is gradually increasing, meanwhile, an initial rise is followed by a decline in overall energy consumption. This trend aligns with expectations: the initial increase reflects a rise in car ownership, leading to shifts in travel habits. The subsequent decline is due to the energy efficiency of electric vehicles, as the average energy consumption of traditional fossil fuel vehicles, when converted to kWh/km, is approximately three times that of electric vehicles. Thus, as the level of transportation electrification increases, total energy consumption begins to decline.

Figure 7.2 illustrates the evolution of renewable energy consumption and total energy consumption within the transportation sector, along with reasonable projections for future trends.

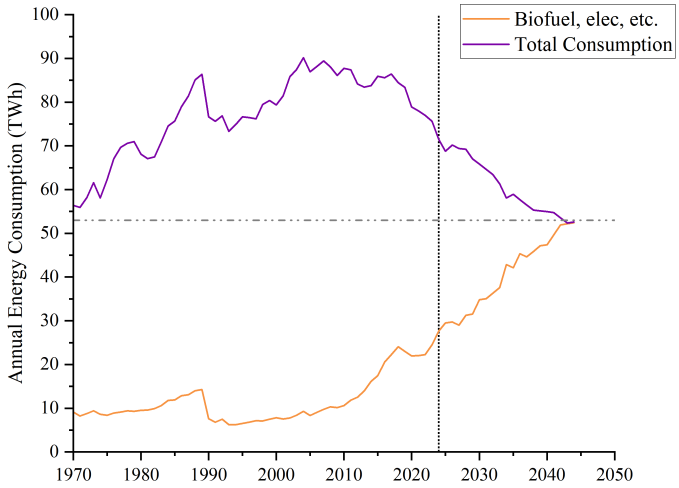

Figure 7.2: Energy consumption trends in the Swedish transport sector, fact from energy agency[49]. With the predicted result for 2024-2045 via the LSTM-GRU model proposed in the study, dual-use of the model.

According to reasonable extrapolation of existing data, it is projected that the transportation sector could reach a balance between renewable energy consumption and total energy consumption by around 2040—a target year also aligned with the ambitious electrification goals set by various countries. The annual energy consumption estimates derived in this study for the transportation sector closely align with the anticipated energy levels at the point of full electrification.

7.2 Placement of Charging Facilities

The study developed a comprehensive plan for charging facility construction to meet Sweden's transportation needs. The detailed data for various cities and highways will be provided in Appendix C. A summary of the different types of charging facilities identified in the study is presented in Table 7.3.

Table 7.3: Charging Facilities in Sweden, suggested by this research, the sum up of the result in Chapter 5.

Type of Charger	Amount
Light Car Charging Station along Highway	141
Heavy Truck Charging Station along Highway	77
Home charger in Sweden	77540
Public charger in Sweden	150192
Total charger	**227732**

It has highlighted the European Commission's recommendations for highway charging infrastructure, specifically, the installation of at least one car charging station every 60 km and one truck charging station every 100 km [31]. According to data from the Swedish Transport Agency [48], Sweden's highways span approximately 6,400 km. Table 7.4 compares the results of this study with the EU's recommendations for charging station.

Table 7.4: Highway Route Length and Vehicle Data Comparison, column 'Research' represents the results derived through the model proposed, column 'EU' obeys the Europeans' recommendation.

Highway	Route Length (km)	Car		Truck	
		Research	EU	Research	EU
E4	1538.87	36	26	17	15
E6	484.05	9	8	6	5
E10	418.74	8	7	6	5
E12	469.76	9	8	7	5
E14	330.64	6	6	5	4
E18	562.97	10	10	6	5
E20	480.86	11	8	6	5
E22	528.49	13	9	5	6
E45	1482.55	37	25	19	15
E65	80.62	2	2	1	1

The number of charging stations derived from the study aligns well with the European Commission's recommendations, further supporting the study's validity. Additionally, the EU has proposed guidelines for the ratio of EV charging points to the total number of vehicles per country, recommending a ratio of 16.6:1 for Sweden [31]. According to data from SCB[47], there are currently around 4 million vehicles in the country. Assuming a stable vehicle count, 240,900 charging points are required to meet this ratio. This is also well-consistent with the 227,732 charging points estimated in the study.

7.3 Energy System Analysis

In the previous analysis, the study assessed the power system from both the energy supply-demand and power market perspectives. The primary conclusions are as follows:

1. As transportation system electrification progresses, the SE4 region faces a potential risk of insufficient energy supply;

2. The complexity of power system dispatch and management has significantly increased, underscoring the urgent need to optimize management strategies;

3. Grid reliability is increasingly challenged, with a growing risk of load loss;

4. The rising energy demand, accompanied by a larger market share of renewable energy, introduces new challenges to the profit and loss dynamics of the power market.

Although specific power system load data were unavailable due to data sensitivity, trends in electricity price changes from the Swedish Energy Agency provide some basis for evaluation. Recent trends in Sweden's electricity prices[49], shown in Figure 7.3, reveal distinct regional behaviors.

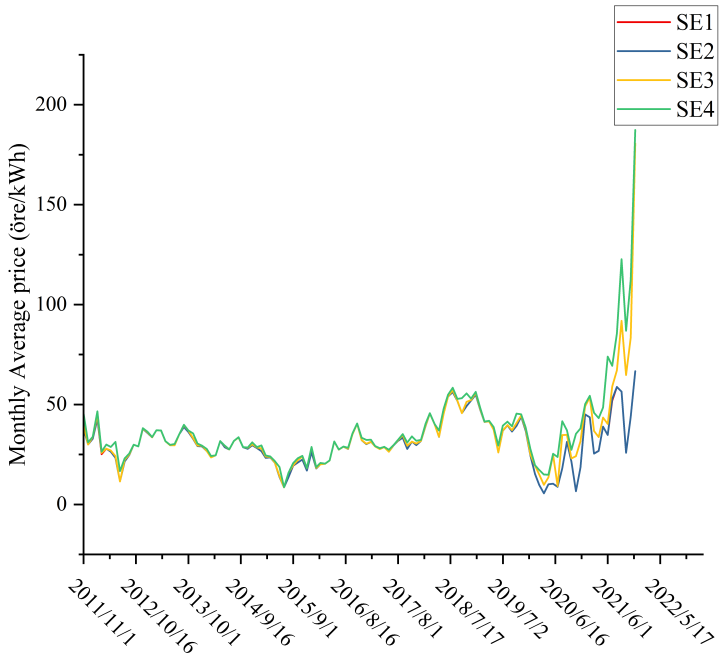

Figure 7.3: Electricity Price in Sweden, data from energy agency[49]

Price fluctuations in SE1 and SE2 are relatively stable and seasonal, reflecting normal market dynamics. However, SE3 and SE4 have exhibited a dramatic upward trend in electricity prices in recent years, aligning with previous analyses. The study

notes that the combined impact of the Merit Order Effect and Quota Obligations has driven destabilizing price balances and caused premiums, as renewable energy has occupied a larger market share as demand rises.

From an energy demand perspective, SE1 and SE2 benefit from sufficient renewable generation and a relatively low concentration of electricity users, allowing the electricity market in these regions to maintain a dynamic balance. In contrast, SE3 and SE4 experience concentrated demand and limited renewable energy generation, leading to higher electricity prices. This outcome aligns with the previous projections, in Chapter 6, indirectly validating the analysis of the power system's response to increased electrification.

8

Discussion

In Chapter 7, the article reviews the relevant results of the study and further demonstrates the rationality of the results. This chapter will review and discuss the research framework and results. Section 8.1 explains the possible deficiencies of the study, and Section 8.2 discusses the ethics and sustainability of the study.

8.1 Deficiency Analysis

Reviewing the results of the study, although in the national dimension, as discussed in Chapter 7, the results of the energy consumption projections for the transportation sector match the future trends in Sweden, and the charging facility siting and construction program is fully in line with the EU recommended standards.

However, the results arriving at the city level lacked corresponding information to validate applicability. In terms of the EOIET framework established by the study, historical macro-statistical data are used as the driving force, optimization algorithms serve as the decision-making tool, and aggregate group characteristics substitute for individual behaviors. The elements that were simplified during the framework deserve to be revisited.

The first is the simplified approach to vehicle energy analysis, where cars, buses, and trucks are studied in terms of average energy consumption per kilometer. The simplification is effective and convenient for studying a macro sample, however, the vehicles used in the calculations are the more dominant vehicles in today's society and it remains fuzzy whether the associated energy consumption will shift with future technological innovations. In the case of Sweden's large cities, the change may take place over an extended period. Yet, some municipalities with a strong focus on high-tech companies, such as Skellefteå, Västerås, etc., might be the first to complete the vehicle replacement. In this context, the energy consumption data obtained in this study may be invalidated in some cities in the future. In addition, geographical location is a critical factor to consider. The colder temperatures in Sweden's high-latitude regions impose greater demands on battery charging technology, potentially limiting the progress of transportation electrification. Conducting sensitivity analyses may help investigate technological innovations' dynamic effects on the energy consumption model.

The study proposed methods for categorizing daily commuters and long-distance travelers in Sweden. In terms of overall development planning, Swedish cities are showing a trend towards decentralization, with an active push for infrastructure development across diverse city types. Under this trend, the distinction between urban and rural areas might be gradually diluted in the future, leading to changes in people's daily commuting habits. Incorporating factors such as infrastructure and population changes could help simulate the shift in transportation demand to ensure the forward-looking nature of the model.

8.2 Ethics and Sustainability

Despite the limitations of the study, several key concepts hold significant generalizable value. First of all, the study not only focuses on urban areas but also takes into account the transportation and energy supply needs of rural areas. This urban-rural perspective highlights the concept of social equality, avoiding the neglect of remote or sparsely populated areas in previous studies. It ensures that both urban and rural residents have access to appropriate infrastructure support in the transition to electrification of the transportation system. This comprehensive coverage provides a reference path for balanced regional development and helps promote more inclusive policymaking.

Moreover, the study adopts a data-driven decision-making process, grounded in historical data and statistical models. This approach ensures accountability and transparency in analysis, minimizing human subjective bias as well. Through the data-driven decision-making model, the study improves the scientific validity and reliability of the results while fostering public trust, contributing to maintaining a fair and transparent policymaking process among multiple stakeholders.

9

Conclusion

The study develops an EOIET framework to address key challenges during the electrification process of Swedish transport system. Specifically, it investigates traffic flow, energy consumption, charging station placement, and the impact on the grid.

In terms of traffic flow and energy consumption, both urban commuters and high-speed travelers are systematically considered. Traffic energy consumption across 290 Swedish cities was modeled using the UCEM and UTEM frameworks. For long-distance travel on 10 major highways, a combination of LSTM-GRU models and Rayleigh distribution was employed to dynamically predict energy demand. Historical trends in Sweden's transportation energy consumption from 1970 to 2020 were analyzed, leading to an estimation of the future convergence range of total energy consumption and electricity consumption required for achieving full electrification by 2040. This is consistent with the results of this research model, confirming the reliability of the research. Regarding the location of charging stations, the above energy consumption demand results are used to determine the distribution of urban charging facilities in consideration of the existing urban layout. The specific number and location distribution of urban charging facilities are shown in Figure 5.2 and Table 5.3. For the highway network, the placement of high-speed charging facilities was optimized through a simulated annealing algorithm integrated with a multi-dimensional road topology analysis, as shown in Figure 5.7 and Table 5.7. The charging station site selection plan obtained from the above study includes 227,732 charging points, which is highly consistent with the EU's recommendation of approximately 240,000 charging points. It supports the practical feasibility of the plan. Moreover, a comprehensive impact assessment of grid carrying capacity is proposed, examining not only the relationship between energy supply and demand but also comprehensively evaluating the grid carrying capacity from multi-dimensional perspectives. Factors such as supply-demand balance, strategy management, system balance, and market operation are considered, establishing a model for analyzing the pressure on the grid arising from the integration of renewable energy into the transportation system.

Despite these contributions, the study still has several limitations. For instance, exhaustive local data support to verify the scheme's feasibility at the city level is limited, leading to uncertainty in city-wide implementation. Additionally, the parameter selection of the model algorithm relies on a heuristic approach, which lacks large-scale data support for refined optimization, and might unexpectedly bring

some bias to the accuracy of the results. Moreover, the dynamic impacts of future technological innovations have not been fully considered in the model. For example, with the upgrading of new energy vehicle technology, the level of energy consumption may change significantly, which will pose a potential challenge to the reliability of the predicted results. These limitations reflect the historical constraints of the study. Future research could address these by conducting small-scale urban analyses and pilot studies to further validate the model's generalizability. As vehicle energy efficiency continues to improve, incorporating more dynamic modeling tools will better capture evolving consumption trends. Expanding grid impact assessments to include a broader range of multidimensional factors is also recommended for more comprehensive evaluations.

Bibliography

[1] J. Van and C. Van Hinsbergen, "Short-Term Traffic and Travel Time Prediction Models."

[2] B. Williams, M. Asce, L. Hoel, and F. Asce, "Modeling and Forecasting Vehicular Traffic Flow as a Seasonal ARIMA Process: Theoretical Basis and Empirical Results," Journal of Transportation Engineering @ ASCE, vol. 129, no. 6, Dec. 2003, doi: https://doi.org/10.1061/(ASCE)0733-947X(2003)129:6(664).

[3] C. Chen, J. Hu, Q. Meng, and Y. Zhang, "Short-time Traffic Flow Prediction with ARIMA-GARCH Model," 2011 IEEE Intelligent Vehicles Symposium (IV), pp. 607–612, Jun. 2011.

[4] K. Li, C. Zhai, and J. Xu, "Short-term Traffic Flow Prediction Using Methodology Based on ARIMA and RBF-ANN," 2017 IEEE, pp. 2004–2207, 2017.

[5] J. Huang, L. Zheng, J. Qin, D. Xia, L. Chen, and D. Sun, "Short-Term Travel Time Prediction on Urban Road Networks using Massive ERI Data," 2019 IEEE SmartWorld, pp. 582–588, Aug. 2019, doi: https://doi.org/10.1109/smartworld-uic-atc-scalcom-iop-sci.2019.00138.

[6] F. G. Habtemichael and M. Cetin, "Short-term traffic flow rate forecasting based on identifying similar traffic patterns," Transportation Research Part C: Emerging Technologies, vol. 66, pp. 61–78, May 2016, doi: https://doi.org/10.1016/j.trc.2015.08.017.

[7] R. Cheng, Z. Liu, and M. Zhang, "An improved traffic flow prediction model: Spatial-Temporal network based on Wavelet and LSTM," 2022 16th IEEE International Conference on Signal Processing (ICSP), pp. 276–280, Oct. 2022, doi: https://doi.org/10.1109/icsp56322.2022.9965226.

[8] T. Wu et al., "Hydrogen Energy Storage System for Demand Forecast Error Mitigation and Voltage Stabilization in a Fast-Charging Station," IEEE Transactions on Industry Applications, vol. 58, no. 2, pp. 2718–2727, Mar. 2022, doi: https://doi.org/10.1109/tia.2021.3089446.

[9] V. N. Katambire, R. Musabe, A. Uwitonze, and D. Mukanyiligira, "Forecasting the Traffic Flow by Using ARIMA and LSTM Models: Case of Muhima Junction," Forecasting, vol. 5, no. 4, pp. 616–628, Nov. 2023, doi: https://doi.org/10.3390/forecast5040034.

[10] Z. Wang, X. Su, and Z. Ding, "Long-Term Traffic Prediction Based on LSTM Encoder-Decoder Architecture," IEEE Transactions on Intelligent Transportation Systems, vol. 22, no. 10, pp. 6561–6571, Oct. 2021, doi: https://doi.org/10.1109/tits.2020.2995546.

[11] M. D. Eddine and Y. Shen, "A deep learning based approach for predicting the demand of electric vehicle charge," The Journal of Supercomputing, vol. 78, no. 12, pp. 14072–14095, Mar. 2022, doi: https://doi.org/10.1007/s11227-022-04428-0.

[12] Z. Wang and W. Han, "Traffic Flow Prediction Based on Optimized LSTM Model," 2023 3rd International Conference on Information Communication and Software Engineering (ICICSE), pp. 60–65, Apr. 2023, doi: https://doi.org/10.1109/icicse58435.2023.10211862.

[13] S. Saleti, L. Y. Panchumarthi, Y. R. Kallam, L. Parchuri, and S. Jitte, "Enhancing Forecasting Accuracy with a Moving Average-Integrated Hybrid ARIMA-LSTM Model," SN Computer Science, vol. 5, no. 6, Jul. 2024, doi: https://doi.org/10.1007/s42979-024-03060-4.

[14] J. Kong, X. Fan, X. Jin, S. Lin, and M. Zuo, "A Variational Bayesian Inference-Based En-Decoder Framework for Traffic Flow Prediction," IEEE Transactions on Intelligent Transportation Systems, vol. 25, no. 3, pp. 2966–2975, Mar. 2024, doi: https://doi.org/10.1109/tits.2023.3276216.

[15] M. Wang, J. Peng, and F. Huang, "Traffic flow prediction model based on multi-time scale space-time graph network," Computer Science, pp. 41–48, Jan. 2022, doi: https://doi.org/10.11896/jsjkx.220100188.

[16] W. Jiang, Y. Xiao, Y. Liu, Q. Liu, and Z. Li, "Bi-GRCN: A Spatio-Temporal Traffic Flow Prediction Model Based on Graph Neural Network," Journal of Advanced Transportation, vol. 2022, pp. 1–12, Feb. 2022, doi: https://doi.org/10.1155/2022/5221362.

[17] D. Huang and D. Tian, "A Long-term Traffic Flow Prediction Model Based on Multiple Features," 2023 3rd International Conference on Electronic Information Engineering and Computer Communication (EIECC), pp. 1–4, Dec. 2023, doi: https://doi.org/10.1109/eiecc60864.2023.10456621.

[18] R. Luo, Y. Song, L. Huang, Y. Zhang, and R. Su, "AST-GIN: Attribute-Augmented Spatiotemporal Graph Informer Network for Electric Vehicle Charging Station Availability Forecasting," Sensors, vol. 23, no. 4, p. 1975, Feb. 2023, doi: https://doi.org/10.3390/s23041975.

[19] Y. Li, S. Chai, X. Zhang, G. Wang, R. Zhu, and E. Chung, "STPNet: Quantifying the Uncertainty of Electric Vehicle Charging Demand via Long-Term Spatiotemporal Traffic Flow Prediction Intervals," IEEE Transactions on Intelligent Transportation Systems, vol. 24, no. 12, pp. 15018–15034, Dec. 2023, doi: https://doi.org/10.1109/tits.2023.3305626.

[20] Y. Wu, H. Tan, L. Qin, B. Ran, and Z. Jiang, "A hybrid deep learning based traffic flow prediction method and its understanding," Transportation Research Part C: Emerging Technologies, vol. 90, pp. 166–180, May 2018, doi: https://doi.org/10.1016/j.trc.2018.03.001.

[21] A. Ermagun and D. Levinson, "Spatiotemporal traffic forecasting: review and proposed directions," Transport Reviews, vol. 38, no. 6, pp. 786–814, Mar. 2018, doi: https://doi.org/10.1080/01441647.2018.1442887.

[22] M. Lippi, M. Bertini, and P. Frasconi, "Short-Term Traffic Flow Forecasting: An Experimental Comparison of Time-Series Analysis and Supervised Learning," IEEE Transactions on Intelligent Transportation Systems, vol. 14, no. 2, pp. 871–882, Jun. 2013, doi: https://doi.org/10.1109/tits.2013.2247040.

[23] Y. Liao, Ç. Tozluoğlu, F. Sprei, S. Yeh, and S. Dhamal, "Impacts of charging behavior on BEV charging infrastructure needs and energy use," Transportation Research Part D: Transport and Environment, vol. 116, p. 103645, Mar. 2023, doi: https://doi.org/10.1016/j.trd.2023.103645.

[24] E. D. Kostopoulos, G. C. Spyropoulos, and J. K. Kaldellis, "Real-world study for the optimal charging of electric vehicles," Energy Reports, vol. 6, pp. 418–426, Nov. 2020, doi: https://doi.org/10.1016/j.egyr.2019.12.008.

[25] M. Neaimeh, S. D. Salisbury, G. A. Hill, P. T. Blythe, D. R. Scoffield, and J. E. Francfort, "Analysing the usage and evidencing the importance of fast chargers for the adoption of battery electric vehicles," Energy Policy, vol. 108, pp. 474–486, Sep. 2017, doi: https://doi.org/10.1016/j.enpol.2017.06.033.

[26] P. Morrissey, P. Weldon, and M. O'Mahony, "Future standard and fast charging infrastructure planning: An analysis of electric vehicle charging behaviour," Energy Policy, vol. 89, pp. 257–270, Feb. 2016, doi: https://doi.org/10.1016/j.enpol.2015.12.001.

[27] B. A. Davis and M. A. Figliozzi, "A methodology to evaluate the competitiveness of electric delivery trucks," Transportation Research Part E: Logistics and Transportation Review, vol. 49, no. 1, pp. 8–23, Jan. 2013, doi: https://doi.org/10.1016/j.tre.2012.07.003.

[28] D. Milakis, M. Kroesen, and B. van Wee, "Implications of automated vehicles for accessibility and location choices: Evidence from an expert-based experiment," Journal of Transport Geography, vol. 68, pp. 142–148, Apr. 2018, doi: https://doi.org/10.1016/j.jtrangeo.2018.03.010.

[29] A. İ. Şimşek, B. Desticioğlu Taşdemir, and E. Koç, "A bibliometric analysis and research agenda of the location of electric vehicle charging stations," Business \& Management Studies: An International Journal, vol. 11, no. 2, pp. 610–625, Jun. 2023, doi: https://doi.org/10.15295/bmij.v11i2.2246.

[30] L. Jis, Z. Hu, Y. Song, and Z. Luo, "Optimal Siting and Sizing of Electric Vehicle Charging Stations."

[31] "European EV Charging Infrastructure Masterplan," 2022.

[32] Y. Huang and K. M. Kockelman, "Electric vehicle charging station locations: Elastic demand, station congestion, and network equilibrium," Transportation Research Part D: Transport and Environment, vol. 78, p. 102179, Jan. 2020, doi: https://doi.org/10.1016/j.trd.2019.11.008.

[33] J. Dong, C. Liu, and Z. Lin, "Charging infrastructure planning for promoting battery electric vehicles: An activity-based approach using multiday travel data," Transportation Research Part C: Emerging Technologies, vol. 38, pp. 44–55, Jan. 2014, doi: https://doi.org/10.1016/j.trc.2013.11.001.

[34] Z. Huang, Q. Zhang, Y. Li, S. Qin, and D. Wang, "Research on charging station demand prediction and layout planning model for TOD," Transport Engineering, vol. 24, no. 4, pp. 72–78, Apr. 2024, doi: https://doi.org/10.13986/j.cnki.jote.2024.04.011.

[35] "Regulation (EU) 2023/1804 of the European Parliament of the Council of 13 September 2023," Official Journal of the European Union, Sep. 2023.

[36] S. Rudnik, "Selected Issues Concerning Transposition to the Polish legal order of the Directive 2014/94/EU of the 22 October 2014 on the deployment of alternative fuels infrastructure," AUTOBUSY – Technika, Eksploatacja, Systemy Transportowe, vol. 19, no. 6, pp. 948–951, Jun. 2018, doi: https://doi.org/10.24136/atest.2018.207.

[37] E. Hatzigeorgiou, "A look into Sweden's EV charging infrastructure," Mer, Sep. 14, 2022. https://uk.mer.eco/news/sweden-ev-charging-infrastructure/

[38] Trafikverket, "Årsredovisningen sammanfattar ett utmanande år," Trafikverket, Sep. 28, 2021. https://www.trafikverket.se/om-oss/nyheter/nationella-nyheter/2024/februari/arsredovisningen-sammanfattar-ett-utmanande-ar/\T1\textbackslash{}#trafikverkets\T1\textbackslash{}_2023\T1\textbackslash{}_i\T1\textbackslash{}_backspegeln\T1\textbackslash{}_ett\T1\textbackslash{}_axplock (accessed Nov. 03, 2024).

[39] J. Taylor, A. Maitra, M. Alexander, D. Brooks, and M. Duvall, "Evaluations of Plug-in Electric Vehicle Distribution System Impacts," 2010 IEEE, 2010.

[40] N. O. Kapustin and D. A. Grushevenko, "Long-term electric vehicles outlook and their potential impact on electric grid," Energy Policy, vol. 137, p. 111103, Feb. 2020, doi: https://doi.org/10.1016/j.enpol.2019.111103.

[41] J. A. P. Lopes, F. J. Soares, and P. M. R. Almeida, "Integration of Electric Vehicles in the Electric Power System," Proceedings of the IEEE, vol. 99, no. 1, pp. 168–183, Jan. 2011, doi: https://doi.org/10.1109/jproc.2010.2066250.

[42] A. Jansson, O. Samuelsson, and F. J. Márquez-Fernández, "Electromobility Impact on the Power Grid - Base Case for Probabilistic Modelling," 2023 IEEE Transportation Electrification Conference \& Expo (ITEC), Jun. 2023, doi: https://doi.org/10.1109/itec55900.2023.10186933.

[43] "Volvo Cars," www.volvocars.com. https://www.volvocars.com/

[44] "Scania Group," Scania Group. https://www.scania.com/

[45] "Kolada," Kolada.se, 2024. https://kolada.se/verktyg/jamforaren/?focus=2328\T1\textbackslash{}&report=206451 (accessed Nov. 07, 2024).

[46] "Geofabrik Download Server," download.geofabrik.de. https://download.geofabrik.de/europe.html

[47] "Finding statistics," Statistiska Centralbyrån, 2019. https://www.scb.se/en/finding-statistics/

[48] "Lastkajen 6.0," Trafikverket.se, 2024. https://lastkajen.trafikverket.se/orderdata/vag (accessed Nov. 07, 2024).

[49] "Statistics," www.energimyndigheten.se. https://www.energimyndigheten.se/en/facts-and-figures/statistics/

[50] "Kommungruppsindelning," skr.se. https://skr.se/skr/tjanster/kommunerochregioner/faktakommunerochregioner/kommungruppsindelning.2051.html (accessed Dec. 09, 2023).

[51] L. Förberg, "Trafikförsörjningsprogram 2020 -2023," Region Blekinge, May 13, 2020. https://regionblekinge.se/regional-utveckling/trafik-och-samhallsplanering/kollektivtrafik.html

[52] Region Dalarna, "Regionalt trafikförsörjningsprogram Dalarna 2023-2032." https://www.regiondalarna.se/verksamhet/kollektivtrafik/

[53] F. Å. Jönsson, " Region Trafikförsörjningsprogram Gävleborg 2022-2032," Region Gävleborg, 2019. https://xtrafik.se/regional-kollektivtrafikmyndighet

[54] "Trafikförsörjningsprogram 2024-2033," Region Gotland, Jul. 17, 2024. https://gotland.se/trafik-gator-och-parker/kollektivtrafik/kollektivtrafik-pa-gotland

[55] Region Halland, "Kollektivtrafikplan 2024 med utblick 2025-2026," Sep. 07, 2023. https://www.regionhalland.se/utveckling-och-tillvaxt/samhallsplanering-och-trafik/kollektivtrafik/hallandstrafiken

[56] M. Zeidlitz, "Rapport Allmän kollektivtrafik 2023," Region Jämtland Härjedalen, Dec. 2020. https://www.regionjh.se/regionalutveckling/kollektivtrafik.4.15591b8415700f7566b4394d.html (accessed Nov. 08, 2024).

[57] Länstrafiken Jököping, "Regionalt trafiksörjningsprogram 2021-2035 för Jönköpings län," Apr. 12, 2021. https://www.jlt.se/om-oss/framtiden/

[58] Region Kalmar län, "Trafikforsorjningsprogram för Kalmar län 2021-2029," Apr. 15, 2021. https://regionkalmar.se/om-oss/resor-och-kollektivtrafik/

[59] A. Englund, "Trafikforsorjningsprogram Kronobergs Län 2021-2030 med Utblick," Region Kronoberg, Nov. 24, 2021. https://www.regionkronoberg.se/trafik-och-samhallsplanering/mal-med-kollektivtrafiken/regional-kollektivtrafikmyndighet/

[60] J. Baggström, P. Trägårdh, and P. Pettersson, "Regionalt Trafikforsorjningsprogram för Norrbotten 2023-2035," Kolletivtrafikmyndigheten i Norrbotten, Oct. 16, 2023. https://utvecklanorrbotten.se/rapporter-blanketter/

[61] L. Ramberg and Rebecca Larsson, "Regionalt Trafikforsorjningsprogram för Örebro län 2022-2030," Region Örebro län, Feb. 15, 2022. https://www.regionorebrolan.se/sv/resor-och-kollektivtrafik/bussar-och-tag/

[62] J. Borggren, N. Ebermark, D. Einar, S. Knape, and K. Wiborn, "Regionalt trafikförsörjningsprogram för Östergötland 2030-Faställd av regionfullmäktige," Nov. 24, 2020. https://www.regionostergotland.se/ro/det-har-gor-vi/kollektivtrafik

[63] J. Gomer, P. Lindblom, and E. Morin, "Trafikforsorjningsprogram för Skane 2020-2030," Regio Skåne, Feb. 25, 2020. https://www.skane.se/om-region-skane/kollektivtrafik/mal-for-kollektivtrafiken/

[64] M. Johansson, "Länsplan för regional Transportinfrastruktur i Södermanlands län 2022-2033," Region Sörmland, Sep. 01, 2022. https://www.skane.se/om-region-skane/kollektivtrafik/mal-for-kollektivtrafiken/

[65] A. Fendert, "Regionalt trafikförsörjningsprogram för Stockholms län 2035," SL, Sep. 10, 2024. https://www.regionstockholm.se/nyheter/2024/09/nytt-regionalt-trafikforsorjningsprogram-siktar-mot-2035/

[66] E. Långsiktig, "Regionalt trafikförsörjningsprogram för Uppsala län 2020-2030," Region Uppsala. https://regionuppsala.se/det-har-gor-vi/kollektivtrafik/utveckling-av-kollektivtrafiken/Regionalt-trafikforsorjningsprogram/

[67] Ø. Lund and L. Malmen, "Regionalt Trafikförsörjningsprogram Värmland 2022-2026," Region Värmland, Jul. 01, 2021. https://regionvarmland.

se/regionvarmland/resor--trafik/kollektivtrafikmyndighet/trafikforsorjningsprogram

[68] B. Byring, A. Åkerlund, and H. Bäckman, "Regionalt Trafikförsörjningsprogram för Västerbottens län 2020-2025," Region Västerbotten, Jun. 16, 2020. https://www.regionvasterbotten.se/naringsliv-och-samhallsbyggnad/infrastruktur-och-kollektivtrafik/kollektivtrafik/trafikforsorjningsprogrammet

[69] S. Nylund, "Regionalt Trafikförsörjningsprogram för framtidens Kollektivtrafik 2024-2030," Din Tur. https://www.dintur.se/om-oss/uppdrag-och-mal/

[70] T. Levinsson and A. Andersson, "Västmanlands Regionala Trafikförsörjningsprogram Antagen av Regionfullmästige," Region Västmanland, Sep. 21, 2021. https://regionvastmanland.se/om-regionen/organisation/kollektivtrafikforvaltningen/

[71] A. Kronvall, M. Elofsson, K. Ryberg, and F. Karlge, "Trafikförsörjningsprogram 2021-2025 Hållbara resor i Västra Götaland," Västra Götalandsregionen, May 18, 2021. https://www.vgregion.se/kollektivtrafik/sa-styrs-kollektivtrafiken/trafikforsorjningsprogrammet/

[72] Gustaver, M. (2020) A Chalmers University of Technology Master's thesis template for LaTeX. Unpublished.

A

Appendix 1

This research benefited from data provided by Statistics Sweden, the Swedish Transport Agency, and the Swedish Energy Agency. It is important to clarify the availability and definitions of the relevant data used in this study.

The original documents are written in Swedish, so to avoid any potential misunderstandings, this appendix includes both the original text and a reference translation by the author. This is intended to assist future researchers who may wish to consult these sources.

- **Vehicle Numbers and Daily Commuting Data**

Statistics Sweden provided data on vehicle counts and daily commuting patterns in Sweden. This data was instrumental in establishing urban commuting flow and energy consumption calculations for this study. Details on the data are provided below.

Swedish Version:
Statistiken beskriver antal fordon i trafik samt antal avställda, i landets län respektive kommuner. Statistiken delas upp på fordonsslag, bränsle och ägandet. Dessutom presenteras antal nyregistrerade personbilar under året. Statistiken omfattar de fordon som fanns i Vägtrafikregsitret den 31 december aktuellt år. Statistik om fordon baseras på Transportstyrelsens vägtrafikregister. Uppgifter avseende ägarens juridiska form matchas på från SCB:s företagsdatabas. Registret innehåller fordon som är i trafik och avställda vid årsskiftet, eller som är avregistrerade under året. Statistiken redovisar hur beståndet per fordonsslag ser ut vid årsskiftet.

Statistiken avser de registreringspliktiga fordon hos Transportstyrelsens vägtrafikregister som utgörs av fordonsslagen personbil, lastbil, buss, släpvagn (inklusive husvagn), motorcykel, moped klass I, snöskoter, terränghjuling och traktor enligt lagen om vägtrafikregister (2001:650). Även terrängvagn, terrängsläp och motorredskap återfinns i vägtrafikregistret men redovisas inte i statistiken.

Att endast registreringspliktiga fordon kan ingå i statistiken innebär att enbart mopeder klass I ingår i statistiken och inte övriga mopeder. I statistiken ingår inte heller militära fordon som tillhör staten eller fordon som enbart används inom in-

hägnat område och för vilka det inte finns någon registreringsplikt.

Translated by Author:
The statistics describe the number of vehicles in traffic/not in traffic in counties and municipalities. The statistics are broken down by vehicle type, fuel and ownership. In addition, the number of newly registered passenger cars during the year is presented. The statistics include the vehicles that were in the Road Traffic Register on 31 December of the year in question.

The statistics are based on the Swedish Transport Agency's Road Traffic Register. Information regarding the owner's legal form is matched from Statistics Sweden's company database. The register includes vehicles in traffic and not in traffic by the end of the year and deregistered vehicles during the past year.

The statistics refer to the vehicles required to be registered in the Swedish Transport Agency's road traffic register of the vehicle types passenger car, lorry, bus, trailer (including caravan), motorcycle, class I moped, snowmobile, all-terrain vehicle, tractor according to the Road Traffic Register Act (2001:650).

This means that only registered vehicles can be included in the statistics and therefore only class I mopeds are included and not other mopeds. Military vehicles belonging to the state and vehicles that are used only within a fenced area and for which there is no registration obligation are not included in the statistics.

- **Average Traffic Volume**

The Swedish Transport Agency provided data on the average daily traffic volume across various road segments for different time periods over recent years. This data, derived from multi-year historical sampling, enabled the development of a research approach that incorporates historical fluctuations to extend, predict, and validate traffic flow and energy consumption models. This methodology provides a concrete foundation for analyzing highway traffic and energy use. Below is the Swedish Transport Agency's description of the data.

Swedish Version:
Vilket år ÅDT-mätningen är gjord framgår av attributet mätårsperiod (ÅÅÅÅMM) under företeelsen Trafik (under vägtrafikdata). På större vägar mäter vi vart fjärde år och på mindre vägar vart 12:e. Du frågar även om specifika tidsperioder. Data finns inte för hela året utan endast under kortare mätperioder. För att skatta ÅDT (Årsmedeldygnstrafik) gör vi mätningar vid fyra tillfällen jämnt fördelat över året. Vid två av tillfällena mäter vi över en helg och vid de två andra tillfällena mäter vi en vardag. Vanligen blir det 10 dygn. Utifrån detta material skattar vi ett medelflöde per dygn. Vid skattningen tar vi hänsyn till hur trafiken brukar variera över året. Vid mätningar görs en fordonsklassning av passerande fordon. Data la-

gras per timme. Med den informationen kan ÅDT delas upp i olika fordonsklasser och olika delar av dygnet. Ser av kvittot du skickade att det är dessa data du laddat ner. Vi har alltså data från de enskilda mättillfällena, men det är inte heltäckande för hela året, och alla platser är inte heller mätta samtidigt. För jämförbarhet är det därför oftast lämpligt att använda det skattade årsmedelvärdet.

Translated by Author:
The year the ÅDT measurement was made is shown by the attribute measurement year period (YYYYMM) under the traffic phenomenon (under road traffic data). On larger roads, it measures every four years, and on smaller roads every 12. You also ask about specific periods. Data is unavailable for the entire year, but only for shorter measurement periods. To estimate ÅDT (annual average daily traffic), we make measurements on four occasions evenly distributed over the year. On two occasions we measure over a weekend and on the other two occasions we measure a weekday. Usually, it will be 10 days. Based on this material, we estimate an average flow per day. When estimating, we consider how traffic tends to vary over the year. During measurements, a vehicle classification is made of passing vehicles. Data is stored hourly. With that information, ÅDT can be divided into different vehicle classes and different parts of the day. Sees from the receipt you sent that this is the data you downloaded. We thus have data from the individual measurement occasions, but it is not comprehensive for the entire year, and not all locations are measured at the same time. For comparability, it is therefore usually appropriate to use the estimated annual average value.

- **Energy System Data**

The Swedish Energy Agency provided data on regional power generation and historical energy consumption in the transportation sector as reference points for this research. Since this data is already standardized using international units, no further clarification is necessary. Below is the Swedish Energy Agency's guidance on data usage.

Swedish Version:
Du får under vissa villkor fritt kopiera och sprida vidare publicerad statistik som finns på webbplatsen. Det gäller såväl tabeller som diagram. Följande villkor gäller:

1. Ange källa. Du ska ange att Energimyndigheten är källa ("Källa: Energimyndigheten").

2. Om du gör bearbetningar. Om du bearbetar statistiken ska du inte ange Energimyndigheten som källa. Men ange gärna att det är bearbetad statistik från Energimyndighetens webbplats.

3. Länkar. Du får gärna länka till våra statistiksidor.

4. Statistikdatabasen och API. Du kan föra över data från statistikdatabasen digitalt via programmeringsgränssnittet API. Det krävs inget särskilt medgivande för det. Samma regler för källangivelse gäller som ovan. Observera att ändringar kan ske i databasen som gör att du måste rikta om din fråga.

Translated by Author:
Under certain conditions, you may freely copy and distribute published statistics on the website. This applies to both tables and diagrams. The following conditions apply:

1. Specify source. You must indicate that the Energy Agency is the source ("Source: The Energy Agency").

2. Processing. If you process the statistics, do not indicate the Energy Agency as the source. But please state that it is processed statistics from the Energy Agency's website.

3. Links. You are welcome to link to our statistics pages.

4. The statistics database and API. You can transfer data from the statistics database digitally via the programming interface API. No special consent is required for it. The same rules for attribution apply as above. Please note that changes may occur in the database which will require you to re-direct your question.

B

Appendix 2

This appendix presents the calculated results for urban energy consumption derived from this study. These results are based on the Urban Consumption Energy Model (UCEM) and the Urban Traffic Energy Model (UTEM) developed within the framework of this research. In short, based on historical commuting data, the driving characteristics of vehicles in each city are classified and identified. Daily energy for cars in the city is calculated through formula 4.3, and energy for buses is determined via formula 4.5.

Type	**City**	**Daily Cars(MWh)**	**Daily Buses(MWh)**
A1	Stockholm	1546.5	155.8
A1	Malmö	408.8	65.57
A1	Göteborg	623.7	237.26
A2	Upplands-Väsby	84.5	0.14
A2	Vallentuna	70.7	0.08
A2	Österåker	81.5	0.71
A2	Värmdö	74.3	17.52
A2	Järfälla	140.5	16.67
A2	Ekerö	48.3	2.04
A2	Huddinge	208.6	0.28
A2	Botkyrka	129.3	16.39
A2	Salem	28.7	0.0
A2	Haninge	144.3	0.14
A2	Tyresö	75.8	29.84
A2	Upplands-Bro	58.6	0.0
A2	Täby	149.6	32.78
A2	Danderyd	119.1	0.14
A2	Sollentuna	182.7	1.81
A2	Nacka	243.9	33.53
A2	Sundbyberg	100.5	33.53
A2	Solna	315.9	20.48
A2	Lidingö	72.8	0.04
A2	Vaxholm	20.2	0.0
A2	Sigtuna	94.0	20.34
A2	Nynäshamn	40.4	1.64
A2	Håbo	47.7	2.47

Type	City	Daily Cars(MWh)	Daily Buses(MWh)
A2	Staffanstorp	59.7	0.18
A2	Burlöv	47.3	0.0
A2	Vellinge	79.5	0.18
A2	Kävlinge	71.1	0.18
A2	Lomma	53.8	0.0
A2	Svedala	55.2	0.0
A2	Skurup	32.9	0.18
A2	Trelleborg	74.3	2.3
A2	Kungsbacka	157.9	12.21
A2	Härryda	94.7	0.1
A2	Partille	80.4	9.68
A2	Öckerö	18.6	1.51
A2	Stenungsund	64.3	11.59
A2	Ale	63.9	0.1
A2	Lerum	81.3	0.0
A2	Bollebygd	22.6	0.0
A2	Lilla Edet	30.4	1.21
A2	Mölndal	207.2	9.58
A2	Kungälv	104.5	4.03
A2	Alingsås	64.1	0.1
B3	Uppsala	204.4	92.2
B3	Linköping	152.7	34.34
B3	Örebro	157.4	21.05
B3	Västerås	155.5	9.37
B3	Helsingborg	192.3	43.55
B3	Norrköping	140.7	25.88
B3	Jönköping	142.2	23.73
B3	Umeå	94.9	17.84
B3	Lund	250.0	45.14
B3	Borås	127.6	50.07
B3	Eskilstuna	97.2	11.95
B3	Halmstad	107.7	17.87
B3	Gävle	101.6	20.04
B3	Södertälje	210.9	23.46
B3	Sundsvall	98.2	113.16
B3	Växjö	96.2	6.87
B3	Karlstad	123.7	46.59
B3	Kristianstad	103.8	17.93
B3	Luleå	81.2	13.71
B3	Kalmar	85.3	38.47
B3	Östersund	69.7	8.23
B3	Trollhättan	89.4	0.74
B3	Borlänge	83.8	6.28
B4	Landskrona	66.6	1.59

Type	City	Daily Cars(MWh)	Daily Buses(MWh)
B4	Enköping	70.5	1.57
B4	Ängelholm	84.0	0.89
B4	Vänersborg	68.1	0.4
B4	Strängnäs	56.3	0.47
B4	Mark	16.7	2.22
B4	Eslöv	63.4	2.3
B4	Mjölby	54.6	4.68
B4	Höganäs	46.2	0.0
B4	Laholm	45.8	3.68
B4	Sala	34.3	0.01
B4	Kumla	45.5	2.22
B4	Tierp	31.3	0.0
B4	Alvesta	35.1	2.02
B4	Sjöbo	40.5	1.06
B4	Knivsta	36.9	0.22
B4	Timrå	37.6	6.04
B4	Klippan	35.6	1.06
B4	Sölvesborg	31.2	1.83
B4	Hammarö	35.1	0.0
B4	Hallstahammar	29.9	0.0
B4	Åstorp	35.1	0.0
B4	Hallsberg	37.3	2.77
B4	Hörby	31.3	0.71
B4	Bjuv	34.8	1.06
B4	Mörbylånga	30.9	0.63
B4	Krokom	30.6	7.25
B4	Östra Göinge	24.2	0.71
B4	Söderköping	28.1	0.77
B4	Vaggeryd	24.4	3.45
B4	Svalöv	31.1	0.18
B4	Trosa	24.2	0.88
B4	Heby	26.2	0.9
B4	Bromölla	24.4	0.18
B4	Habo	25.9	6.52
B4	Kil	26.6	5.75
B4	Forshaga	21.7	0.0
B4	Gnesta	19.1	0.1
B4	Åtvidaberg	18.3	0.88
B4	Säter	23.3	0.0
B4	Nykvarn	24.7	1.41
B4	Svenljunga	20.6	0.0
B4	Nora	16.8	6.09
B4	Örkelljunga	19.8	7.43

Type	City	Daily Cars(MWh)	Daily Buses(MWh)
B4	Gagnef	21.2	0.13
B4	Surahammar	18.5	0.0
B4	Kinda	15.2	0.0
B4	Älvkarleby	16.8	0.0
B4	Herrljunga	17.7	0.1
B4	Vännäs	15.9	2.27
B4	Grums	18.0	0.14
B4	Lessebo	12.2	0.0
B4	Lekeberg	17.8	0.55
B4	Valdemarsvik	10.7	0.0
B4	Perstorp	12.7	0.18
B4	Mullsjö	14.1	1.02
B4	Nordmaling	11.1	2.57
B4	Torsås	12.8	0.2
B4	Aneby	13.7	5.07
B4	Robertsfors	10.2	1.51
B4	Ockelbo	8.7	1.13
B4	Grästorp	12.6	0.1
B4	Bjurholm	3.7	0.0
B5	Uddevalla	84.3	5.43
B5	Hässleholm	74.1	3.54
B5	Motala	55.2	2.46
B5	Sandviken	53.8	12.86
B5	Nässjö	44.8	11.42
B5	Boden	40.3	7.43
B5	Köping	66.0	1.57
B5	Ulricehamn	38.6	2.72
B5	Kristinehamn	30.8	0.69
B5	Lindesberg	31.8	5.54
B5	Östhammar	31.9	6.05
B5	Finspång	32.2	2.8
B5	Nybro	30.8	12.36
B5	Tingsryd	20.4	5.65
B5	Tranemo	21.5	0.4
B5	Askersund	19.3	3.88
B5	Hylte	15.5	0.77
B5	Uppvidinge	15.2	0.0
B5	Älvsbyn	11.2	5.83
B5	Berg	10.8	1.05
B5	Bräcke	9.0	0.0
B5	Laxå	9.5	0.0
B5	Vindeln	7.7	2.27
B5	Munkfors	5.9	0.0
C6	Skellefteå	56.2	12.01

Type	City	Daily Cars(MWh)	Daily Buses(MWh)
C6	Karlskrona	66.6	4.53
C6	Varberg	82.1	9.54
C6	Norrtälje	75.3	0.04
C6	Gotland	48.1	5.86
C6	Falun	76.3	14.49
C6	Nyköping	66.1	28.08
C6	Skövde	90.8	22.58
C6	Örnsköldsvik	44.0	4.44
C6	Falkenberg	61.4	7.96
C6	Piteå	44.3	7.86
C6	Lidköping	58.6	2.22
C6	Hudiksvall	39.0	8.83
C6	Västervik	29.5	5.78
C6	Katrineholm	37.3	2.39
C6	Värnamo	46.5	7.81
C6	Falköping	43.4	1.21
C6	Karlshamn	42.5	2.66
C6	Ystad	49.3	8.32
C6	Karlskoga	41.5	0.55
C6	Ljungby	31.6	12.12
C6	Oskarshamn	30.1	1.54
C6	Ludvika	30.3	0.0
C6	Härnösand	26.9	4.7
C6	Mariestad	35.2	2.55
C6	Avesta	29.6	27.06
C6	Kiruna	20.6	7.03
C7	Ronneby	42.8	3.85
C7	Skara	36.9	0.5
C7	Älmhult	29.5	7.67
C7	Eksjö	29.3	2.98
C7	Höör	33.0	1.59
C7	Flen	22.2	0.05
C7	Vara	31.9	0.81
C7	Tjörn	30.9	6.75
C7	Hedemora	25.6	0.0
C7	Orust	28.3	0.1
C7	Hultsfred	18.6	0.89
C7	Arboga	22.3	0.56
C7	Tomelilla	27.7	0.0
C7	Olofström	22.8	1.73
C7	Mönsterås	21.2	0.36
C7	Fagersta	18.2	0.11
C7	Götene	30.5	0.4
C7	Osby	23.3	0.35

Type	City	Daily Cars(MWh)	Daily Buses(MWh)
C7	Tidaholm	19.7	0.2
C7	Åmål	16.1	0.2
C7	Oxelösund	20.2	0.07
C7	Vårgårda	25.1	11.49
C7	Sävsjö	16.5	1.57
C7	Tibro	20.3	0.1
C7	Smedjebacken	19.7	0.0
C7	Munkedal	22.4	1.71
C7	Markaryd	18.7	2.42
C7	Hofors	13.2	0.69
C7	Degerfors	16.8	2.22
C7	Gnosjö	21.5	2.22
C7	Nordanstig	15.0	0.99
C7	Emmaboda	14.9	0.54
C7	Töreboda	15.7	0.2
C7	Mellerud	13.1	0.0
C7	Hjo	15.6	0.0
C7	Vingåker	14.6	0.03
C7	Kungsör	16.9	0.01
C7	Vadstena	13.5	1.77
C7	Karlsborg	11.9	0.2
C7	Färgelanda	12.3	1.61
C7	Högsby	8.7	0.36
C7	Norberg	9.8	0.15
C7	Essunga	12.0	0.1
C7	Boxholm	10.8	0.75
C7	Ödeshög	9.1	0.48
C7	Gullspång	8.0	0.71
C7	Dals-Ed	7.6	0.0
C7	Ljusnarsberg	6.6	0.0
C7	Skinnskatteberg	7.2	0.08
C7	Storfors	8.3	0.0
C7	Ydre	6.2	0.27
C8	Gislaved	41.6	8.25
C8	Vetlanda	33.5	3.61
C8	Bollnäs	32.7	2.22
C8	Arvika	29.5	0.57
C8	Söderhamn	27.0	7.95
C8	Tranås	21.2	1.99
C8	Sollefteå	18.8	2.55
C8	Ljusdal	19.9	7.3
C8	Kramfors	20.7	3.75
C8	Kalix	17.1	1.45

Type	City	Daily Cars(MWh)	Daily Buses(MWh)
C8	Vimmerby	22.3	1.79
C8	Säffle	20.4	4.87
C8	Lysekil	18.9	5.75
C8	Sunne	19.8	0.72
C8	Lycksele	12.1	0.3
C8	Ovanåker	14.8	0.33
C8	Hagfors	13.1	0.29
C8	Strömsund	11.8	0.3
C8	Torsby	15.9	0.14
C8	Filipstad	11.9	0.0
C8	Haparanda	8.7	0.59
C8	Bengtsfors	12.9	10.99
C8	Ånge	10.7	1.98
C8	Hällefors	6.9	0.0
C8	Vansbro	8.3	0.0
C8	Vilhelmina	7.0	8.01
C8	Arvidsjaur	7.2	1.09
C8	Pajala	6.9	1.84
C8	Ragunda	7.2	0.0
C8	Övertorneå	4.7	1.19
C8	Norsjö	5.4	0.54
C8	Överkalix	4.1	1.28
C8	Malå	4.1	0.45
C8	Åsele	3.0	0.91
C8	Dorotea	3.2	1.06
C9	Mora	30.4	0.26
C9	Simrishamn	27.0	0.18
C9	Gällivare	17.5	2.55
C9	Leksand	24.3	0.0
C9	Båstad	30.1	1.24
C9	Strömstad	13.3	0.1
C9	Tanum	19.8	5.14
C9	Åre	15.5	2.24
C9	Rättvik	17.9	0.26
C9	Borgholm	14.7	0.63
C9	Malung	12.6	4.62
C9	Härjedalen	11.5	15.69
C9	Årjäng	10.5	0.72
C9	Sotenäs	13.0	0.1
C9	Eda	11.9	0.72
C9	Älvdalen	9.7	1.67
C9	Orsa	12.3	0.0
C9	Storuman	5.8	1.66

Type	**City**	**Daily Cars(MWh)**	**Daily Buses(MWh)**
C9	Jokkmokk	5.1	0.0
C9	Arjeplog	3.2	0.78
C9	Sorsele	3.1	1.97

C

Appendix 3

This appendix presents the calculated vehicle energy consumption results for highways obtained in this study. The results are based on the LSTM-GRU model and the Rayleigh distribution-based traffic energy consumption model developed as part of this research. Detailly, the traffic agency offered ÅDT values for 6:00-18:00, 18:00-22:00, and 22:00-6:00, respectively. Then, after prediction through the LSTM-GRU model proposed, the study utilizes Rayleigh distribution parameters for different road sections according to formulas 4.9-4.11. After iterative optimization and verification, the following results are obtained.

Highway	**Route**	**Light Cars (MWh)**			**Heavy Trucks (MWh)**		
		6:00-18:00	**18:00-22:00**	**22:00-6:00**	**6:00-18:00**	**18:00-22:00**	**22:00-6:00**
E4	Ljungby S-Kropp	1083.9	249.08	120.38	1102.7	372.92	448.71
	Lagan N-Ljungby S	111.24	26.32	9.882	126.52	42.036	48.84
	Jönköping-Lagan N	1494.5	342.92	163.38	1242.2	419.27	620.55
	Mjölby- Jönköping	755.8	183.39	74.666	582.98	220.52	327.48
	Norrköping-Mjölby	621.43	147.45	67.584	449.89	139.03	196.03
	Nyköping-Norrköping	550.67	147.2	55.969	363.37	118.07	176.33
	Södertälje-Nyköping	842.61	212.4	91.038	443.83	143.77	204.86
	Norrtull-Södertälje	174.92	40.5	16.762	105.91	30.455	37.598
	Järva krog-Norrtull(STHL)	7.0638	1.4602	0.56112	5.1661	1.2972	1.4114
	Märsta-Järva krog (STHL)	329.65	77.098	48.384	172.7	44.207	53.083
	Uppsala - Märsta	271.48	60.595	33.631	114.71	26.558	30.868
	Gävle -Uppsala	1179.4	268.04	121.84	786.43	241.9	319.8
	Bergby - Gävle	138.27	30.651	12.488	84.144	23.034	28.189
	Söderhamn - Bergby	222.45	53.581	24.776	145.08	43.872	53.277
	Ångersjön - Söderhamn	101.59	24.445	9.4813	88.081	26.139	30.259
	Sundsvall - Ångersjön	390.58	98.139	41.718	305.35	102.03	157.17
	Härnösand - Sundsvall	616.07	136.09	60.33	274.85	71.762	97.688
	Utansjö-Härnösand	150.7	31.189	11.73	87.417	23.203	27.389
	Umeå - Utansjö	1198.6	274.53	135.68	925.2	287.95	371.47
	Piteå - Umeå	1566.6	373.23	184.46	1358.5	389.84	486.34
	Gäddvik Södra (Luleå) - Piteå	224.61	49.584	22.168	148.61	37.415	45.176
	Rutvik (Luleå)-Gäddvik Söder (Luleå)	7.2148	1.2903	0.53822	3.5454	0.57024	0.67561
	Töre-Rutvik (Luleå)	137.1	31.008	14.059	86.105	21.477	25.45
	Haparanda (Border SE/FI) - Töre	361.69	79.922	36.342	210.26	40.346	47.469
E6	Vellinge-Trelleborg	224.83	45.219	20.942	173.42	36.057	34.18
	Petersborg-Vellinge	181.42	36.112	16.538	118.66	24.334	22.891
	Fredriksberg-Petersborg	51.549	9.9579	4.5365	43.461	8.6684	8.8885
	Kronetorp-Fredriksberg	183.32	36.003	16.424	115.4	23.973	22.733
	Helsingborg S-Kronetorp	1334	302.71	157.6	889.13	211.97	245.28
	Kropp-Helsingborg S	150.88	29.91	13.654	96.234	19.93	18.929
	Helsingborg S- Helsingborg	150.27	34.842	18.322	83.426	15.887	14.925
	Ängelholm-Kropp	343.5	73.013	34.452	246.21	53.942	52.282

Highway	Route	Light Cars (MWh)			Heavy Trucks (MWh)		
		6:00-18:00	18:00-22:00	22:00-6:00	6:00-18:00	18:00-22:00	22:00-6:00
	Kallebäcksmotet-Ängelholm	5536.2	1275.3	715.14	4659.6	1250.4	1470.5
	Gullbergsmotet-Kallebäcksmotet	58.612	11.464	5.3213	28.409	5.1978	4.855
	Stora Höga-Gullbergsmotet	717.56	160.21	80.462	442.26	99.914	104.79
	Munkedal-Stora Höga	912.27	211.91	109.87	625.61	156.38	171.16
	Rabbalshede-Munkedal N	355.76	74.953	35.359	242.61	57.038	53.36
	Strömstad-Rabbalshede	863	195.25	100.03	566.42	135.87	143.16
	Svinesund-Strömstad	334.35	69.085	32.816	214.51	46.443	45.841
E10	Riksgränsen (Border SE/NO) - Svappavaara	167.88	42.485	24.167	84.194	17.499	13.134
	Svappavaara - Gällivare	26.427	6.759	3.7546	21.913	5.1784	6.3479
	Gällivare - Töre	149.91	42.92	21.146	168.32	45.302	58.141
E12	Umeå-Holmsund	37.956	7.6508	2.9857	21.319	1.8151	3.0764
	Storuma-Umeå	825.77	182.07	92.507	317.85	69.078	102.54
	Norges riksgräns-Storuman	99.919	23.184	6.9189	51.442	12.108	5.8088
E14	Storlien - Östersund	510.29	94.842	35.894	229.7	37.207	20.207
	Östersund-Brunflo	126.57	24.657	9.479	42.369	6.4995	9.0872
	Brunflo - Sundsvall	842.03	181.26	83.388	408.63	108.28	137.57
E18	Töcksfors W-Valnäs(Segmon S)	612.69	149.82	68.706	474.66	129.12	120.31
	Segmon-Vålberg	137.73	28.054	11.067	90.187	18.047	13.586
	Vålberg-Segmon	55.857	11.327	4.2039	31.865	6.3523	4.8443
	Vålberg - Bergviksmotet(Karlstad W)	350.33	70.37	28.832	152.31	31.657	27.305
	Bergviksmotet-Skattkärrsmotet	606.02	111.19	40.936	327.54	53.539	46.284
	Skattkärrsmotet - Väse	1037.4	233.02	107.96	515.95	130.69	133.51
	Väse-Lekhyttan	658.78	145.97	67.537	363.23	91.656	92.33
	Lekhyttan-Örebro	489.59	96.097	38.371	230.05	51.822	55.413
	Örebro-Arboga	430.87	102.21	38.332	333.62	103.05	109.44
	Arboga- Köping	106.26	21.328	8.1855	83.047	21.234	20.195
	Köping-Dingtuna	72.047	13.589	7.1717	46.469	12.081	13.029
	Dingtuna-Hällamotet	883.46	174.31	80.73	340.26	63.043	73.053
	Hällamotet-Hummelsta	130.98	26.746	11.742	76.442	15.459	16.333
	Enköping-Kungsängen	813.8	182.72	87.635	343	74.941	78.941
	Kungsängen-Hjulsta	352.46	70.467	32.411	197.99	36.598	32.978
	Hjulsta-Tpl Kista	101.22	19.802	8.0786	49.19	9.6748	9.4443
	Märsta - Järva krog (STHL)	18.073	3.4412	1.2706	6.1087	1.2475	1.0606
	Järva krog-Rosenkälla	1033	208.19	84.411	264.94	44.707	32.834
	Rosenkälla-Söderhall	220.96	42.699	16.719	89.709	19.6	10.058
	Söderhall-Norrtälje	130.55	26.244	9.8421	64.69	17.4	8.4717
	Norrtälje-Kapellskär	33.466	7.1146	1.8256	45.388	16.851	4.1955
E20	Göteborg - Örebro	4855.7	1141.2	567.79	4559.2	1395.8	1560.6
	Lekhyttan-Örebro	650.36	135.08	56.586	320.86	74.487	78.549
	Örebro-Arboga	419.56	99.381	37.902	323.78	98.212	104.08
	Arboga-Öster Tibble	168.6	35.477	14.364	117.44	28.497	23.234
	Öster Tibble-Eskilstuna	123.73	24.69	10.975	65.301	12.741	10.376
	Eskilstuna-Södertälje	667.98	142.8	81.172	342.08	68.987	78.646
	Södertälje-Norrtull	258.8	53.421	23.459	150.36	34.66	32.949
	Norrtull-Värtahamnen	36.062	7.1708	2.9881	21.732	4.8166	4.3324
	Stockholm - Nynäshamn	1362.2	333.41	184.19	578.2	115.65	126.14
E22	Norrköping-Söderköping	493.41	95.811	39.031	144.15	20.627	22.722
	Söderköping-Oskarshamn	864.38	169.61	75.77	467.68	90.831	105.22
	Oskarshamn-Linsdal	408.56	89.15	39.407	196.63	36.66	43.836
	Linsdal-Ljungbyholm	330.05	58.707	21.482	91.033	10.572	12.682

Highway	Route	Light Cars (MWh)			Heavy Trucks (MWh)		
		6:00-18:00	18:00-22:00	22:00-6:00	6:00-18:00	18:00-22:00	22:00-6:00
	Ljungbyholm-Söderåkra	114.84	20.676	8.6892	54.623	8.6097	7.0143
	Söderåkra-Karlskrona	215.57	41.848	16.767	115.69	19.85	15.364
	Karlskrona-Listerby	263.46	44.909	17.798	77.598	11.322	9.5408
	Listerby-Mörrum W	428.5	81.239	39.442	171.56	25.096	25.412
	Mörrum W-Sölvesborg	2.183	0.37352	0.14152	1.2964	0.1507	0.12802
	Sölvesborg-Kristianstad	589.09	106.35	46.528	252.41	32.945	33.674
	Kristianstad-Hurva	741.9	148.93	65.986	310.11	52.24	58.014
	Hurva-Lund	78.255	13.975	5.6403	24.331	3.4694	3.6315
	Lund-Kronotorp	130.85	21.714	8.9358	59.982	9.3167	8.2848
	Kronetorp-Fredriksberg	92.518	15.799	6.4026	35.783	4.9573	4.6171
	Fredriksberg-Petersborg	109.01	18.346	7.8288	56.603	10.14	10.883
	Petersborg-Vellinge	100.64	18.042	7.3042	40.262	5.9764	5.7117
	Vellinge-Trelleborg	137.36	25.322	10.544	53.584	8.003	8.1529
E45	Gällivare-Storuman	526.67	154.53	99.274	270.44	61.172	50.224
	Storuman-Strömsund	155.26	37.696	18.204	91.411	25.245	21.97
	Strömsund-Lit	150.74	33.762	14.607	59.493	13.493	11.859
	Lit-Östersund	51.563	10.145	4.0781	15.453	2.4611	2.0927
	Östersund - Brunflo	126.51	24.644	9.4734	42.348	6.4978	9.084
	Brunflo-Åsarna	174.21	40.266	16.863	77.749	15.913	24.524
	Åsarna-Orsa	210.72	47.82	20.165	138.41	48.875	56.27
	Orsa-Mora	82.69	14.646	5.1606	19.525	4.3519	3.7585
	Mora-Malung	473.52	102.9	41.909	117.36	25.211	32.93
	Malung-Torsby	134.98	35.236	11.822	53.434	15.182	16.697
	Torsby- Vålberg	309.48	81.658	34.372	179.98	32.122	33.618
	Vålberg-Segmon	134.88	29.861	11.974	82.776	17.502	14.504
	Segmon-Valnäs	18.121	3.7382	1.3037	11.344	2.3007	1.6397
	Valnäs-Vänersborg	1045.2	219.78	95.804	610.02	139.85	126.89
	Vänersborg-Trollhättan	170.93	31.577	14.14	93.665	14.072	12.088
	Trollhättan-Älvängen	666.86	158.15	88.402	240.26	46.009	49.847
	Älvängen-Gullbergsmotet	624.19	147.02	88.586	192.18	24.868	24.862
	Gullbergsmotet-Göteborg	75.556	16.072	9.4103	27.661	3.3385	3.5818
E65	Öresundsbron-Petersborg	370.15	69.534	31.362	170.7	25.528	24.708
	Petersborg-Fredriksberg	101.22	17.795	8.1054	37.334	6.1396	6.4855
	Fredriksberg-Svedala	228.87	45.398	21.65	91.262	13.473	12.946
	Svedala-Skurup	158.91	28.685	13.314	69.09	8.8963	7.5921
	Skurup-Ystad	254.59	52.802	23.703	89.245	14.976	14.933

D

Appendix 4

This appendix provides the recommended number of charging points for each model in urban areas as determined in this study, which were calculated in Chapter 5. As the proposed charging infrastructure plan for highways has already been presented in detail in previous sections, it is not reiterated here in the appendix. According to formula 5.1, the required number of charger in cities are shown in the table.

City	Number of AC Chargers			Number of DC Chargers				
	3.7-7.4kW	11kW	22kW	25kW	50kW	100kW	150kW	350kW
Stockholm	42	6742	3371	151	47	71	1429	501
Malmö	67	1712	856	39	12	30	366	129
Göteborg	83	2607	1304	59	18	108	556	198
Upplands-Väsby	116	388	194	10	3	2	89	32
Vallentuna	233	289	163	64	31	1	84	27
Österåker	239	331	183	62	30	7	93	30
Värmdö	244	298	168	68	33	8	87	28
Järfälla	114	668	334	16	5	8	148	53
Ekerö	271	164	111	96	47	20	65	19
Huddinge	158	1012	506	24	8	3	223	79
Botkyrka	118	605	303	15	5	8	135	48
Salem	179	95	68	65	32	0	41	11
Haninge	136	673	337	16	5	2	150	54
Tyresö	181	326	173	38	18	14	84	29
Upplands-Bro	141	255	136	30	14	0	66	22
Täby	183	699	350	17	6	15	158	56
Danderyd	200	560	282	18	7	2	131	47
Sollentuna	147	879	440	21	7	18	194	69
Nacka	135	1178	589	27	9	31	257	91
Sundbyberg	25	509	255	12	4	0	109	38
Solna	13	1635	818	37	12	10	347	122
Lidingö	149	318	165	25	12	1	79	28
Vaxholm	209	44	48	84	42	0	35	8
Sigtuna	119	437	219	11	4	10	99	36
Nynäshamn	189	142	90	64	32	16	51	16
Håbo	248	168	109	86	42	24	64	19
Staffanstorp	234	235	139	71	35	2	74	23
Burlöv	135	205	112	33	16	0	56	18
Vellinge	295	311	181	88	43	2	96	30
Kävlinge	239	287	163	67	33	2	84	27
Lomma	245	203	125	79	39	0	70	20
Svedala	229	215	129	72	35	0	70	21
Skurup	266	90	76	102	51	2	51	13
Trelleborg	219	294	163	58	28	23	84	27
Kungsbacka	269	689	350	31	13	118	164	60
Härryda	250	411	221	57	27	1	109	37
Partille	165	359	186	27	12	93	88	33

City	Number of AC Chargers			Number of DC Chargers				
	3.7-7.4kW	**11kW**	**22kW**	**25kW**	**50kW**	**100kW**	**150kW**	**350kW**
Öckerö	317	5	45	133	67	15	41	8
Stenungsund	248	253	149	76	37	6	80	25
Ale	226	254	146	65	32	1	77	25
Lerum	266	328	185	73	35	0	95	30
Bollebygd	284	37	55	116	58	0	43	9
Lilla Edet	299	70	71	119	60	12	52	12
Mölndal	164	1018	509	24	8	92	225	82
Kungälv	215	457	237	37	17	39	114	40
Alingsås	213	247	141	61	30	1	73	24
Uppsala	114	764	382	18	6	42	168	61
Linköping	138	554	277	14	5	16	125	45
Örebro	130	578	289	14	5	203	130	53
Västerås	152	559	280	14	5	5	127	46
Helsingborg	122	743	372	18	6	20	164	59
Norrköping	150	502	251	13	4	12	115	41
Jönköping	168	497	249	13	4	228	115	47
Umeå	157	304	159	31	15	9	77	27
Lund	118	1011	506	24	8	21	221	78
Borås	170	454	229	19	8	23	108	38
Eskilstuna	153	328	170	26	12	115	81	32
Halmstad	194	360	190	40	18	172	92	37
Gävle	160	349	181	26	12	193	86	35
Södertälje	106	843	422	20	6	11	185	66
Sundsvall	194	319	172	45	21	52	85	30
Växjö	173	324	171	35	16	66	84	31
Karlstad	160	451	227	14	6	22	106	38
Kristianstad	230	345	188	57	27	9	94	31
Luleå	184	260	143	47	23	7	73	24
Kalmar	181	287	155	43	21	18	77	26
Östersund	161	224	124	42	20	4	63	21
Trollhättan	172	319	169	36	17	8	82	28
Borlänge	203	285	157	52	25	61	80	27
Landskrona	140	252	134	30	14	16	65	23
Enköping	209	245	140	59	29	16	73	24
Ängelholm	225	306	169	59	28	9	87	28
Vänersborg	214	238	137	63	31	4	73	23
Strängnäs	211	183	112	68	33	5	62	19
Mark	285	0	36	114	57	22	34	7
Eslöv	210	222	129	63	30	23	69	22
Mjölby	234	178	112	78	38	45	63	20
Höganäs	269	128	94	99	49	0	58	15
Laholm	323	110	93	124	62	36	61	17
Sala	251	79	70	98	48	1	47	12
Kumla	222	143	95	77	38	22	55	16
Tierp	273	61	64	108	54	0	46	10
Alvesta	284	77	73	112	56	20	50	13
Sjöbo	344	86	85	135	68	11	60	14
Knivsta	202	111	78	73	37	3	47	13
Timrå	262	97	79	100	50	58	51	15
Klippan	270	85	75	105	53	11	50	13
Sölvesborg	303	55	66	122	61	18	49	11
Hammarö	242	92	74	92	46	0	48	12
Hallstahammar	222	72	62	85	42	0	42	10
Åstorp	216	100	74	80	40	0	47	12
Hallsberg	271	95	80	104	52	27	53	14

City	Number of AC Chargers			Number of DC Chargers				
	3.7-7.4kW	11kW	22kW	25kW	50kW	100kW	150kW	350kW
Hörby	326	51	67	133	66	7	51	12
Bjuv	252	89	74	97	49	11	49	13
Mörbylånga	332	47	66	135	67	7	51	11
Krokom	330	46	65	134	67	70	50	13
Östra Göinge	296	27	52	123	61	7	43	9
Söderköping	278	50	60	112	56	8	45	11
Vaggeryd	272	34	52	112	56	34	42	10
Svalöv	288	62	66	115	57	2	48	12
Trosa	224	46	51	90	45	9	37	9
Heby	314	32	56	129	64	9	46	10
Bromölla	300	29	53	124	62	2	44	9
Habo	262	45	56	106	53	63	43	11
Kil	287	41	57	117	58	56	44	11
Forshaga	312	13	48	131	65	0	42	7
Gnesta	262	14	41	109	55	1	36	8
Åtvidaberg	298	0	39	126	63	9	38	7
Säter	309	21	51	129	64	0	43	8
Nykvarn	232	49	54	93	46	14	39	10
Svenljunga	326	4	45	137	69	0	42	7
Nora	271	1	37	115	58	59	35	8
Örkelljunga	310	5	44	131	66	72	41	10
Gagnef	360	0	46	148	74	2	45	8
Surahammar	282	7	41	119	60	0	37	6
Kinda	312	0	32	103	52	0	31	5
Älvkarleby	296	0	37	118	59	0	36	6
Herrljunga	311	0	39	123	62	1	38	7
Vännäs	274	0	35	111	56	22	34	7
Grums	308	0	39	126	63	2	38	7
Lessebo	297	0	26	85	43	0	25	4
Lekeberg	313	0	39	126	63	6	38	7
Valdemarsvik	336	0	23	72	37	0	22	4
Perstorp	223	0	28	90	45	2	27	6
Mullsjö	293	0	31	100	50	10	30	6
Nordmaling	346	0	24	76	38	25	23	5
Torsås	365	0	28	89	45	2	27	6
Aneby	309	0	30	97	49	49	29	7
Robertsfors	359	0	22	69	35	15	22	5
Ockelbo	351	0	19	59	30	11	18	4
Grästorp	334	0	28	90	45	1	27	6
Bjurholm	365	0	8	26	14	0	9	2
Uddevalla	197	287	157	50	24	53	79	27
Hässleholm	267	225	138	86	43	34	77	24
Motala	232	156	102	80	40	24	59	17
Sandviken	238	151	101	83	41	6	58	17
Nässjö	249	114	85	92	46	110	53	18
Boden	261	91	77	100	50	72	50	15
Köping	198	212	123	59	29	16	65	21
Ulricehamn	268	84	74	104	52	27	50	13
Kristinehamn	239	59	59	94	47	7	42	10
Lindesberg	285	50	60	115	57	54	46	12
Östhammar	290	51	62	117	58	59	46	12
Finspång	240	66	62	94	47	27	44	11
Nybro	271	52	60	109	54	6	44	11
Tingsryd	341	0	41	132	66	55	40	8
Tranemo	317	5	45	134	67	4	41	8

City	Number of AC Chargers			Number of DC Chargers				
	3.7-7.4kW	**11kW**	**22kW**	**25kW**	**50kW**	**100kW**	**150kW**	**350kW**
Askersund	319	0	39	125	63	38	38	8
Hylte	302	0	31	101	51	8	31	6
Uppvidinge	328	0	31	100	50	0	30	5
Älvsbyn	339	0	22	70	36	56	22	6
Berg	391	0	22	69	35	11	21	5
Bräcke	384	0	18	58	30	0	18	3
Laxå	335	0	20	62	32	0	20	3
Vindeln	346	0	16	50	26	22	16	4
Munkfors	338	0	12	39	20	0	12	2
Skellefteå	227	134	91	81	40	6	54	16
Karlskrona	241	186	117	80	39	44	66	21
Varberg	228	256	147	67	33	5	77	25
Norrtälje	265	219	135	86	42	1	75	23
Gotland	247	98	77	93	47	57	50	14
Falun	223	239	139	66	33	7	73	23
Nyköping	174	210	119	49	24	13	62	20
Skövde	186	314	168	42	20	11	83	28
Örnsköldsvik	287	77	74	113	57	43	52	14
Falkenberg	255	172	112	88	43	77	65	21
Piteå	274	91	78	105	53	76	52	15
Lidköping	233	169	108	79	39	22	62	18
Hudiksvall	268	74	69	105	52	85	48	14
Västervik	259	38	52	106	53	56	41	10
Katrineholm	196	92	68	73	36	23	43	12
Värnamo	235	119	86	86	43	75	53	17
Falköping	253	103	81	95	48	12	52	14
Karlshamn	260	98	79	99	50	26	51	14
Ystad	207	144	93	71	35	80	53	18
Karlskoga	228	104	78	84	42	6	49	13
Ljungby	271	48	58	109	54	117	43	13
Oskarshamn	245	50	55	98	49	15	41	10
Ludvika	244	52	56	97	48	0	41	9
Härnösand	244	39	51	99	49	46	38	10
Mariestad	237	76	66	92	45	25	45	12
Avesta	247	49	56	99	49	13	41	10
Kiruna	212	18	36	88	44	68	31	9
Ronneby	298	93	82	115	58	37	56	15
Skara	230	94	73	87	44	5	47	13
Älmhult	258	54	59	103	51	74	43	12
Eksjö	255	54	58	102	51	29	43	10
Höör	313	55	67	127	63	16	50	12
Flen	260	22	44	107	54	1	37	8
Vara	327	46	64	133	66	8	50	11
Tjörn	336	40	63	137	68	65	50	12
Hedemora	291	27	51	121	60	0	42	8
Orust	358	22	57	149	74	1	50	10
Hultsfred	308	0	37	119	60	9	36	7
Arboga	231	31	45	95	47	6	36	8
Tomelilla	300	37	57	123	61	0	45	9
Olofström	297	16	47	125	62	17	41	8
Mönsterås	323	1	44	136	68	4	42	8
Fagersta	196	22	36	81	41	2	30	7
Götene	310	47	63	126	63	4	48	11
Osby	288	21	48	120	60	4	41	9
Tidaholm	284	5	40	120	60	2	37	7

City	Number of AC Chargers			Number of DC Chargers				
	3.7-7.4kW	**11kW**	**22kW**	**25kW**	**50kW**	**100kW**	**150kW**	**350kW**
Åmål	274	0	32	103	52	2	31	6
Oxelösund	188	35	41	76	38	1	31	8
Vårgårda	268	35	52	110	55	6	41	9
Sävsjö	290	0	33	106	53	16	32	6
Tibro	272	13	42	114	57	1	37	8
Smedjebacken	339	0	40	129	65	0	39	6
Munkedal	321	9	47	136	68	17	43	8
Markaryd	306	0	39	124	62	24	38	7
Hofors	281	0	26	85	43	7	25	5
Degerfors	320	0	35	111	56	22	34	7
Gnosjö	275	19	46	115	57	22	39	8
Nordanstig	361	0	30	98	49	10	29	6
Emmaboda	335	0	30	98	49	6	29	6
Töreboda	309	0	32	104	52	2	31	6
Mellerud	329	0	26	84	42	0	25	4
Hjo	290	0	32	103	52	0	31	5
Vingåker	302	0	30	97	49	1	29	6
Kungsör	275	0	35	113	57	1	34	7
Vadstena	258	0	28	91	46	18	27	6
Karlsborg	305	0	24	79	40	2	24	5
Färgelanda	341	0	26	82	41	16	25	5
Högsby	372	0	18	57	29	4	18	4
Norberg	279	0	21	65	33	2	20	4
Essunga	342	0	25	81	41	1	25	5
Boxholm	310	0	23	72	37	8	22	5
Ödeshög	353	0	19	60	31	5	18	4
Gullspång	361	0	17	52	27	7	16	4
Dals-Ed	337	0	16	49	25	0	15	3
Ljusnarsberg	346	0	14	43	22	0	13	2
Skinnskatteberg	355	0	15	48	25	1	15	4
Storfors	385	0	18	56	29	0	18	3
Ydre	370	0	13	41	21	3	13	3
Gislaved	265	90	76	102	51	80	51	15
Vetlanda	287	50	61	116	58	35	46	12
Bollnäs	270	52	59	108	54	2	44	10
Arvika	283	35	54	116	58	6	42	9
Söderhamn	269	29	49	111	55	77	39	11
Tranås	213	25	40	87	44	20	32	7
Sollefteå	337	0	34	109	55	25	33	6
Ljusdal	323	0	37	117	59	71	36	9
Kramfors	358	0	39	124	62	2	38	7
Kalix	327	0	31	101	51	14	31	6
Vimmerby	280	12	43	117	59	1	38	8
Säffle	316	0	39	125	63	47	38	8
Lysekil	273	1	37	116	58	56	35	8
Sunne	336	0	38	121	61	7	36	7
Lycksele	259	0	22	70	36	3	22	5
Ovanåker	317	0	28	90	45	4	27	6
Hagfors	355	0	24	78	39	3	24	5
Strömsund	358	0	21	68	35	3	21	5
Torsby	372	0	30	96	48	2	29	6
Filipstad	316	0	23	72	37	0	22	4
Haparanda	268	0	16	51	26	6	16	4
Bengtsfors	349	0	25	80	40	5	24	5
Ånge	360	0	20	63	32	20	20	4

City	Number of AC Chargers			Number of DC Chargers				
	3.7-7.4kW	**11kW**	**22kW**	**25kW**	**50kW**	**100kW**	**150kW**	**350kW**
Hällefors	321	0	13	41	21	0	13	2
Vansbro	371	0	16	50	26	0	16	3
Vilhelmina	346	0	13	41	21	77	13	5
Arvidsjaur	301	0	14	44	23	11	14	3
Pajala	385	0	13	41	21	18	13	3
Ragunda	394	0	14	44	23	0	14	2
Övertorneå	389	0	9	29	15	12	9	3
Norsjö	340	0	11	33	17	6	11	3
Överkalix	386	0	8	25	13	13	8	3
Malå	317	0	8	26	14	5	9	3
Åsele	371	0	6	19	10	9	6	2
Dorotea	385	0	6	20	11	11	7	2
Mora	309	40	59	126	63	3	47	10
Simrishamn	316	26	54	131	65	2	45	9
Gällivare	235	3	33	100	50	25	31	6
Leksand	326	13	49	137	68	0	44	8
Båstad	316	44	62	129	64	12	48	11
Strömstad	242	0	26	83	42	1	25	5
Tanum	352	0	40	129	65	50	39	8
Åre	287	0	31	99	50	22	30	6
Rättvik	326	0	36	117	59	3	36	7
Borgholm	372	0	29	95	48	7	29	6
Malung-Sälen	356	0	24	78	39	45	24	6
Härjedalen	382	0	22	70	36	8	22	5
Årjäng	319	0	20	63	32	7	20	4
Sotenäs	337	0	26	85	43	1	26	5
Eda	335	0	24	78	39	7	24	5
Älvdalen	382	0	19	61	31	16	18	4
Orsa	329	0	26	83	42	0	25	4
Storuman	374	0	11	36	19	16	11	3
Jokkmokk	343	0	10	32	17	0	11	2
Arjeplog	383	0	7	21	11	8	7	2
Sorsele	385	0	6	20	11	19	7	2

DEPARTMENT OF SOME SUBJECT OR TECHNOLOGY
CHALMERS UNIVERSITY OF TECHNOLOGY
Gothenburg, Sweden
www.chalmers.se

CHALMERS
UNIVERSITY OF TECHNOLOGY